การสังเคราะห์ซีโอไลต์บีต้าจากเถ้าลอยถ่านลิกไนต์

นายภาณุสิทธิ์ ธุระทำ

วิทยานิพนธ์นี้เป็นส่วนหนึ่งของการศึกษาตามหลักสูตรปริญญาวิศวกรรมศาสตรมหาบัณฑิต
สาขาวิชาวิศวกรรมเคมี ภาควิชาวิศวกรรมเคมี
คณะวิศวกรรมศาสตร์ จุฬาลงกรณ์มหาวิทยาลัย
ปีการศึกษา 2544
ISBN 974-03-1321-3

SYNTHESIS OF ZEOLITE BETA FROM LIGNITE FLY ASH

Mr. Panusit Turatum

A Thesis Submitted in Partial Fulfillment of the Requirements
for the Degree of Master of Engineering in Chemical Engineering
Department of Chemical Engineering
Faculty of Engineering
Chulalongkorn University
Academic Year 2001

ISBN 974-03-1321-3

Thesis Title	Synthesis of zeolite beta from lignite fly ash
By	Mr. Panusit Turatum
Field of Study	Chemical Engineering
Thesis Advisor	Suphot Phatanasri, D.Eng.
Thesis Co-advisor	Professor Piyasan Praserthdam, Dr.Ing.
Thesis Co-advisor	Assistant Professor Metta Chareonpanich, D.Eng.

Accepted by the Faculty of Engineering, Chulalongkorn University in Partial Fulfillment of the Requirement for the Master's Degree

……...Dean of Faculty of Engineering
(Professor Somsak Panyakeow, D.Eng.)

Thesis Committee

……Chairman
(Professor Wiwat Tanthapanichakoon, Ph.D.)

……..Thesis Advisor
(Suphot Phatanasri, D.Eng.)

……..Thesis Co-advisor
(Professor Piyasan Praserthdam, Dr.Ing.)

……Thesis Co-advisor
(Assistant Professor Metta Chareonpanich, D.Eng.)

……Member
(Aticha Chaisuwan, Ph.D.)

ภาณุสิทธิ์ ธุระทำ : การสังเคราะห์ซีโอไลต์บีต้าจากเถ้าลอยถ่านลิกไนต์ (SYNTHESIS OF ZEOLITE BETA FROM LIGNITE FLY ASH) อ. ที่ปรึกษา : อ.ดร.สุพจน์ พัฒนะศรี, อ.ที่ปรึกษาร่วม : ศ.ดร.ปิยะสาร ประเสริฐธรรม และ ผศ.ดร.เมตตา เจริญพานิช, 111 หน้า ISBN 974-03-1321-3

ในการศึกษาภาวะที่เหมาะสมต่อการสังเคราะห์ซีโอไลต์บีต้าจากเถ้าลอยถ่านลิกไนต์ ปัจจัยที่นำมาศึกษาคือ อุณหภูมิขณะคนสารตั้งต้นและอุณหภูมิช่วงตกผลึก อัตราส่วนโดยโมลของ $TEAOH/SiO_2$ และอัตราส่วนอะตอมของ Si/Al ปรากฏว่าการสังเคราะห์ซีโอไลต์บีต้าจากเถ้าลอยถ่านลิกไนต์ที่อุณหภูมิขณะคนสารตั้งต้นและอุณหภูมิช่วงตกผลึกเท่ากันจะได้ซีโอไลต์บีต้าที่มีความเป็นผลึกสูง เนื่องจากการเปลี่ยนอุณหภูมิจะให้ขนาดของผลึกซีโอไลต์บีต้าที่ได้มีขนาดไม่สม่ำเสมอ อุณหภูมิขณะคนสารตั้งต้นและอุณหภูมิช่วงตกผลึกที่เหมาะสมประมาณ 140 องศาเซลเซียส อัตราส่วนโดยโมลของ $TEAOH/SiO_2$ และอัตราส่วนอะตอมของ Si/Al ที่เหมาะสมประมาณ 0.5 และ 50 ตามลำดับ ปัจจัยที่เหมาะสมเหล่านี้ทำให้ได้ซีโอไลต์บีต้าจากการสังเคราะห์จากเถ้าลอยถ่านลิกไนต์มีความเป็นผลึกสูงสุดประมาณ 98 เปอร์เซ็นต์ พื้นที่ผิวประมาณ 630 ตารางเมตรต่อกรัม และขนาดของผลึกประมาณ 0.25 ไมโครเมตร เมื่อเปรียบเทียบกับซีโอไลต์บีต้าที่ใช้ในอุตสาหกรรมซึ่งมีพื้นที่ผิวประมาณ 700 ตารางเมตรต่อกรัม และมีขนาดผลึกประมาณ 0.5 ไมโครเมตร ปรากฏว่ามีความแตกต่างกันเพียงเล็กน้อย และผลของปฏิกิริยาการเปลี่ยนเมทานอลค่อนข้างไม่แตกต่างกัน แต่อย่างไรก็ตามยังพบออกไซด์ของเหล็กและออกไซด์ของโลหะอื่นๆปนเปื้อนอยู่ในผลึกที่สังเคราะห์ได้ ซึ่งมีผลต่อการเลือกเกิดผลิตภัณฑ์ในปฏิกิริยาการเปลี่ยนเมทานอล

ภาควิชา.....วิศวกรรมเคมี.....
สาขาวิชา.....วิศวกรรมเคมี.....
ปีการศึกษา.....2544.....

ลายมือชื่อนิสิต.....
ลายมือชื่ออาจารย์ที่ปรึกษา.....
ลายมือชื่ออาจารย์ที่ปรึกษาร่วม.....
ลายมือชื่ออาจารย์ที่ปรึกษาร่วม.....

#4270481021: MAJOR CHEMICAL ENGINEERING
KEY WORD: ZEOLITE BETA / FLY ASH / SINTHESIS

PANUSIT TURATUM: SINTHESIS ZEOLITE BETA FROM LIGNITE FLY ASH. THESIS ADVISOR: SUPHOT PHATANASRI, D.Eng, THESIS CO-ADVISOR: PROF. PIYASAN PRASERTHDAM, Dr.Ing. and ASST. PROF. METTA CHAREONPANICH, D.Eng. 111 pp. ISBN 974-03-1321-3

The optimum conditions of synthesis of zeolite beta from lignite fly ash were investigated. The parameters studied were stirring and aging temperature, $TEAOH/SiO_2$ mole ratio and Si/Al atomic ratio. The temperatures of stirring stage effected on the crystallinity of zeolite beta synthesized from lignite fly ash. During the crystallization, the temperature of aging with stirring and crystallization without stirring stage should be the same temperature since changing of the temperature effected on distribution of crystal size. The optimum aging and crystallization temperature were 140^{o}C. The optimum $TEAOH/SiO_2$ mole ratio was 0.5 and Si/Al atomic ratio was 50. This condition gave the highest crystallinity of zeolite beta synthesized from lignite fly ash (about 98% crystallinity) and BET surface area about 630 m^2/g and uniform crystal size of 0.25 μm. At this condition, the characteristics of zeolite beta synthesized from lignite fly ash are not much different from commercial zeolite beta which has BET surface area and average crystal size about 0.5 μm and 700 m^2/g, respectively. Furthermore, result of methanol conversion reaction is not quite different. However, there were Fe_2O_3 and other metal oxides presented in obtained crystal which effect to the product selectivity of methanol conversion reaction.

Department……Chemical Engineering.…. Student's signature…….
Field of study…….Chemical Engineering…. Advisor's signature……
Academic year…….2001……... Co-advisor's signature……
Co-advisor's signature ……...

ACKNOWLEDGEMENT

The author would like to sincerely thank and express his gratitude to Dr. Suphot Phatanasri, his advisor, for his continuous guidance, enormous number of invaluable discussions, helpful suggestions and warm encouragement. He wishes to give his gratitude to Professor Dr. Piyasarn Praserthdam and Assistant Professor Metta Chareonpanich, the thesis co-advisor, for their kind guidance and encouragement. In addition, he is also grateful to Professor Dr. Wiwat Tanthapanichakoon and Dr. Aticha Chaisuwan for serving as chairman and member of the thesis committee, respectively, whose comments are especially helpful.

Most of all, the author would like to express his highest gratitude to his parents for their inspiration and encouragement during his research.

Special thanks to petrochemical laboratory members who had encouraged and guided him over the years of his study.

CONTENTS

PAGE

CONTENTS (Cont.)

PAGE

LIST OF TABLES

TABLE **PAGE**

LIST OF FIGURES

FIGURE **PAGE**

LIST OF FIGURES (Cont.)

FIGURE **PAGE**

LIST OF FIGURES (Cont.)

FIGURE **PAGE**

LIST OF FIGURES (Cont.)

FIGURE **PAGE**

CHAPTER I

INTRODUCTION

The need of electric power has resulted in the construction of electricity generating plants at Mae Moh district in Lam Pang province in the north of Thailand, because there is the great reserve of lognite, which can used as the solid fuel in electricity generating plants. This causes the increase of coal consumption and consequently increased combustion waste generation. In a production of electricity, the coal are pulverized as powder and blown into a furnace by high velocity hot air. The pulverized coal is burnt, while it is floating at the temperature of 900-1200°C, which is higher than a melting point of almost minerals in the coal and cause the transformation of physical and chemical properties. Amounts of fly ash and slag are generated as a waste from the result of the high coal consumption and the high mineral matter content of coal, although high combustion efficiencies are reached in power station [15]. The fly ash production can be estimated as 3,000 $tday^{-1}$ for 2,625 MW power station with a normal coal consumption of 12,000 $tday^{-1}$to produce enough domestic electricity [10].

Fly ash is generally hazardous in nature therefore, many technologies have been developed for the disposal treatment, utilization of the special waste. At least a half of fly ash is disposed of by landfills, which become increasingly expensive and brings about environmental pollution. The another way is the use of fly ash in agriculture, because it contains alkaline oxides, sulfur, plant nutrients and use as a soil additive to decrease acidity and to promote root growth [15]. The other is the use of fly ash as the filler in concrete [1,22].

It should be recognized that, where the demand for industrial and domestic energy results in the production of large volumes of fly ash, these should not only be disposed of safely to prevent environmental pollution but should wherever possible be treated as a valuable resource. Nevertheless, given the potential industrial value of some of fly ash, other application must be investigated to enhance the value of products and to recycle the high fly ash output. Some authorities forecast fly ash

volumes of more than treble the current world output to some 800 x 10^6 tons by the year 2010 [1,22].

The typical fly ash is an agglomerated microspheres (cenospheres (hollow pheres) and pleurospheres (smaller spheres)) of 1-100 μm in diameter. These microsheres are composed of Si and Al as the major elements and minor amounts of Fe, Na, K, Ca, P, Ti, and S. The major compounds are aluminosilicate (glass) and other crystalline minerals are also present such as mullite, quartz, lime anhydrite and feldspars [1,15,20,22]. These chemicals make fly ash as a very suitable and economical starting material for zeolite synthesis and this is one alternative. Accordingly, a new field open up for research on industrial applications of fly ash.

At present, the environmental pollution becomes a very serious problem, because the growing up of industries bring about the pollution to the environment directly. Therefore, this problem must be realized and solved urgently. Zeolites are one alternative that has been studied to apply the solution to this problem because zeolites are the porous materials having high surface area, which are suitable to use as the adsorbents and they have cation-exchange properties. Accordingly, zeolites were brought to apply to many industries such as water treatment, detergent production and the use of zeolites as the catalysts in petroleum and petrochemical industries. There are many zeolites used in petrochemical industry such as ZSM-5, Y and zeolite beta. ZSM-5 zeolite is generally used as the catalyst in catalytic cracking and reforming consequently [2,6,19]. Especially, zeolite beta is the interesting zeolite, which has been studied as the catalyst in petrochemical reactions. Zeolite beta is used as the catalyst in the isomerization of C_4-C_7 hydrocarbons to gasoline fraction with increasing octane number [8,12], the transalkylation of xylenes [17], and the condensation of benzene and formaldehyde [3].

Recently, several researches have reported the preparation of zeolite from fly ash, the study deals with the synthesis of zeolite by alkaline activation of fly ash as a function of temperature, compositions and concentration of solution in opened and closed system. The results show that zeolite formation depends on the reaction conditions [5,7,11,15,16,20].

Therefore, this research has been studied the synthesis of zeolite beta from fly ash that can be the feasible to produce zeolite beta from fly ash in industrial scale. This present work is arranged as follows:

Chapter II presents the literature reviews of investigation the synthesis of zeolite Beta from fly ash and the applications.

Chapter III presents the theoretical consideration on zeolite Beta and fly ash.

Following by the description o experimental systems and the operational procedures in chapter IV.

The experimental results obtained from a laboratory scale reactor and standard measurement are reported and discussed in chapter V.

Chapter VI gives overall conclusions emerged from this work and presents some recommendations for any future works.

Finally, the sample of calculation of catalyst preparation, calculation of crystallity percent and data of experiments are including in appendix at the end of this thesis.

The Objective of this Study

To study the synthesis of zeolite beta from lignite fly ash by hydrothermal process

The Scope of this Study

1. To study the synthesis of zeolite beta from lignite fly ash by hydrothermal process
2. To study and elucidate the optimum conditions of the synthesis of zeolite beta from lignite fly ash as the function of following parameters:
    2.1 The temperature of aging with stirring stage (80-135°C)
    2.2 The temperature of crystallization without stirring stage (110-150°C)
    2.3 The Si/Al mole ratio of mixture (5-100)
    2.4 The amounts of template added into the solution ($(TEAOH/SiO_2)$ = 0-0.75)
3. To characterize by following method:
    3.1 Determining chemical compositions of fly ash by X-Ray Fluorescence (XRF)
    3.2 Determining the structure of zeolites by X-Ray Diffraction (XRD)
    3.3 Determining the functional group in zeolites by Infrared Spectroscopy (IR)
    3.4 Determining shape and size of zeolites crystals and fly ash by Scanning Electron Microscope (SEM)
    3.5 Determining surface areas of zeolites by BET Surface Area Measurement

CHAPTER II

LITERATURE REVIEWS

From the past, the synthesis of zeolite had focused on studying to find economical materials to decrease the cost of the zeolite synthesis. Therefore, many authors had the effort to use natural resources such as kaolinite and montmorilloite as the starting materials . At present, the synthesis of zeolite have focused on studying to try to use the waste such as fly ash as the starting material of the zeolite synthesis.

E.B. Drag et al. [5] studied the synthesis of zeolite from kaolinite, halloysite and montmorillonite. They found that at SiO_2/Al_2O_3 molar ratio in gel changed with in the limits from 2.00 to 19.8, A, X and Y zeolite were crystallized from halloysite, kaolinite and montmorillonite consequently.

S. Phumethum and V. Siriadhul [14] studied the synthesis of zeolite type A from kaolinite at the optimum condition obtained from the synthesis of A zeolite from chemicals; aluminium hydroxide ($Al(OH)_3$) and sodiumsilicate (Na_2SiO_3). Before synthesized zeolite A, kaolinite was prepared by calcining at 700°C for 3 h to obtain metakaonite. Calcined kaolinite was stirred with 50 wt%/vol NaOH at 95°C. After a half hour, added with warm distilled water and left for one and a half hour to crystallize zeolite A. The obtained A zeolite was characterized by IR, XRD and SEM.

R. Yingyuad and N. Shinaphan [23] studied zeolite synthesis from Kaolinite by hydrothermal process and studied the influence of synthesis parameters on the formation of zeolite crystals. The parameters were pH of solvent, Si/Al molar ratios by modifying pH of solvent (3,5,7,9 and 12). By using distilled water as the solvent, analcime was crystallized at pH of 12, which had the maximum amounts of Na and quartz was crystallized at pH of 3, 5, 7, 9. The use of ethanol as the solvent, at pH of 12 quartz was crystallized and also the unknowns were presented and quartz was crystallized at the other pH too. Furthermore, by modifying Si/Al molar ratio of 2.233, quartz was crystallized, and at Si/Al molar ratios of 40 and 400, quartz was not crystallized only but unknown amorphous was also presented.

X. Querol et al. [15] studied the synthesis of zeolite from fly ash by alkaline hydrothermal activation. High-Fe fly ash from Teruel power station in NE Spain was the starting material. The activation was performed by 0.1 M NaOH and KOH solution in the closed system. Zeolite formation was studied as the function of temperature (60 and 150°C), reaction time (24, 48, and 336 h) and sample/solution ratio (30,60,100, and 200 g/l). The synthesized zeolitic products were phillipsite, merlinaite, analcime, NaP1 zeolite and unknown. Other identified reaction products were portlandite and bayerite. The activated material in fly ash was mainly glass and quartz, the highest zeolite synthesis efficiency was 75%.

X. Querol et al. [16] studied the synthesis of zeolite from fly ash. Fly ash was activated by NaOH and KOH solution in closed system. The zeolite conversion was studied as a function of temperature (150-200°C), reaction time (8-100 h) and solution concentration (0.1-1 M). The estimated pressure during activation ranged from 0.48 MPa at 150°C to 1.55 MPa at 200°C. The activation was performed using a sample concentration of 0.055 gm/L. The synthesized zeolites were NaP1, NaP derivatives (mainly sodalite hydrate), analcime, gmelinite and nepheline hydrate after NaOH activation, and phillipsite after KOH activation. Subsequent experiments focused on short reaction times for high conversion efficiencies and monomineral synthesis of zeolite. High synthesis efficiencies for NaP1 zeolite and analcime were obtained with the fly ash types studied. The results highlight the importance of the mineralogical composition of the fly ash. Fly ashes with very similar SiO_2/Al_2O_3 ratios show different zeolites synthesis behavior under the same activation conditions. These differences could be attributed to different SiO_2/Al_2O_3 ratios of the glass matrix inferred from the differences in mineralogy at the same bulk chemical composition.

E. Lopez-Salinas et al.[11] studied the zeolitization of fly ash into NaP faujasite-type zolites were carried out. After incorporating Cu with CO. Thus for example, 306 wt.% Cu-impregnated NaP and faujasite-type zeolites show 47 and 36 mol% conversion of NO, respectively, at 230^{o}C. the untreated fly ash was almost inactive in this reaction.

M. Samran and M. chareonpanich [18] studied the synthesis of zeolite from lignite fly ash from electricity generating plant at Mae Moh in Lam Pang in the north of Thailand by hydrothermal process. The alkaline activation by using NaOH solution, the reaction was carried out at the initial pressure of 4.8 kPa and reaction time of 24, 72 and 120 h. At pH was about 13 by using 1 M NaOH, P zeolite was obtained at the reaction time of 72 and 120 h.

The conversion of fly ash into zeolites by incubation of the fly ash with alkaline solutions which well known process however usually results in a zeolitic product, which still contains significant amounts of residual fly ash. Therefore, G. G. Hollman et al. [7] modified the method to two-step process by which part of silicon in fly ash can be used for the synthesis of 85 g pure zeolite per kg of fly ash prior to the residual being converted into zeolite by the tradition method. The cation exchange capacities ranged from 3.6 to 4.3 meq/g for the pure zeolites and from 2.0 to 2.5 meq/g for the zeolites containing residual fly ash. Tests showed that the pure zeolites are suitable for the removal of ammonia and heavy metal ions from waste water.

X.S. Zhao et al. [28] studied the effect of aging and seeding on the formation of zeolite Y from coal fly ash. They found that zeolite Y was selectively synthesized by treating Tarong fly ash in hydrothermal system. The effects of aging and seeding on the formation of the resultant phases, crystallisation kinetics, and gel chemistry of Si and Al were investigated. Most of the Si and Al components in Tarong fly ash could be effectively transformed into zeolite Y in presence of seeds but not the mineral phase, like mullite. The maximum crystallinity of zeolite Y obtained was 72%. Crystallization of zeolite materials from fly ash is quite different from that of normal zeolite synthesis because the sources of Si and Al are relatively less reactive other cations (e.g., K^+, Mg^+) are present in fly ash. Zeolite P is a competitive phase present in the resulting products that could be eliminated by employing the seeding method. NMR study demonstrated that aging plays an important role in enhancing the hydrothermal condition during which both Si and Al in fly ash dissolved into a basic solution and reacted to form ring-like structures, and further to zeolite materials. Seeding can selectively induce the formation of zeolite Y and eliminate the processes of induction and nucleation.

The mesoporous aluminosilicate had been also studied by H. L. Chang et al [26]. Mesoporous aluminosilicate in the hexagonal phase (MCM-41) has been synthesized from fly ash solution and cations cetyltrimethylammonium bromide (CTAB) surfactants. The study provide direct evidence that and MCM-41 aluminosilicate with a homogeneous chemical composition of Si/Al = 13.4 can be prepared with cationic surfactant. The results indicate that coal combustion byproducts can be utilized for producing mesoporous molecular sieves even though they contain significant amounts of impurities.

The effect of fly ash particle size on the synthesis of zeolites from coal fly ash was investigated by F. Kunihiro et al. [24], and also proposed and formulated the formation mechanism of zeolite. It was found that the treatment time for the zeolites to synthesize decreased with decreasing feed fly ash particle size. When the feed size is small, both phillopsite and hydroxysodalite were synthesized by hydrothermal treatment with NaOH solution. Only phillipsite was synthesized when large fly ash particles were used. The zeolite from the fly ash having 2.1 μm mass median diameter indicated the maximum NH_4^+-adsorption capacity. The change in liquid ion concentrations calculated by the newly proposed model agreed with the experimental results, it was assumed that dissoluble silica is contained by about twice the mass of dissoluble alumina in the large fly ash particles, while in the case of small ones, they were almost equal.

Beside coal fly ash, municipal incinerator fly ash was used as the raw material of zeolite synthesis. G.C.C. Yang and T.Y. Yang [25] studied the synthesis of zoelite-like materials from a municipal incinerator fly ash (MIFA) was carried out by means of hydrothermal processing. In this investigation, conversion of MIFA to zeolite-like materials was conducted in reaction bombs that were subjected to heating in a rocking chamber. Aqueous NaOH was used as a mineralizer to assist the conversion reaction. Experimental parameters studied include the mineralizer concentration, solid/liquid (i.e., MIFA/mineralizer) ratio, reaction time, and operating temperature. Powder patterns of X-ray diffraction analysis have shown that several types of zeolite such as gismondine and gmelinite were successfully synthesized under certain experimental conditions. Therefore, it is technically feasible to synthesis zeolites from MIFA.

The other natural materials were used to synthesize or upgrade to be zeolite such as clinoptilolite, which coexcists with quartz and feldspars. S.J. Kang et al.[27] studied hydrothermal treatment of low-grade Korean natural zeolite with NaOH solution. The low-graded Korean natural zeolite in which clinopotilolite coexists with quartz and feldspars was treated hydrothermally with 3, 4 and 5 M NaOH solutions during different times raging from 4 to 40 h, either with or without fusion with NaOH powder at 550^{o}C during 2 h as a pretreatment. Zeolite Na-P, zeolite Na-X and hydroxysodalite were identified as the reacted products, depending on the reaction conditions such as NaOH concentration and reaction time. The fusion with NaOH powder prior to the hydrothermal reaction brought about zeolization of feldspars in the starting material, whereas it hardly occurred in the hydrothermal reaction without the fusion treatment.

From the reviews, fly ash and other natural materials were used as the source of Si and Al in zeolite synthesis such as zeolite A, P, Y, ZSM-5 and MCM-41, etc. It was shown that fly ash can be also used as the raw material in the synthesis of zeolite Beta by hydrothermal processing because fly ash has SiO_2 and Al_2O_3 as main conpositions.

CHAPTER III

THEORY

3.1 Fly Ash

The term “fly ash” is often used to describe any fine particle material precipitates from the stack gases of industrial furnaces burning solid fuels. In the electricity production, fly ash is generated from the pulverized coal sent into and burnt in power stations in order to generate the heat required to turn water into steam, which can be used to drive steam turbine to generate electricity. Pulverization of coal for the large furnaces used in power station boilers creates an immediate, urgent problem; dry fly ash has to be collected from the stack gases by mechanical or electrostatic separators. Each year, Mae Moh electricity generating plants produce the fly ash as the waste, which can be estimated about 10,000,000 tons [10].

3.2 Definition and Specifications of Fly Ash

Fly ash is a solid, fine-grained material resulting from the combustion of pulverized coal in power station furnaces. The materials collected in mechanical or electrostatic separators. The term fly ash is not applied to the residue extracted from the bottom of boilers.

Fly ashes may be sub-divided into two categories, according to their origins:

- Class F: Fly ash normally produced by burning anthracite or bituminous coal.
- Class C: Fly ash normally produced by burning lignite or subbituminous coal. Some Class C fly ashes may have lime contents in excess 10 %.

Many other forms of classification can be accepted, e.g. classification according to carbon content, SiO_2 reactivity, SiO_2 solubility, e.g. [1,22].

3.3 Mineralogical Composition of Fly Ash

The chemical and mineralogical composition of fly ashes depends upon the characteristics and composition of coal burned in the power plant. Owing to the rapid cooling of the material, fly ashes are composed mainly (50-90%) of mineral matter in the form of glassy particles. A small amount of ash occurs in the form of crystals. Unburned coal is collected with the fly ash particle of carbon, which may constitute up to 16% of the total, depending on the rate and temperature of combustion, the degree of pulverization of the original coal, the fuel/air ratio, the nature of the coal being burned, etc. Low-angle X-ray diffractometry can be used to ascertain the glass phase.

Infrared and Mössbauer Spectroscopy, X-ray diffraction and other specialized techniques provide powerful tools for researching the crystalline phases in fly ashes. The most important minerals found in fly ashes from bituminous coal are:

- Magnetite	0.8-6.5%
- Hematite	1.1-2.7%
- Quartz	2.2-8.5%
- Mullite	6.5-9.0%
- Free calcium oxide	up to 3.5%

Other minerals like wüstite, goethite, pyrite, calcite, anhydrite and periclade range from trace amounts to 2.5%.

3.3.1 Chemical Composition of Fly Ash

Fly ashes are particularly rich in SiO_2, Al_2O_3, and also contain other oxides such as CaO, MgO, MnO, TiO_2, Na_2O, K_2O, SO_3, etc.

Fly ashes can be sub-divided into four groups, depending on the percentage of main compounds.

Type I

SiO_2	>50%
$Al_2O_3 + Fe_2O_3$	medium
CaO	< 7%
Other components	small quantities

Type II

SiO_2	35-50%
Al_2O_3	high
Fe_2O_3	medium
CaO	more than type I

Type III

SiO_2	< 35%
CaO	very high
$Al_2O_3 + Fe_2O_3$	
Other components	wide differences, but lower than Type I and Type II

Type IV

SiO_2	very low
CaO	very high
Free CaO	
$CaSO_4$	
$Al_2O_3 + Fe_2O_3$	
Other components	low

The color of fly ashes depends on the Fe_2O_3 and carbon contents, which can be brown up to gray. [1,22]

3.4 Granulometry

The fineness of fly ashes is commonly measured by sieve analysis, which can be performed using dry or wet methods. Other techniques are also utilized. Generally speaking, it is important to know the amount of material retained by 200, 150, 87 and 44/45 micron sieves.

In general, the amount of fly ash retained on the 80 μm sieve ranges from 6 to 25%, on the 50 μm sieve from about 16 to 40%, and on the 45 μm sieve from about 3 to 14% (all mass percentages).

Optical and scanning electron microscopy of fly ashes have shown that these can vary in size and shape, including fly ashes of spherical, rounded, irregular and angular shape. Spherical and rounded fly ashes vary in size from 0.5-200 μm. fly ashes of irregular and angular shape are usually but not necessarily larger.

A particle may be defined as a simple, continuous unit of solid (in the case of fly ash) or liquid material of larger than molecular dimensions. In certain cases, a particle may be formed by the agglomeration of a number of small unit, a phenomenon commonly encouraged in fly ashes.

Microscopic examination of fly ashes reveals a wide variety of particle sizes and shapes. Grain size may be varied from 0.2 to 200 μm, most particles being larger than 1 μm in size.

Particles are spherical, irregular or angular, etc., depending on the nature and granulometry of the coal burned and on the combustion conditions in the power plant. If the combustion temperature is low, the mineral ash fails to melt and the final shape is irregular. At high combustion temperatures, the mineral matter in the coal melts, forming hollow spheres referred to as cenospheres, sometimes containing a number of smaller spheres (pleospheres). At a combustion temperature of roughly 1500°C, the majority of particles are round-shaped and hollow, with smooth or rough surfaces.

Particle shape is an important parameter affecting a variety of processes, such as particle motion in a fluid medium, the formation of electrostatic charges, light scattering, etc. In the case of fine particles, spherical, cubic, flake, floc, platelet and irregular shapes are the most significant.

Recent SEM studied have confirmed this observation. In a few cases only, the spheres [22] as presented in Figure 3.1.

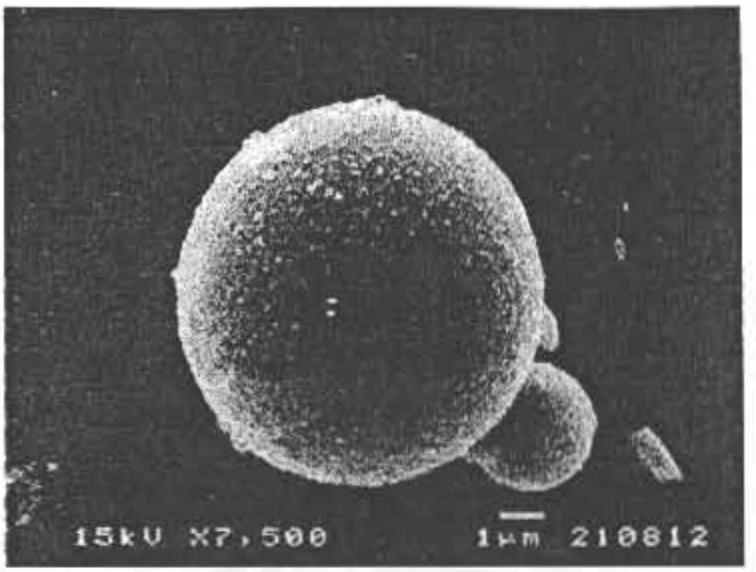

Figure 3.1 SEM photograph of fly ash

3.5 Zeolite

In 1756, Cronstedt, a Swedish mineralogist, discovered a new mineral, which visibly lost water when heated. Because of this easily observed intumescence he coined the word "zeolite" from two Greek words "zein" and " lithos", meaning "boiling stone", to name the new species. Cronstedt's mineral was later named stilbite.

This facile loss of water was shown to be reversible by Damuor in 1840 and, in 1858, Eichorn showed that the zeolite chabazite contained alkali and alkaline earth metals, which were capable of being reversibly replaced, i.e. the zeolite exhibited cation exchange properties. Analysis of zeolite minerals showed them to be aluminosilicates and their easy loss of water and cation exchange was evidence for the open nature of their structures, often likened to a sponge. The description "zeolitic water" has been widely used to describe loosely held water in any solid

The need for commercial water softeners prompted attempts to synthesize zeolites. These were not successful, althoughin 1862 St Claire Deville claimed to be

able to make levyne and de Schulten analcime in 1862. Lack of available, definitive, Characterization methods makes it difficult to confirm their work.

Ultimately the need was satisfied by the production of amorphous aluminosilicates, pioneered by Gans in a series of patents around 1900. These are the "permutite" materials and are still being produced. Permutite have often been describes and marketed as "zeolites", and this has created misconceptions in many elementary texts suggesting that they are widely used as commercial cation exchanges; in fact, it is only within the last decade that zeolites have been extensively used for this purpose, as will be described later. It is also unfortunate that elementary texts often ascribe the cation exchange properties of soils to the presence of zeolites. In fact this is a reflection of the soil clay mineral content and, although some soils do contain zeolites, this is comparatively rare.

Progress to 1925 was largely through mineralogical identification of new zeolite species but in this year Weigel and Steinhoff reported that chabazite sorbed water, methyl and ethyl alcohols, and formic acid but excluded acetone, ether, and benzene. The significance of this observation was expressed by McBain. Who described it as a "molecular sieving" effect in 1926. In 1930, Taylor solved the structure of analcime and Pauling published a series of seminal papers based upon single-crystal X-ray studies which showed how silicates and aluminosilicates were constructed form tetrahedral building blocks, i.e. the $[SiO_4]^{-4}$ and $[AlO_4]^{5-}$ units of structure. His work included the zeolite natrolite and the felspathoids sodalite and cancrinite, which are now known to have structures closely related to the zeolite minerals. Figure 3.2 [9] shows the Si/Al coordination tetrahedra and their linkage to create the chain-like element of structure identified in natrolite. The importance of Pauling's work was that it illustrated the way in which the tetrahedral units linked by sharing all corners to produce the three dimensional framework structures associated with the zeolite and felspathoid minerals. It is this regular and reproducible molecular architecture that confers on the zeolites their uniquely useful properties.

This was evident to R.M. Barrer who from the mid-1930s to the present has provided the scientific base upon which the current widespread industrial use of zeolites has been founded. His pioneering work on zeolite synthesis, ion exchange,

gas sorption, and structures, from both theoretical and practical standpoints, has spawned the continuing growth of zeolite science and technology encouraged by the discovery of their catalytic properties in early 1960s [9].

Figure 3.2 Si, AlO_4 tetrahedra linked as in the zeolite natrolite [9]

Zeolites can be viewed as solid analogues of such classical acids as sulfuric or aluminum chloride. These all have in common the ability to promote a large number of acid-catalysted reactions, including polymerization; cracking; isomerization of loefins, parafins and aromatics; alkylation of aromatics and parafins; transalkylation, and many others. Some reactions, such as gas oil cracking, are among the largest-scale catalytic processes.

Zeolites lend themselves very well to catalyst design for a variety reasons. Zeolites have well-defined pore system and large intracrystalline surface area [29,30] It was discovered in the late 1950s at the Mobil laboratories that catalytic reactions can take place inside these structures. This discovery marked the real beginning of zeolite cataysis.

Two aspects make zeolites unique. The intracrystalline surface is an inherent part of the crystal structure and hence topologically well defined, in sharp distinction to amorphous and even most crystalline solids whose outer surface may be considered

a crystal defect with atoms whose coordination number differs from atoms in the crystal. The second distinctive feature of zeolites is that the diameter of their pores is uniform and of similar magnitude as that of many organic molecules of interest. Molecular sieving and shape selectivity previously unknown with synthetic catalysts become possible.

The world's zeolite literature continues to grow at a rate of close to 100 publications per week. This is almost entirely devoted to synthetic materials of zeolite structure type, and has caused a reassessment of the strict mineralogical concept of zeolite as aluminosilicates containing mobile cation exchange and water molecules which promote the properties of cation exchange and reversible water uptake [6,9].

3.6 Structure of Zeolite

Zeolite are highly crystalline, hydrated aluminosilicates that upon dehydration develop in the ideal crystal a uniform pore structure having minimum channel diameters (aperture) of from about 0.3 to 1.0 nm. The size depends primarily on the type of zeolite and secondarily on the cations present and the nature of treatments such as calcination, leaching, and various chemical treatments. Zeolites have been of intense interest as catalysts for some three decades because of the high activity and unusual selectivity they provide, mostly in a variety of acid-catalyzed reaction. In many cases, but not all, the unusual selectivity is associated with the extremely fine pore structure, which permits only certain molecules to penetrate into the interior of the catalyst particles, or only certain products to escape from the interior. In some cases unusual selectivity seems to stem instead from constrains that the pore structure sets on allowable transition states, sometimes termed spacio-selectivity.

The structure of the zeolite consists of a three-dimensional framework of the SiO_4 and AlO_4 tetrahedra as presented in Figure 3.3 [9], each of which contains a silicon or aluminum atom in the center. In 1982, Barrer defined zeolites as the porous tectosilicates [29], that is, three-dimensional networks built up of TO_4 tetrahedra where T is silicon or aluminum. The oxygen atoms are sheared between adjoining tetrahedra, which can be present in various ratios and arrange in a variety of

ways. The framework thus obtained contains pores, channels, and cages, or interconnected voids.

A secondary building unit (SBU) consists of selected geometric groupings of those tetrahedral. There are sixteen such building units, which can be used to describe all of known zeolite structures; for example, 4 (S4R), 6 (S6R), and 8 (S8R)-member single ring, 4-4 (D6R), 8-8 (D8R)-member double rings. The topologies of these units are shown in Figure 3.4 [31]. Also listed are the symbols used to describe them. Most zeolite framework can be generated from several different SBU's. Descriptions of known zeolite structures based on their SBU's are list in Table 3.1 [32]. Both zeolite ZSM-5 and Ferrierite are described by their 5-1 building units. Offertile, Zeoite L, Cancrinite, and Erionite are generated using only single 6-member rings. Some zeolite structures can be described by several buildings. The sodalite framework can be built from either the single 6-member ring or the single 4-member ring. Faujasite (type X or type Y) and Zeolite A and be constructed using 4 ring or 6 ring building units. Zeolite a can also be formed using double 4 ring building units, whereas Faujasite cannot.

Zolites may be represented by the empirical formula:

$$M_{2/n} \cdot Al_2O_3 \cdot xSiO_2 \cdot yH_2O$$

or by a structural formular:

$$M_{x/n}[(Al_2O_3)_x(SiO_2)_y] \cdot wH_2O$$

Where the bracketed term is the crystallographic unit cell. The metal cation (of valence n) is present it produces electrical neutrality science for each aluminum tetrahedron in the lattice there is an overall charge of –1. Access to the channels is limited by aperture consisting of a ring of oxygen atoms of connected tetrahedra. There may be 4, 5, 6, 8, 10, 0r 12 oxygen atoms in the ring. In some cases an interior cavity exists of larger diameter in the aperture; in others, the channel is of uniform diameter like a tube [19].

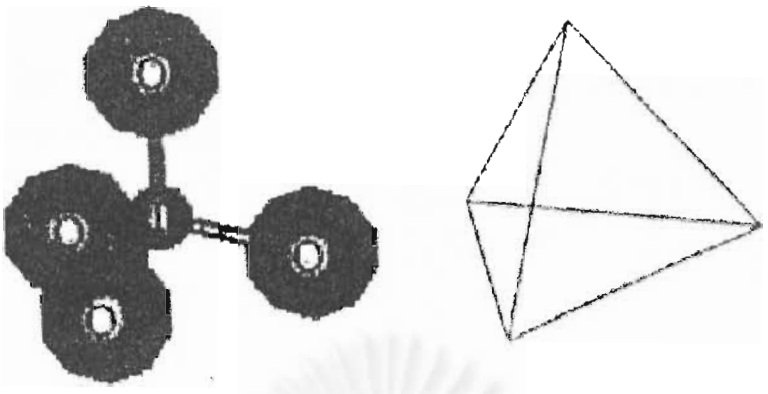

Figure 3.3 TO_4 tetrahedra (T = Si or Al) [9]

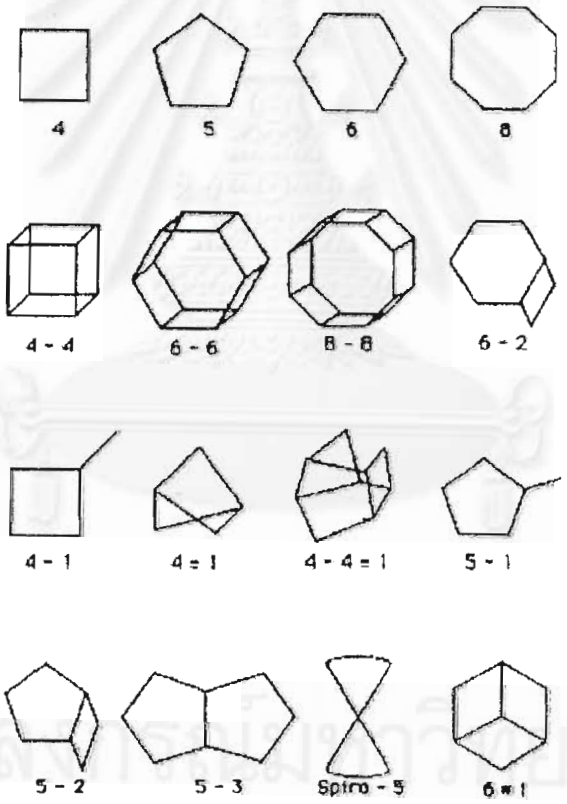

Figure 3.4 Secondary building units (SBU's) found in zeolite structures [32]

Table 3.1 Zeolites and their secondary building units. The nomenclature used is consistent with that presented in Figure 3.4 [32]

ZEOLITE	SECONDARY BUILDING UNITS								
	4	6	4	4-4	6-6	8-8	4-1	5-1	4-4=1
Bikilaite								X	
Li-A (BW)	X	X	X						
Analcime	X	X							
Yagawaralite	X		X						
Episibite								X	
ZSM-5								X	
ZSM-11								X	
Ferrierite								X	
Cachiardite								X	
Brewsterite	X								
Laumonite		X							
Mordenite								X	
Sodalite	X	X							
Henulandite									X
Stibite									X
Natrolite							X		
Thomsonite							X		
Edingtonite							X		
Cancrinite		X							
Zeolite L		X							
Mazzite	X								
Merlinoite	X		X			X			
Philipsite	X		X						
Zeolite Losod		X							
Erionite	X	X							
Paulingite	X								
Offretite		X							
TMA-E(AB)	X	X							
Gismondine	X		X						
Levyne		X							
ZK-5	X	X	X		X				
Chabazite	X	X			X				
Gmelinite	X	X	X		X				
Rho	X	X	X			X			
Type A	X	X	X	X					
Faujasite	X	X			X				

3.7 Category of Zeolite

There are over 40 known natural zeolites and more than 150 synthetic zeolites have been reported [33]. The number of synthetic zeolites with new structure morphologies grows rapidly with time. Based on the size of their pore opening, zeolites can be roughly divided into five major categories, namely 8-, 10-, and 12-member oxygen ring systems, dual pore systems and mesoporous system [2]. Their pore structures can be characterized by crystallography, adsorption, measurements and/or through diagnostic reactions. One such diagnostic characterization test is the "constraint index" test. The concept of constraint index was defined as the ratio of the cracking rate constant of *n*-hexane to 3-methylpenthane. The constraint index of a typical medium-pore zeolite usually ranges from 3 to 12 and those of the large-pore zeolites are the range 1-3. For materials with an open porous structure, such as amorphous silica alumina, their constraint indices are normally less than 1. On the index for erionite is 38.

A comprehensive bibliography of zeolite structures has been published by the International Zeolite Assosiation [33]. The structural characteristics of assorted zeolites are summarized in Table 3.2.

Zeolites with 10-membered oxygen rings normally possess a high siliceous framework structure. They are of special interest in industrial applications. In fact, they were the first family of zeolites that were synthesized with organic ammonium salts. With pore openings close to the dimensions of many organic molecules, they are particularly useful in shape selective catalysis. The 10-membered oxygen ring zeolites also possess other important characteristic properties including high activity, high tolerance to coking and high hydrothermal stability. Among the family of 10-membered oxygen ring zeolites, the MFI-type (ZSM-5) zeolite as presented in Figure 3.5is probably the most useful one. ZSM-5 zeolite has two types of channel systems of similar sized, one with a straight channel of pore opening 5.3x5.6 Å and the other with a tortuous channel of pore opening 5.1x5.5 Å. Those intersecting channels are perpendicular to each other, generating a three-dimensional framework. ZSM-5 zeolites with a wide range of SiO_2/Al_2O_3 ratio can easily be synthesized. High

siliceous ZSM-5 zeolites are more hydrophobic and hydrothermally stable compared with many other zeolites. Although the first synthetic ZSM-5 zeolite was discovered more than two decades ago (1972) new interesting applications are still emerging to this day. For example, its recent application in NO_x reduction, especially in the exhaust of lean-burned engine, has drawn much attention. Among various zeolite catalyst, ZSM-5 zeolite has the greatest number of industrial applications, covering from petrochemical production and refinery processing to environmental treatment.

Table 3.2 Structural characteristics of selected zeolites [34]

Zeolite	Number of rings	Pore opening Å	Pore/Channel structure	Void volume (ml/g)	D_{Frame}[a] (g/ml)	CI[b]
8-membered oxygen ring						
Erionite	8	3.6x5.1	Intersecting	0.35	1.51	38
10-membered oxygen ring						
ZSM-5	10	5.3x5.6 5.1x5.5	Intersecting	0.29	1.79	8.3
ZSM-11	10	5.3x5.4	Intersecting	0.29	1.79	8.7
ZSM-23	10	4.5x5.2	One-dimensional	-	-	9.1
Dual pore system						
Ferrierite (ZSM-35, FU-9)	10,8	4.2x5.4 3.5x4.8	One-dimensional 10:8 intersecting	0.28	1.76	4.5
MCM-22	12 10	7.1 Elliptical	Capped by 6 rings	-	-	1-3
Mordenite	12 8	6.5x7.0 2.6x5.7	One-dimensional 12:8 intersecting	0.28	1.70	0.5
Omega (ZSM-4)	12	7.4	One-dimensional	-	-	2.3
	8	3.4x5.6	One-dimensional	-	-	0.6
12membered oxygen ring						
ZSM-12	12	5.5x5.9	One-dimensional	-	-	2.3
Beta	12	7.6x6.4 5.5x5.5	Intersecting	-	-	0.6
Faujasite (X,Y)	12 12	7.4 7.4x6.5	Intersecting 12:12 intersecting	0.48	1.27	0.4
Mesoporous system						
VPI-5	18	12.1	One-dimensional	-	-	-
MCM41-S	-	16-100	One-dimensional	-	-	-

[a]Framework density

[b]Constraint index

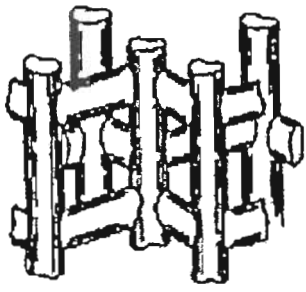

(a) channel pattern

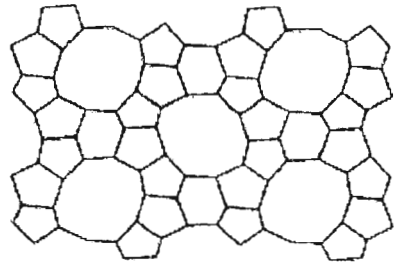

(b) framework projection

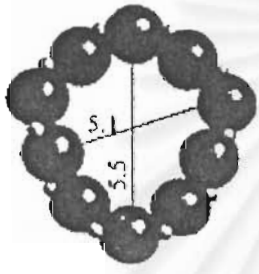

(c) tortous channel

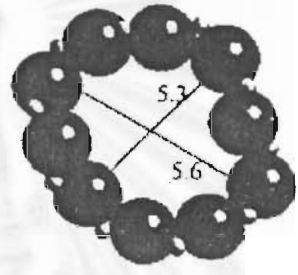

(d) straight channel

Figure 3.5 Structure of ZSM-5 [33]

Although the 10-membered oxygen ring zeolites were found to possess remarkable shape selectivity, catalysis of large molecules may require a zeolite catalyst with a large-pored opening. Typical 12-membered oxygen ring zeolites, such as faujasite-type zeolites , normally have pore opening greater than 5.5 Å and hence are more useful in catalytic applications with large molecules, forexample in trimethylbenzene (TMB) conversions. Faujasite (X or Y; Figure 3.6 [33]) zeolites can be synthesized using inorganic salts and have been widely used in catalytic cracking since 1960s. The framework structures of zeolite Beta and ZSM-12 are shown in Figure 3.6 [33] and Figure 3.7 [33], respectively.

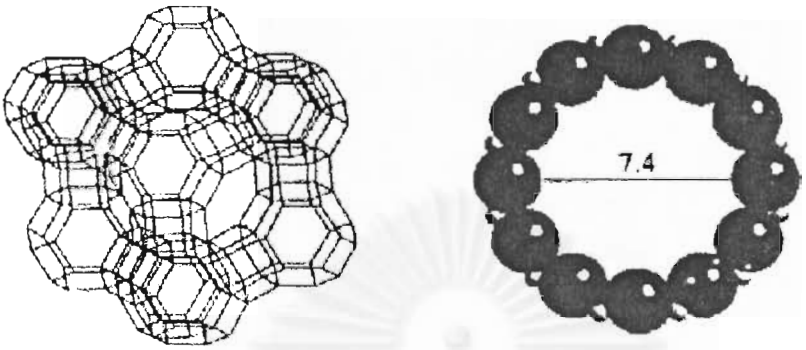

(a) framework structure (b) pore opening

Figure 3.6 Structure of Faujasite [33]

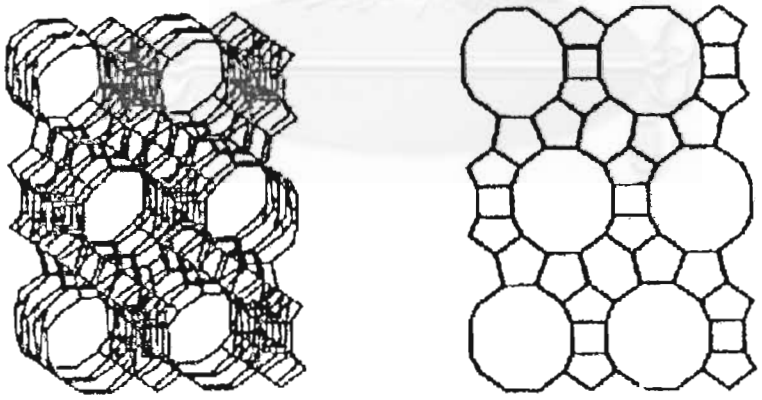

(a) framework structure (b) framework projection

Figure 3.7 Structure of zeolite beta [33]

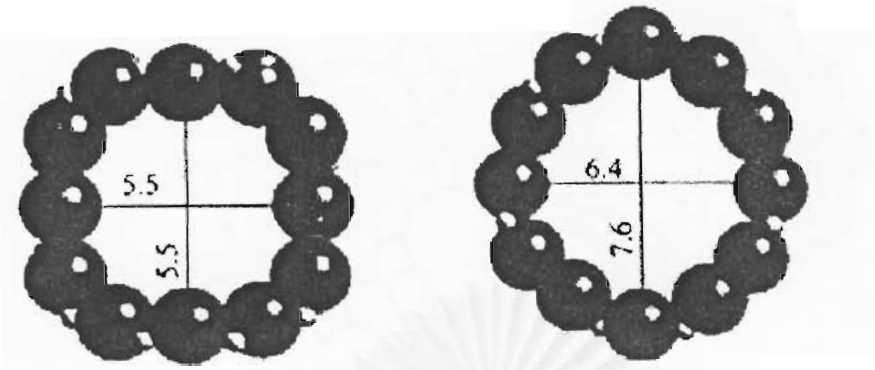

(c) tortous channel (d) straight channel

Figure 3.7 Structure of zeolite beta [33]

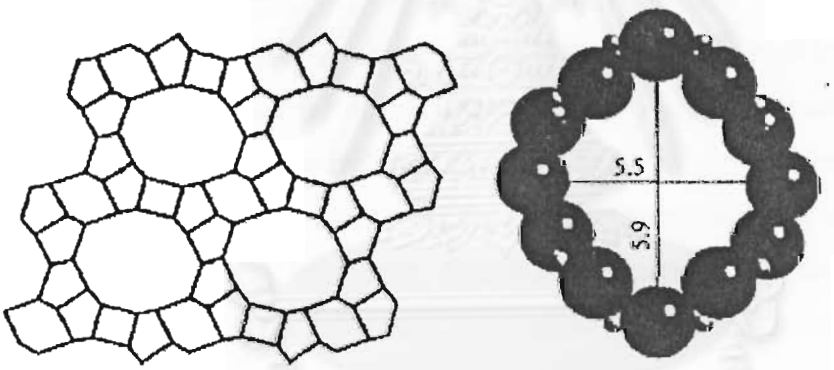

(a) framework projection (b) pore opening

Figure 3.8 Structure of zeolite ZSM-12 [33]

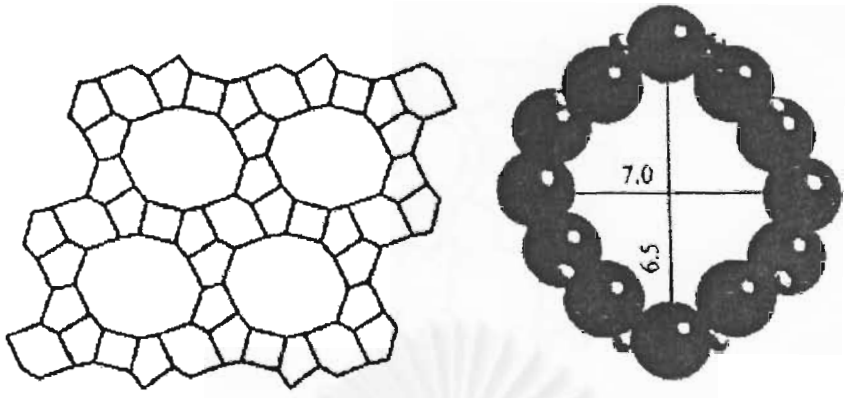

(a) framework projection (b) pore opening

Figure 3.9 Structure of Mordenite [33]

Zeolites with a dual pore system normally possess interconnecting pore channels with two different pore opening sizes. Mordenite is a well-known dual pore zeolite having a 12-membered oxygen ring channel with pore opening 6.5x6.7 Å which id interconnected to 8-membered oxygen ring channel with opening 2.6x5.7 Å (Figure 3.9 [33]). MCM-22, which was found more than 10 years, also possesses a dual pore system. Unlike Mordenite, MCM-22 consists of 10- and 12-membered oxygen rings (Figure 3.10 [33]) and thus shows prominent potential in future applications.

In the past decade, many research efforts in synthetic chemistry have been invested in the discovery of large-pored zeolite with pore diameter greater than 12-membered oxygen rings. The recent discovery of mesoporous materials with controllable pore opening (from 12 to more than 100 Å) such as VPI-5, MCM-41S undoubted will shed new light on future catalyst applications.

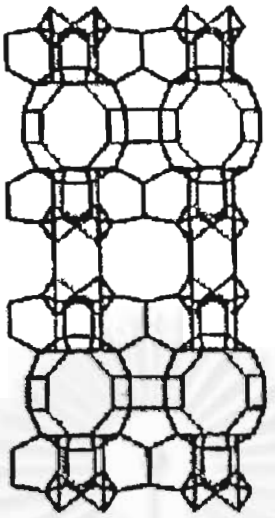

Figure 3.10 Framework structure of MCM-22 [33]

3.8 Zeolite Active Sites

3.8.1 Acid sites

Classical Brønsted and Lewis acid models of acidity have used to classify the active sites on zeolites. Brønsted acidity is proton donor acidity; a tridiagonally coordinated alumina atom is an electron deficient and can accept an electron pair, therefore behaves as a Lewis acid [35,36].

Ingenral, the increase in Si/Al ratio will increase acidic strength and thermal stability of zeolite [37]. Since the numbers of acidic OH groups depend on the number of aluminium in zeolites framework, decrease in Al content is expected to reduce catalytic activity of zeolite. If the effect of in crease in the acidic centers, increase in Al content, shall result in enhancement of catalytic activity.

Based on olectrostatic consideration, the charge density at a cation site increases with increasing Si/Al ratio. It was conceived that these phenomena are related to reduction of electrostatic interaction between framework sites, and possibly

to difference in the order of aluminum in zeolite crystal-the location of Al in crystal structure [36].

An improvement in thermal or hydrothermal stability has been ascribed to the lower density of hydroxyl groups, which id parallel to that of Al content [35]. A longer distance between hydroxyl groups decreases the probability of dehydroxylation that generates defects on structure of zeolites.

3.8.2 Generation of Acid Centers

Protonic acid centers of zeolite are generated in various was. Figure 3.11 depicts the thermal decomposition of ammonium-exchanged zeolites yielding the hydrogen form [32].

The Br∅nsted acidity due to water ionization on polyvalent cations, described below, is depicted in Figure 3.12 [38].

$$M^{n+} + xH_2O \longrightarrow M(OH)_x^{(n-x)} + xH^+ \quad (3.1)$$

The exchange of monovalent ions by polyvalent cations could improve the catalytic property. Those highly charged cations create very centers by hydrolysis phenomena. Br∅nsted acid sites are also generated by the reduction of transition metal cations. The concentration of OH groups of zeolite containing transition metals was note to increase by hydrogen at 2.5-450^{o}C to increase with the rise of the reduction temperature [38].

$$Cu^{2+} + H_2 \longrightarrow Co^0 + 2H^+ \quad (3.2)$$

$$Ag^+ + 1/2H_2 \longrightarrow Ag^0 + H^+ \quad (3.3)$$

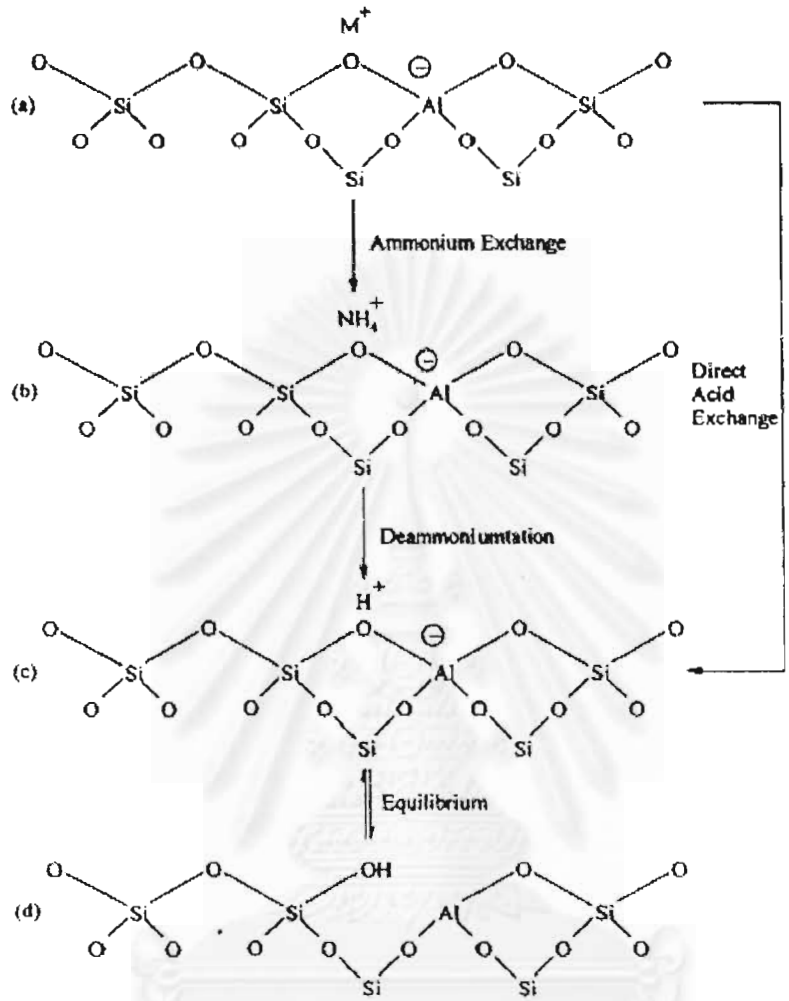

Figure 3.11 Diagram of the surface of a zeolite framework [32].

a) In the as-synthesis form M^+ either an organic cation or an alkali metal cation.

b) Ammonium in exchange produces the NH_4^+ exchanged form.

c) Thermal treatment is used to remove ammonia, producing the H^+, acid form

d) The acid form in (c) is in equilibrium with the form shown in (d), where is a silanol group adjacent to tricoordinate aluminium.

The formation of Lewis acidity from Brønsted acid sites is depicted in Figure 3.13 [38]. The dehydration reaction decreases the number of protons and increases that of Lewis sites. Brønsted (OH) and Lewis (-Al-) sites can be present simultaneously in the structure of zeolite at high temperature. Dehydroxylation is thought to occur in ZSM-5 zeolite above 500°C and calcinations at 800 to 900°C Produces irreversible dehydroxylation, which causes defection in crystal structure of zeolite.

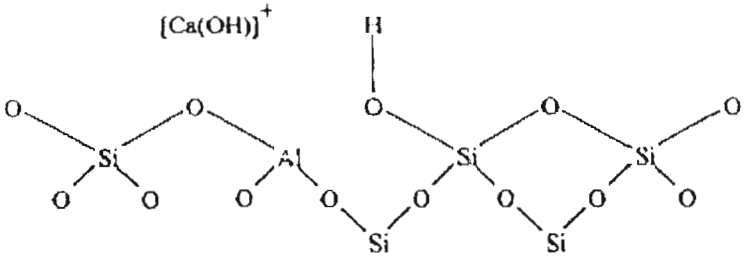

Figure 3.12 Water moluclues co-ordinated to polyvalent cation are dissiciated by heat treatment yielding Brønsted acidity [38].

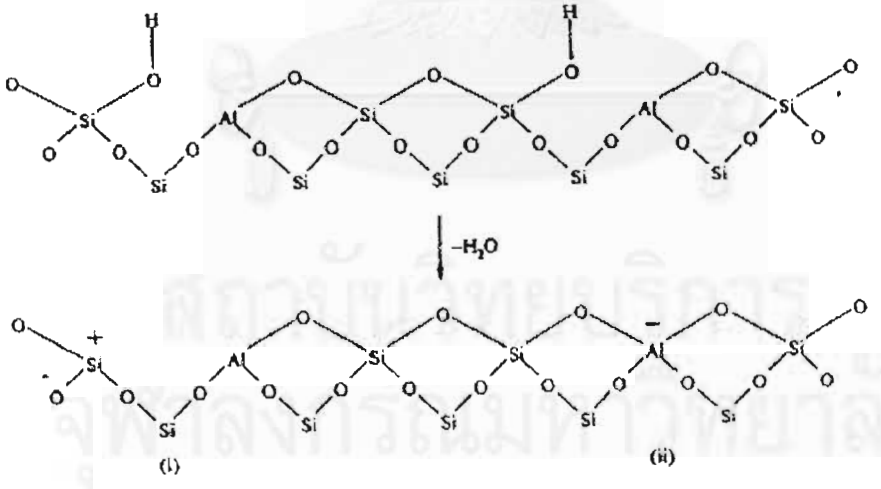

Figure 3.13 Lewis acid site developed by dehydroxylation of Brønsted acid site [38].

Dealumination is believed to occur during dehydroxylation, which may result from the steam generation within the sample. The dealumination is indicated by an increase in the surface concentration of aluminum on the crystal. Th dealumination process is expressed in Figure 3.14 [38]. The extent of dealumination monotonously increases with the partial pressure of team.

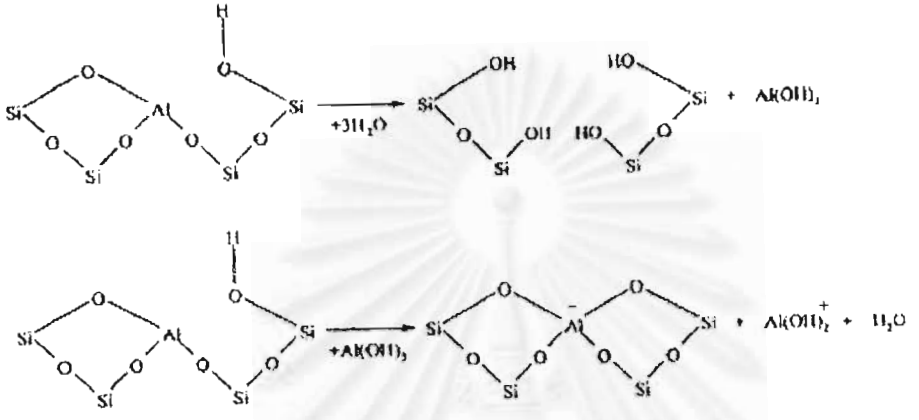

Figure 3.14 Steam dealumination process in zeolite [38]

The enhancement if the acid strength of OH groups is recently proposed to be pertinent to their interaction with those aluminum species sites tentatively expressed in Figure 3.15 [38]. Partial dealumination might therefore yield a catalyst of higher activity while severe steaming reduces the catalytic activity.

3.8.3 Basic Sites

In certain instances reactions have been shown to be catalyzed at basic (cation) site in zeolite without any influences from acid sites. The best-characterized example of this is that K-Y which splits n-hexane isomers at 500°C. The potassium cation has been shown to control the unimolecular cracking (β-scission). Free radial mechanisms also contribute to surface catalytic reactions in these studies.

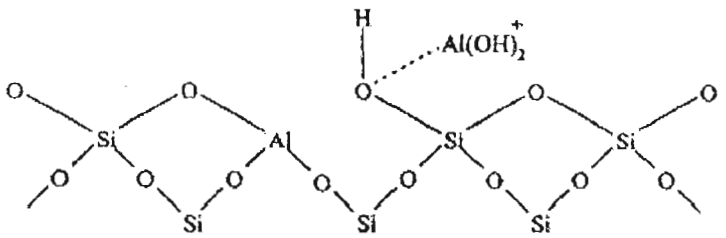

Figure 3.15 The enhancement of the acid strength of OH groups by their interaction with dislodged aluminum species [38]

3.9 Shape Selective

Many reactions involving carbonium intemediates are catalyzed by acidic zeolite. With respects to a chemical standpoint the reaction mechanisms are nor fundamentally different with zeolites or with any the acidic oxides. What zeolite add is shape selectivity effect. The shape selective characteristics of zeolites influence their catalytic phenomena by three modes: shape selectivity, reactants shape selectivity, products shape selectivity and transition states shape selectivity. These types of selectivity are illustrated in Figure 3.16 [32].

Reactants of charge selectivity results from the limited diffusibility of some of the reactants, which cannot effectively enter and diffuse inside crystal pore structures of the zeolites. Product shape selectivity occurs as slowly diffusing product molecules cannot escape from the crystal and undergo secondary reactions. This reaction path is established by monitoring changes in product distribution as a function of varying contact time.

Restricted transition state shape selectivity is a kinetic effect from local environment around the active site, the rate constant for a certain reaction mechanism is reduced of the space required for formation of necessary transition state is restricted.

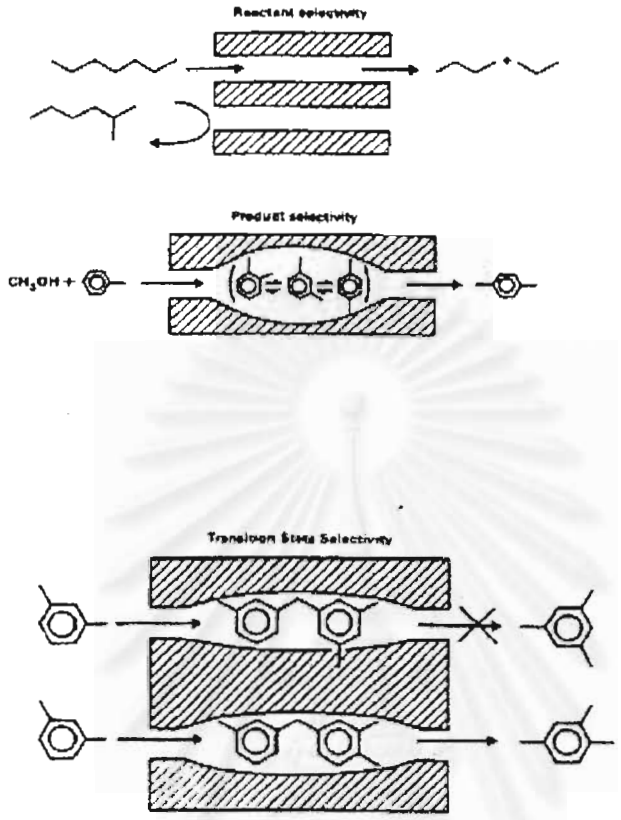

Figure 3.16 Diagram depicting the tree type of selectivity [32]

The critical diameter (as opposed to the length) of the molecules and the pore channel diameter of zeolites are important in predicting shape selective effects. However, molecules are deformable and can pass through opening, which are smaller than their critical diameters. Hence, not only size but also the dynamics and structure of the molecules must be taken into account.

3.10 Zeolite Synthesis

Zeolites are generally synthesizes by a hydrothermal process from a source of alumina (e.g., sodium aluminate or aluminium sulfate) and of silica (e.g., a silica sol, fumed silica, or sodium water glass) and an alkali such as NaOH, and /or a quaternary ammonium compound. An inhomogeneous gel is produced which gradually

crystallizes, in some cases forming more than one type of zeolite in succession. Nucleation effects can be important, and an initial induction period at near ambient temperature may be followed by crystallization temperature that may range up to 200° C or higher. The pressure is equal to the saturated vapor pressure of the water present.

The final product depends on a complex interplay between many variables including SiO_2/Al_2O_3 ratio in the starting medium, nucleating agents, temperature, pH, water content, aging, stirring, and the presence of various inorganic and organic cations. Much remains to be learned about how the initial reaction mixture forms the precursor species and how these arrange into the final crystalline products. A key concept is that the cations present give rise to a templating action, but clearly the process is more complex.

Bauer and coworkers in the early 1960s developed the use of reaction mixtures containing quaternary ammonium ions or other or other cations to direct the crystallization process. In their work and succeeding studies, a primary motivation was to attempt to synthesize zeolites with large apertures than X and Y. This did not occur, but instead organic species were found to modify the synthesis process in a variety of ways that led to discovery of many new zeolites, and new methods of synthesizing zeolites with structures similar to previously know zeolites.

The mechanism of action of the organic species is still controversial. It was originally thought to be primarily a templating effect, but later it was found that a least some of zeolites could be synthesized without an organic template. Further,

organic species other than quaternary ammonium compounds had directing effects not readily ascribed to their size or shape. However, an important result was the zeolites of higher SiO_2/Al_2O_3 ratio than before could be synthesized. Previously, only structures with SiO_2/Al_2O_3 ratios of about 10 or less could be directly forms, but with organic additives, zeolites with ratio of 20 to 100 or more can be directly prepared.

After synthesis the zeolite are washed, dried heated to remove water of crystallization, and calcined in air, e.g., at about 550°C. Organic species are also thus

removed. For most catalytic purpose, the zeolite is converted into acidic form. For some zeolites this can be achieved by treatment with aqueous HCl without significantly altering the framework structure. For other zeolites Na^+ is replaced with NH_4^+ via an ammonium compound such as NH_4OH, NH_4Cl or NH_4NO_3. Upon heating NH_3 is driven off, leaving the zeolite in the acid form. For some reaction a hydrogenation component such as platinum or nickel is introduced by impregnation or ion exchange [19].

3.11 Zeolite beta

Zeolite beta is an old zeolite discovered before Mobil began the "ZSM" naming sequence.Zeolite beta was initially synthesized by Wadlinger et al. [4] using tetraethylammonium hydroxide as the organic template. The structure of zeolite beta was recently determined because the structure is very complex and interest but was not high until it becomes important for some dewaxing process.

The tetrahedral framework structure of zeolite beta is disordered along the [001]. The disordered structure and the three simple ordered polytypes are related through layer displacements on 001 planes. These polytypes have mutually perpendicular 12-ring channel systems, and zeolite beta exhibits characteristic properties of the presence of 12-member-ring channels and the intersecting 6.5x5.6 and 7.5x5.7 Å. The smaller building units are double six-ring units connected by two four-rings and four five-rings unit. These are connected to form chains along the [001] direction. Polytypes A and B contain 9 unique T sites, whereas polytype C contain 32 [21].

The chemical composition of zeolite beta is:

$$(TEA,Na)_2O \cdot Al_2O_3 \cdot 5\text{-}100SiO_2 \cdot 4H_2O$$

This zeolite may offer interesting opportunities as a catalyst, since it combines three important characteristics: large pore (12 membered oxygen ring), high silica to alumina synthesis ratio, three dimension network or pores. In addition, The

dimensions of on type of pores (5.5 Å) can give a certain level of shape selectivity. This has been suitable for isomerization of C_4-C_7 hydrocarbons to gasoline fraction with increasing octane number [8,15], to transalkylation of xylenes [17], and to condensation of benzene and formaldehyde [3].

CHATER IV

EXPERIMENT

The synthesis of zeolite beta from fly ash and its characterization are explained in the following section.

4.1 Preparation of zeolite Na, NH_4 and H-beta

The preparation procedures and reagents used are shown in Figure 4.1 and Table 4.1, Table 4.2, Table 4.3 (for calculation see Appendix A-1).

In the synthesis of zeolite beta from fly ash, because fly ash used as the source of Si and Al is solid powder and after stirring reagents together they were not homogeneous therefore gel composition can not be assessed. The stirring of gel was important since without stirring cause dissolution and deposition of fly ash together while they were heated and aged in autoclave. This is the first stage called aging with stirring stage. And the second stage is crystallization without stirring stage, this stage was unstirred therefore crystal can be crystallized entirely. The optimum temperatures at two stages were studied. However, at aging with stirring stage, crystallization of zeolite crystals may be occurred.

In the synthesis of zeolite beta, tetraethylammonium was used as organic template and source of Si were effected on characterizations of obtained zeolite beta.

Therefore, there were four parameters: 1. Temperatures at aging with stirring stage, 2. Temperature at crystallizing without stirring stage, 3. TEAOH/SiO_2 mole ratio and 4. Si/Al atomic ratio.

4.1.1 Reagents

Zeolite beta was prepared by using the following reagents: untreated fly ash (from Mae Moh generating plants) as the source of SiO_2 and Al2O3, cataloid as a

source of SiO_2 (SiO_2 30% by weight aqueous solution), tetraethylammonium hydroxide (Fluka, 40% by weight aqueous solution), sodium hydroxide (MERCK, analytical grade), potassium chloride (AJAX CHEMICALS, analytical grade), sodium chloride (MERCK, analytical grade).

Table 4.1 Reagents used for the preparation of zeolite Na-beta for the study of effect of the temperature at aging with stirring stage and crystallization without stirring stage

Reagents	Weights (g)
Fly ash	1.000
TEAOH	46.018
Cataloid for Si/Al = 50	48.508
KCl	0.372
NaOH	0.603
NaCl	0.193

Table 4.2 Reagents used for the preparation of zeolite Na-Beta for the study of effect of TEAOH/ SiO_2 mole ratio

Reagents	Weights (g)
Fly ash	1.000
TEAOH	
For $TEAOH/SiO_2 = 0.00$	0.000
$TEAOH/SiO_2 = 0.25$	23.009
$TEAOH/SiO_2 = 0.30$	27.611
$TEAOH/SiO_2 = 0.40$	36.815
$TEAOH/SiO_2 = 0.50$	46.018
$TEAOH/SiO_2 = 0.75$	69.028
Cataloid at Si/Al = 50	48.508
KCl	0.372
NaOH	0.603
NaCl	0.193

Table 4.2 Reagents used for the preparation of zeolite Na-Beta for the study of effect of SiO_2/Al_2O_3 mole ratio

Reagents	Weights
Fly ash	1.000
TEAOH	
For Si/Al = 5	4.602
Si/Al = 25	23.009
Si/Al = 50	46.018
Si/Al = 60	55.223
Si/Al = 75	69.028
Si/Al = 100	92.038
Cataloid	
For Si/Al = 5	3.445
Si/Al = 25	23.473
Si/Al = 50	48.508
Si/Al = 60	58.522
Si/Al = 75	73.543
Si/Al = 100	98.578
KCl	0.372
NaOH	0.603
NaCl	0.193

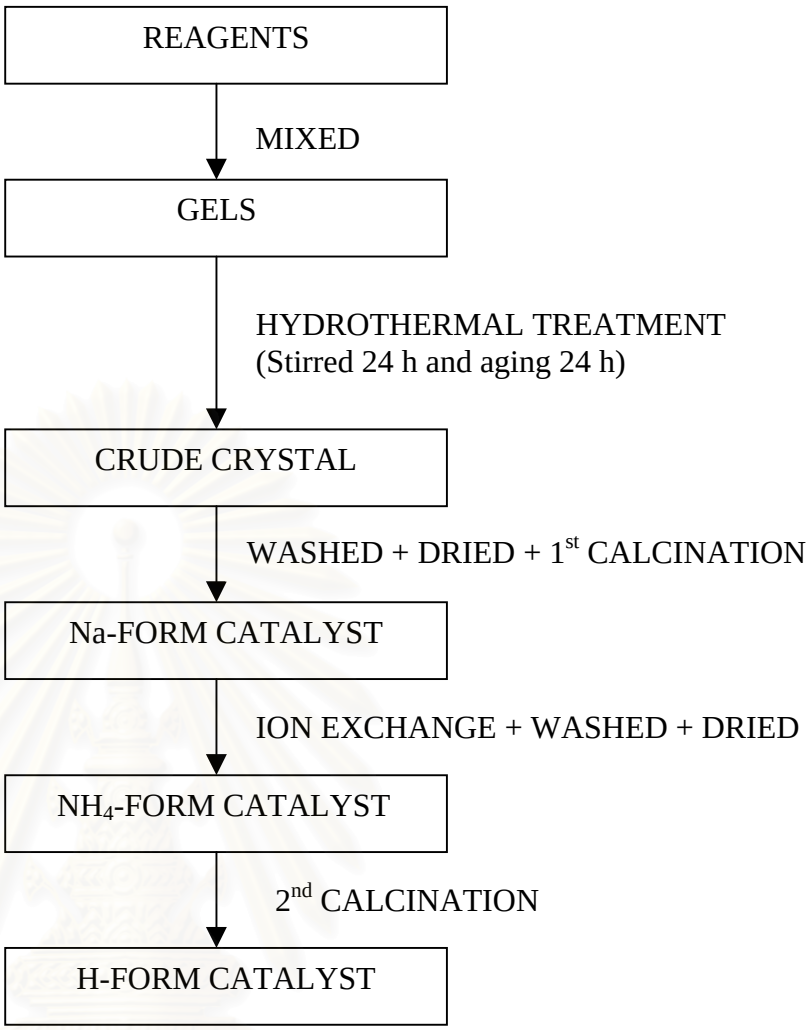

Figure 4.1 Preparation procedures of zeolite beta from lignite fly ash

4.1.2 Crystallization

The gel obtained was stirred thoroughly in teflon vessel before transferring to a stainless steel autoclave. At the aging with stirring stage, gel was heated and stirred at 120 rpm for crystallization in the autoclave from room temperature to first set temperature at heating rate of 1°C/min under initial pressure 3 kg/cm^2 (gauge) of nitrogen gas. At the crystallization with stirring stage, stirring was stopped after 24 h and heated at the same heating rate to second set temperature for 24 h. After the process finished, autoclave was cooled to room temperature. The crystal product obtained was centrifuged at 2,500 rpm for 15 minute for each time. The recovered solid products were then washed until pH ≈ 9 and dried in an oven at 90°C overnight.

4.1.3 First Calcination

The solid products were calcined in an air stream at 540^{o}C for 3.5 hr by heating them from room temperature to 540^{o}C in 60 min in order to burn off the organic template and to leave the cavities and channels in the crystals. Then, The calcined crystals were cooled to room temperature in desicator. After this step the crystals form zeolite Na-Beta.

4.1.4 Ion-exchange with Ammonium Nitrate

The ion-exchange step was carried out by mixing the calcined crystals with 2 M NH_4NO_3 (ratio of crystals and solution is 1 g : 30 ml) and heated on a stirring hot plate at 80^{o}C for 1 hr. Then, the mixtures were cooled down to room temperature. And then, the ion-exchange step was repeated again. After that, the ion-exchange crystals were washed twice with deionized water by using centrifugal separator. And then, the ion-exchange crystals were dried at 90^{o}C for at least 3 hr in oven. The dried crystals (zeolite NH_4-Beta) were then obtained.

4.1.5 Second Calcination

Unstable species, i.e. NH_3, NO_x were decomposed by thermal treatment of the ion-exchanged crystals in a furnace by heating form room temperature to 500^{o}C in 60 min in air stream and maintained at this temperature for 2 hr. After this step the catalysts formed were called zeolite H-beta.

The crystals were tableted by a tablet machine. The tableted catalysts were crushed and sieved to the size of 8-16 mesh to use in the reaction.

4.2 Characterization of the Catalysts

4.2.1 X-ray Diffraction Spectroscopy

X-ray diffraction (XRD) analysis of the catalysts were performed with SIEMENS XRD D5000, accurately in the 5-40^{o} 2θ angular region, at Petrochemical Engineering Research Laboratory, Chulalongkorn University.

4.2.2 Morphology

The shape and the distribution of size of crystal were observed by JEOL Scanning Electro Microscope (SEM) at the Scientific and Technological Research Equipment Center, Chulalongkorn University (STREC).

4.2.3 Chemical Analysis

Percentage of metal was analyzed by X-ray fluorescence spectrometer (XRF) technique. The silicon and aluminum content of the prepared catalyst was analyzed by X-ray fluorescence spectrometer (XRF) at the Scientific and Technological Research Equipment Center, Chulalongkorn University (STREC).

4.2.4 Reaction Testing

4.2.4.1 Chemicals and Reagents

Methanol is available from MERCK, 99.9 % for methanol conversion.

4.2.4.2 Instruments and Apparatus

a) Reactor: The reactor is a conventional microreactor made from a quartz tube with 6 mm inside diameter. The reaction was carried out under N_2 gas flow and atmospheric pressure.

b) Automatic Temperature Controller: This consists of a magnetic switch connected to a variable voltage transformer and a RKC temperature controller connected to a thermocouple attached to the catalyst bed in reactor. A dial setting establishes a set point at any temperatures within the range between 0^{o}C to 600^{o}C.

c) Electric Furnace: This supplies the required heated to the reactor for reaction. The reactor can be operated from room temperature up to 700^{o}C at maximum voltage of 220 volt.

d) Gas Controlling System: Nitrogen is equipped with pressure regulator (0-120 psig), an on-off valve and a needle valve were used to adjust flow rate of gas.

e) Gas Chromatographs: Operating conditions are shown in Table 4.2.

Table 4.2 Operating condition for gas chromatograph

Gas chromatographs	Shimadzu GC-14A	Shimadzu GC-14B	Shimadzu GC-8A
Detector	FID	FID	TCD
Column	Silicon OV-1 ϕ 0.25 x 50 m	VZ-10	Porapak-Q
Carrier gas	N_2 (99.999%)	N_2 (99.999%)	He (99.999%)
Column temperature			
-Initial	40^{o}C	70^{o}C	90^{o}C
-Final	140^{o}C	70^{o}C	90^{o}C
Detector temperature	150^{o}C	150^{o}C	100^{o}C
Injector temperature	150^{o}C	100^{o}C	100^{o}C
Analyzed gas	Hydrocarbon	C_1-C_4	CH_3OH

4.2.4.3 Reaction Method

The methanol conversion was carried out by using a conventional flow as shown in Figure 4.2. A 0.3 portion of the catalyst was packed in the quartz tubular reactor. The reaction was carried out under the following procedure:

1) Adjust the pressure of nitrogen to 1 kg/cm^2, and allow the gas to flow through a rotameter (See Appendix A-2), measure the outlet gas flow rate by using a bubble flowmeter. Gas flow rate was about 22.62 ml/min at GHSV about 2000 h^{-1}.

2) Heat up the reactor (under N_2 flow) by raising the temperature from room temperature to 450^{o}C in 45 min and then hold at this temperature about 30 min for preheating catalyst.

3) Put methanol 20 ml in saturator and set the temperature of water bath at 25^{o}C at this temperature. The concentration of methanol in saturator were 20% mol.

4) Start to run the reaction by adjusting 2 three way valves to allow nitrogen gas to pass through reactants inside saturator in water bath.

5) Take sample for analyzed by gas chromatograph after the reaction ran for 1 h..

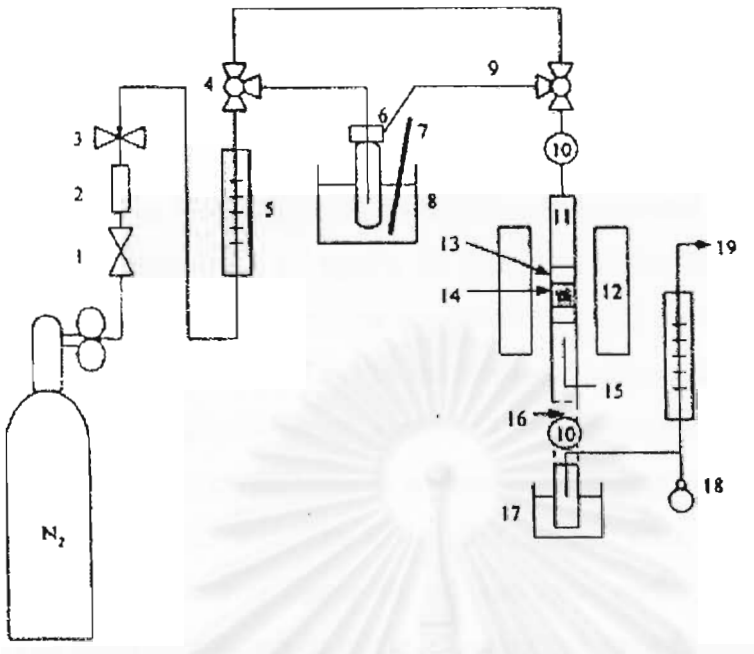

1. On-off valve 2. Gas filter 3. Needle valve 4. Three-way valve
5. Flow meter 6. Saturator 7. Thermocouple 8. Water bath
9. Heating line 10. Sampling port 11. Tubular reactor 12. Electric furnace
13. Quartz wool 14.Catalyst 15. Thermocouple 16. Heating tape
17. Trap 18. Soap-film flowmeter 19. Purge

Figure 4.2 Schematic diagram of the reaction apparatus for reactions.

CHAPTER V

RESULTS AND DISCUSSION

In this chapter, the results and discussions are separated to two sections. First section 5.1, characterizations of lignite fly ash and zeolite beta are included. As mentioned Chapter III, there were four parameters studied in the synthesis of zeolite beta from lignite fly ash which affect to the characterizations of the synthetic crystals were concentrated on the following aspects: 1. Temperature at aging with stirring stage, 2. Temperature at crystallization without stirring stage, 3. TEAOH/SiO_2 mole ratio, and 4. Si/Al atomic ratio. The XRD, BET, surface area, FTIR, SEM and XRF. For XRF used to characterize lignite fly ash and some zeolites beta used for testing reactions. The experimental results of these parameters were discussed in section 5.1.

The second, section 5.2, catalytic behavior of zeolite beta synthesized from lignite fly ash are explained.

5.1 Charaterizations

5.1.1 Characterizations of lignite fly ash

XRD diffraction pattern of lignite fly ash as presented in Figure 5.1 at 2θ from 4 to 40^{o}. It showed that lignite fly ashes are amorphous material which BET surface area was about 15 m^2/g. FTIR spectra of lignite fly ash also presents in Figure 5.2 at wave number ranged from 400 to 2000 cm^{-1}. From IR spectra, it shows board band at from 900 to 1200 cm^{-1}.

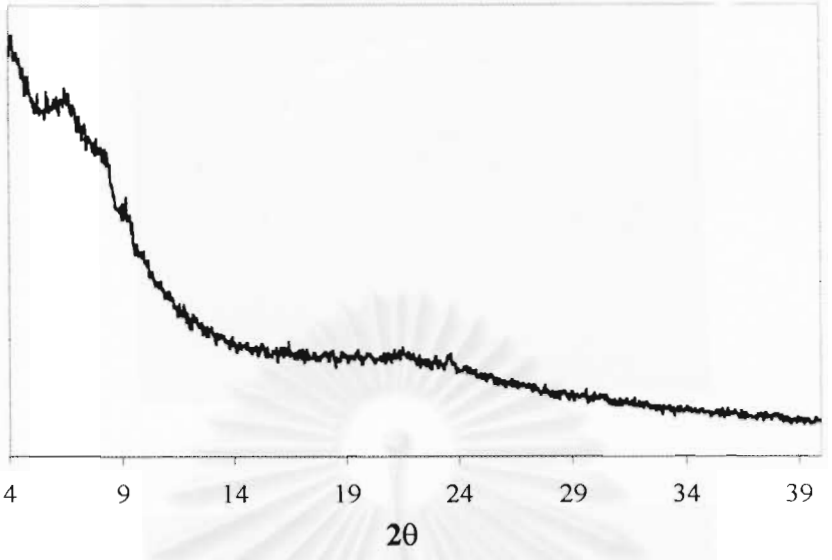

Figure 5.1 X-ray diffraction pattern of Mae Moh lignite fly ash

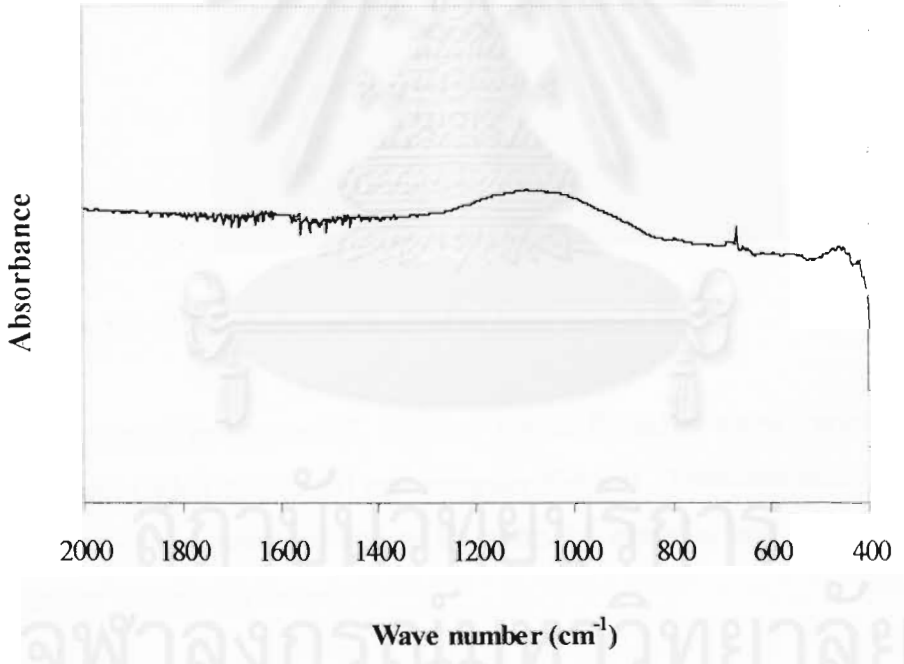

Figure 5.2 FTIR spectra of Mae Moh lignite fly ash

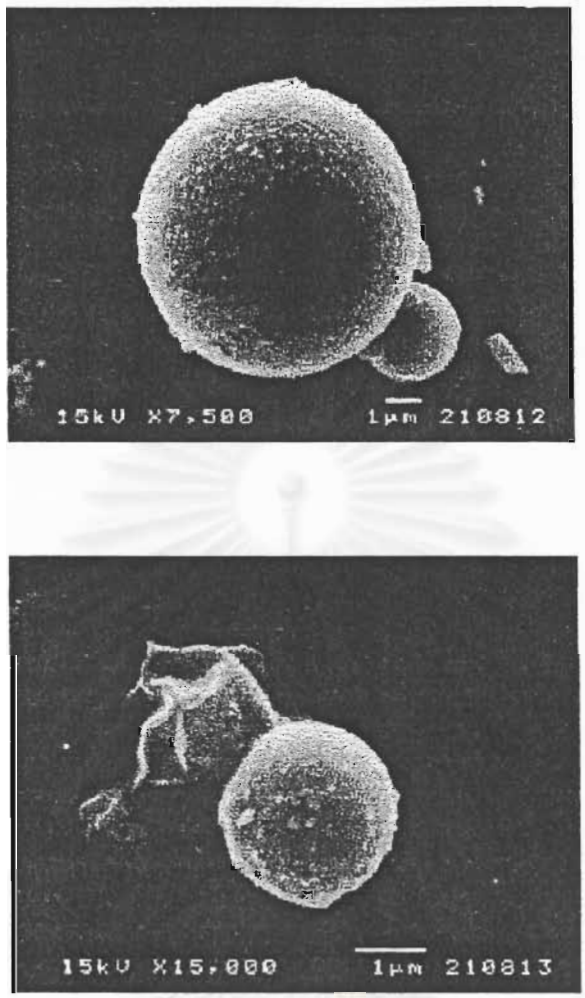

Figure 5.3 SEM photographs of Mae Moh lignite fly ash

As presented in Figure 5.3, SEM of lignite fly ashes show various sized and shape of fly ash (spherical, round and irregular shapes). Spherical and round lignite fly ashes vary in size however lignite fly ashes of irregular and angular shape are usually but not necessarily larger.

The chemical compositions of lignite fly ash characterized by XRF are summarized in Table 5.1. The major chemical compositions of lignite fly ash from Mae Moh are SiO_2 and Al_2O_3 and minor composition of Fe_2O_3 and CaO are found. Amount of SiO_2 and Al_2O_3 are about 46.8 and 25.6 % by weight and amount of Fe_2O_3 and CaO are 10.4 and 9.9 % by weight, respectively.

Table 5.1 Chemical compositions of Mae Moh lignite fly ash

Chemical compositions	Constituent (wt %)
SiO_2	46.8
Al_2O_3	25.6
Fe_2O_3	10.4
Na_2O	0.87
K_2O	2.59
MgO	2.67
CaO	9.9

5.1.2 Characterization of crystals

5.1.2.1 Effect of temperatures at aging with stirring stage

The aging temperatures (with stirring) were varied as the following: 80, 90, 100, 120 and, 135^{o}C. The crystallizing temperature (without stirring), TEAOH/SiO_2 mole ratio, and Si/Al atomic ratio were fixed at 135^{o}C, 0.5 and 50, respectively.

(a) Characterizations of product crystals by crystallinity

The XRD pattern for zeolite beta synthesized from lignite fly ash at various aging temperatures were shown in Figure 5.5. Each XRD pattern was the same compared with the XRD pattern of commercial zeolite beta as shown in Figure 5.4. This approach used for characterization the type of zeolite crystals by comparing with the data of powder diffraction file [21], XRD pattern was specified for each crystals.

The intensity of XRD patterns developed in the same direction from 80 to 135^{o}C. And the XRD pattern also showed that the other components such as Fe_2O_3 were concealed by intensity of zeolite beta.

The crystallinities of each pattern were calculated by choosing six points of 2θ, which have maximum intensity (see appendix A-3). The results of calculation were shown in Figure 5.6, the crystallinity increased with the increasing aging temperatures. In addition, tend of crystallinity increased was similar to intensity as shown above.

The results indicated that as the aging temperatures ranging from 80 and 135, the crystallinity of zeolites beta synthesized from lignite fly ash increased with increasing aging temperatures and at aging temperature of 135^{o}C showed the highest crystallinity of 75 % in this range.

(b) External structure (Morphology) analysis by scanning electron microscope

SEM photograph of zeolites beta synthesized from lignite fly ash at aging temperature ranging from 80 to 135^{o}C were shown in Figure 5.8 to 5.12, respectively and SEM photograph of commercial zeolite beta was shown Figure 5.7. The shape of commercial zeolite was cuboid form.

From Figure 5.8, SEM photograph showed that the product crystals were crystalline forms as cuboid shape [39,41] (about 0.5 – 1 μm) which was similar to commercial zeolite beta. It was showed that there were zeolite beta crystals, which had been developed in the synthesis at aging temperature of 80^{o}C. And there were a little Fe_2O_3 crystals also presented in bar shape.

From Figure 5.9, SEM photograph at aging temperature of 90^{o}C, the product crystals contained amorphous forms in irregular shape and the cubic forms of zeolite beta, which had the average size about 0.8 μm. And the crystals of Fe_2O_3 also presented.

For the SEM photograph at aging temperature of 100^{o}C, in Figure 5.10, product crystal almost contained of cuboid form of zeolite beta and Fe_2O_3. The size of zeolite beta was varied from 0.2 to 1 μm. The amounts of Fe_2O_3 were less than

product crystals synthesized at aging temperature of 80 and 90^{o}C and therefore, this was better condition.

The SEM photograph of product crystals obtained from aging temperature of 120^{o}C are shown in Figure 5.11. At this condition, the cubic crystals of zeolite beta were almost the same size of about 0.5 μm and the amount of impurity still presented but less than the condition at aging temperature of 80 to 100^{o}C.

At the aging temperature of 135^{o}C showed in SEM photograph Figure 5.12. The results were the same as at aging temperature of 120^{o}C.

The SEM photograph from Figure 5.8 to 5.12 indicated that at the aging temperature in range of 120 to 135^{o}C were the best conditions for the synthesis of zeolite beta from lignite fly ash. This was consistent to the results of crystallinity calculated from XRD diffraction pattern.

(c) Functional group analysis

The infrared (IR) spectra of zeolites beta synthesized from lignite fly ash at various aging temperature are shown in Figure 5.14. The area each band was divided into three parts. First part, at range of wave number from around 1100 to 1250, was assigned as asymmetric stretching of T-O-T bond of external linkages modes and the second part, at 440 to 630 cm^{-1}, was illustrated bending mode of O-T-O and T-O-T bond of internal tetrahedral linkages modes. The last part, at around wave number 795, assigned as symmetric stretching of T-O-T bond of external linkage modes [39,41].

IR spectra of zoelite Beta typical for crystalline zeolite beta had strong band at wave number of 1230 and 1090 cm^{-1} assigned as the asymmetric stretching of T-O-T and medium weak band around 800 cm^{-1} assigned as symmetric stretching of T-O-T. The wave number of 460, 535 and 560 were medium strong, which assigned as bending vibration of T-O-T and O-T-O [40].

At aging temperature of 135°C, IR spectra of zeolite beta obtained showed strong shoulder band at around 1090 and 1230 cm^{-1} like the IR spectra of commercial zeolite beta in Figure 5.13. A similar IR spectra has also been reported by Perez-Pariente et al. [41]. From each IR spectra of zeolite beta in Figure 5.14, as the crystallization progressed, the stronger shoulder of this two band developed. Similarly to abroad medium strong band of 800 cm^{-1} due to external tetrahedral linkages is shifted to be higher and medium strong band of 460, 534, and 560 showed the same behavior.

(d) BET surface area

The results of BET surface area showed in Figure 5.15. BET surface area of obtained crystals were not quite different, about 370 m^2/g. It showed that the BET surface area of zeolite beta synthesized from lignite fly ash at low aging temperature was lower compared with BET surface area of commercial zeolite beta which was about 700 m^2/g.

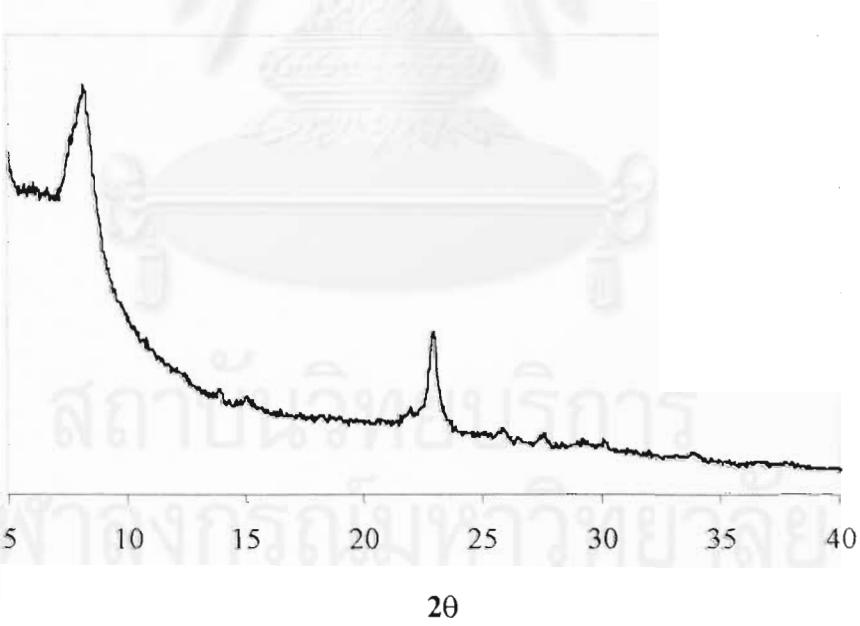

Figure 5.4 X-ray diffraction pattern of commercial zeolite beta

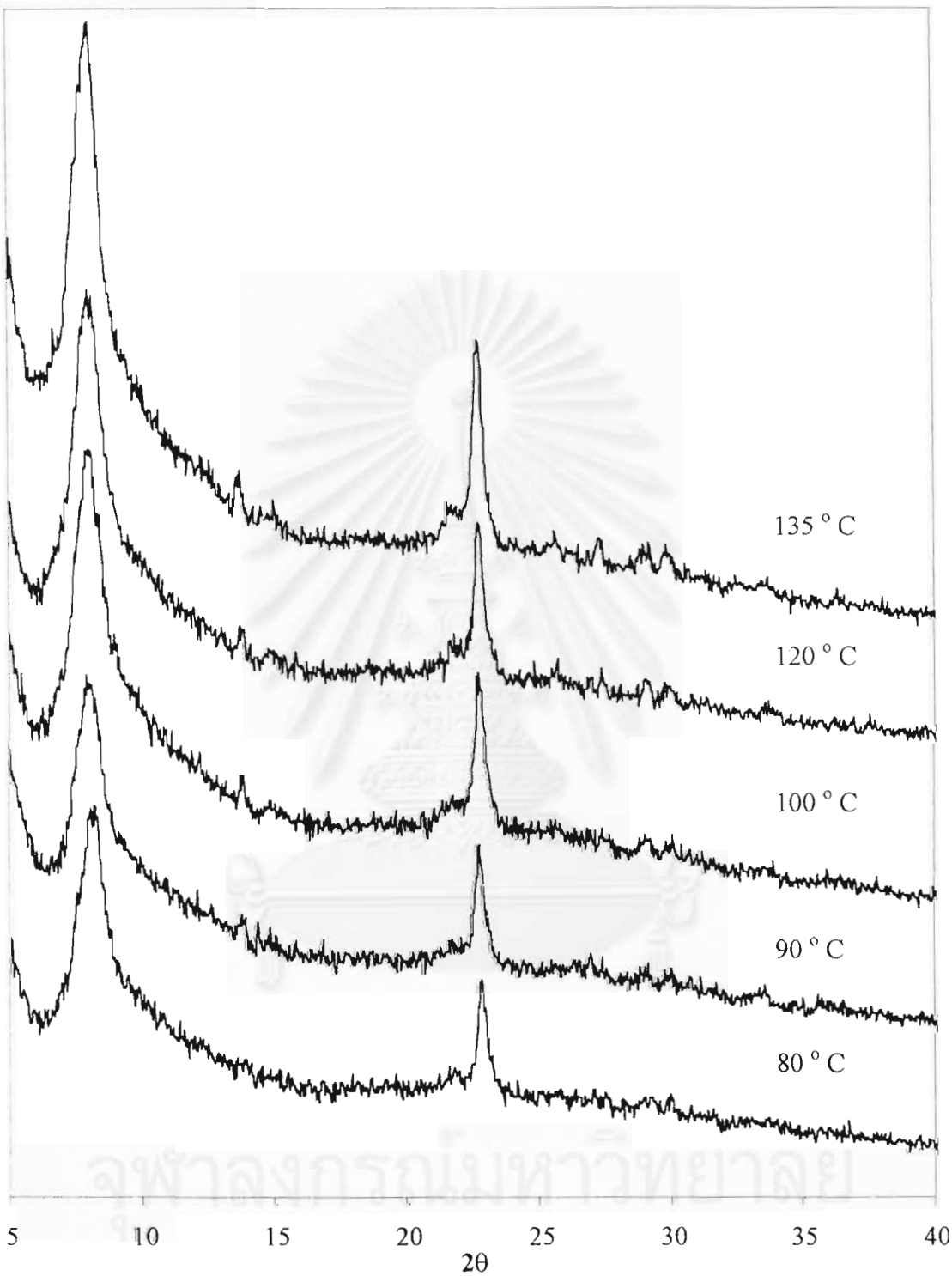

Figure 5.5 X-ray diffraction pattern of zeolite beta synthesized from lignite fly ash at various aging temperature

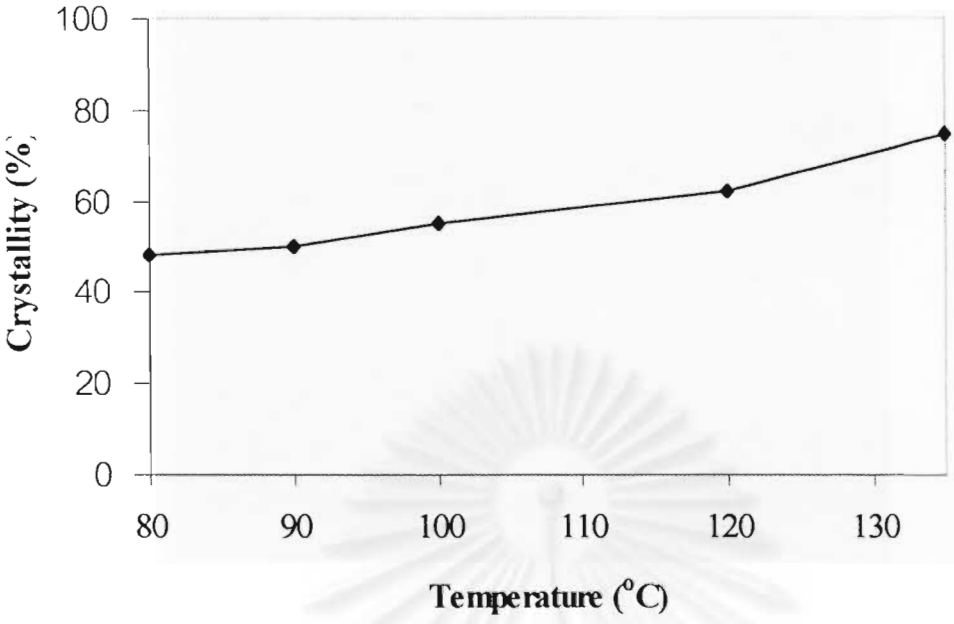

Figure 5.6 Percent crystallinity of synthesized zeolite beta from lignite fly ash at aging temperature in the range of 80 to 135°C

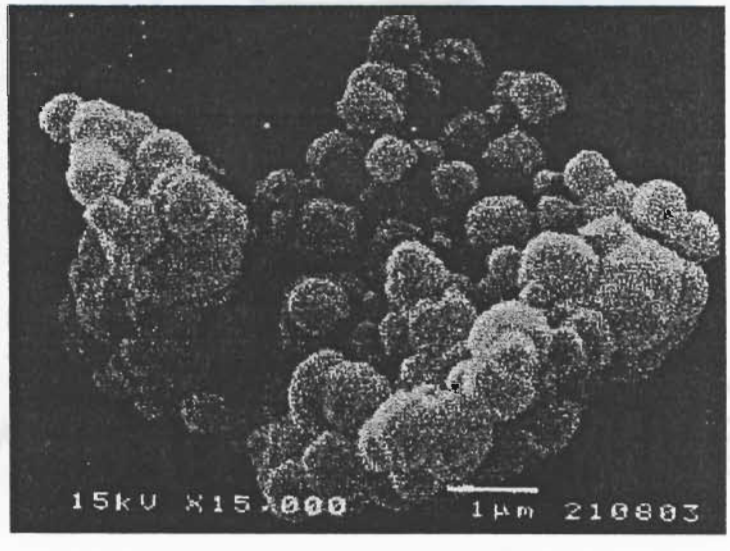

Figure 5.7 SEM photograph of commercial zeolite beta

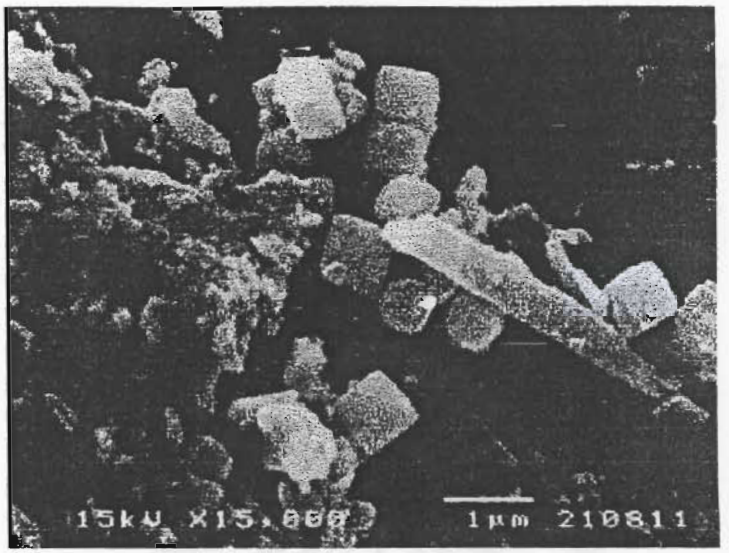

Figure 5.8 SEM photograph of zeolite beta synthesized from lignite fly ash at aging temperature of 80 ° C and crystallization temperature of 135 ° C

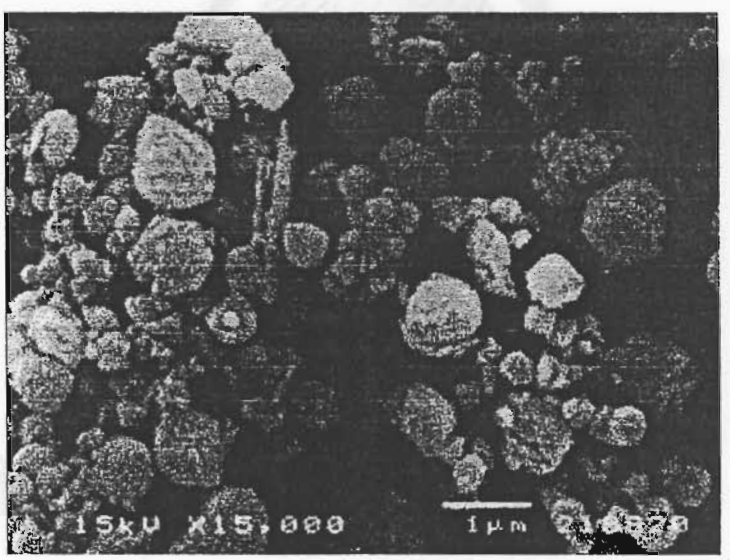

Figure 5.9 SEM photograph of zeolite beta synthesized from lignite fly ash at aging temperature of 90 ° C and crystallization temperature of 135 ° C

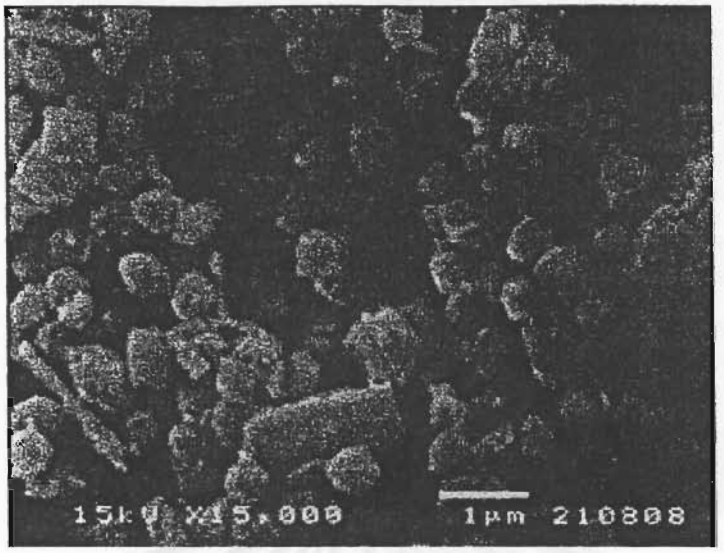

Figure 5.10 SEM photograph of zeolite beta synthesized from lignite fly ash at aging temperature of 100 ° C and crystallization temperature of 135 ° C

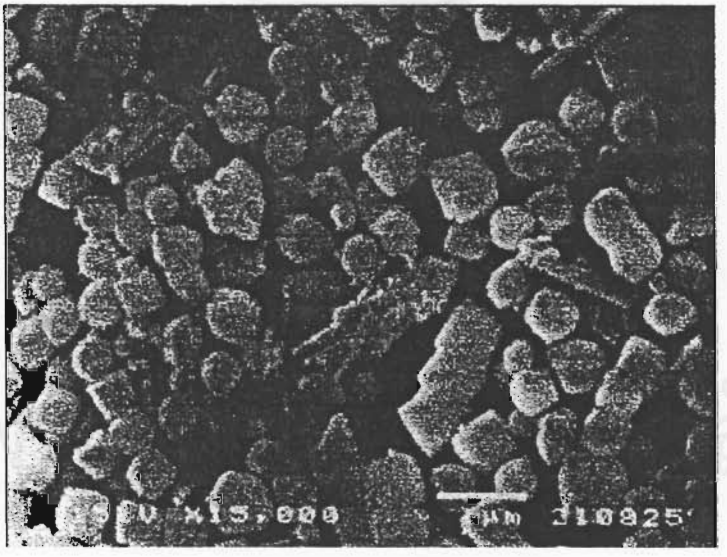

Figure 5.11 SEM photograph of zeolite beta synthesized from lignite fly ash at aging temperature of 120 ° C and crystallization temperature of 135 ° C

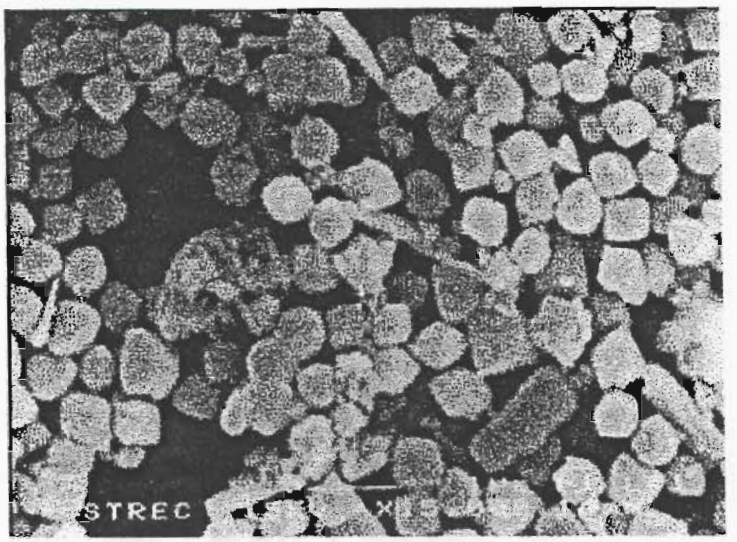

Figure 5.12 SEM photograph of zeolite beta synthesized from lignite fly ash at aging temperature of 135 ° C and crystallization temperature of 135 ° C°

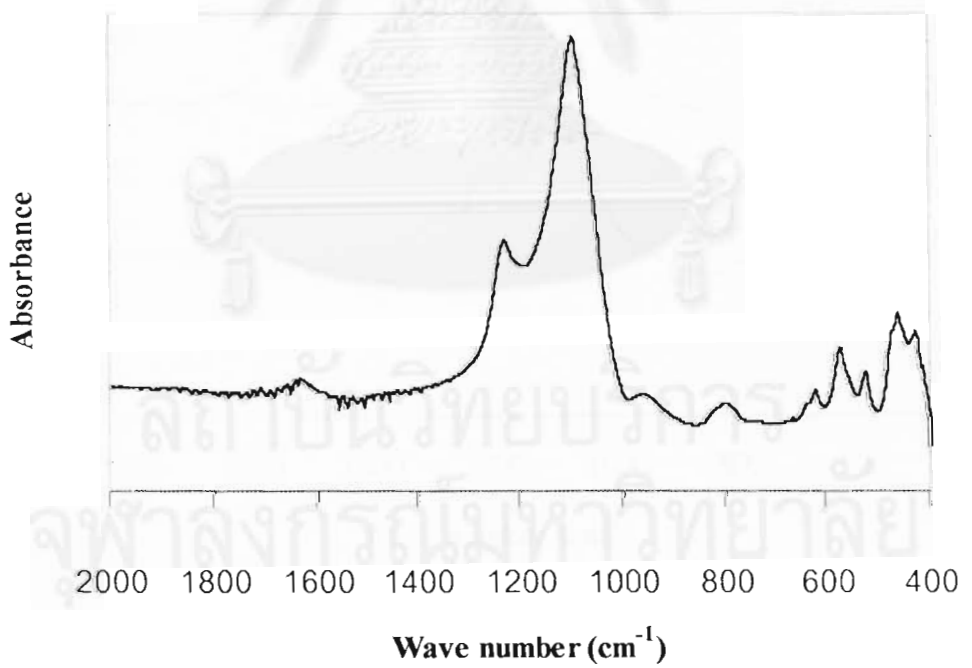

Figure 5.13 FTIR spectra of commercial zeolite beta

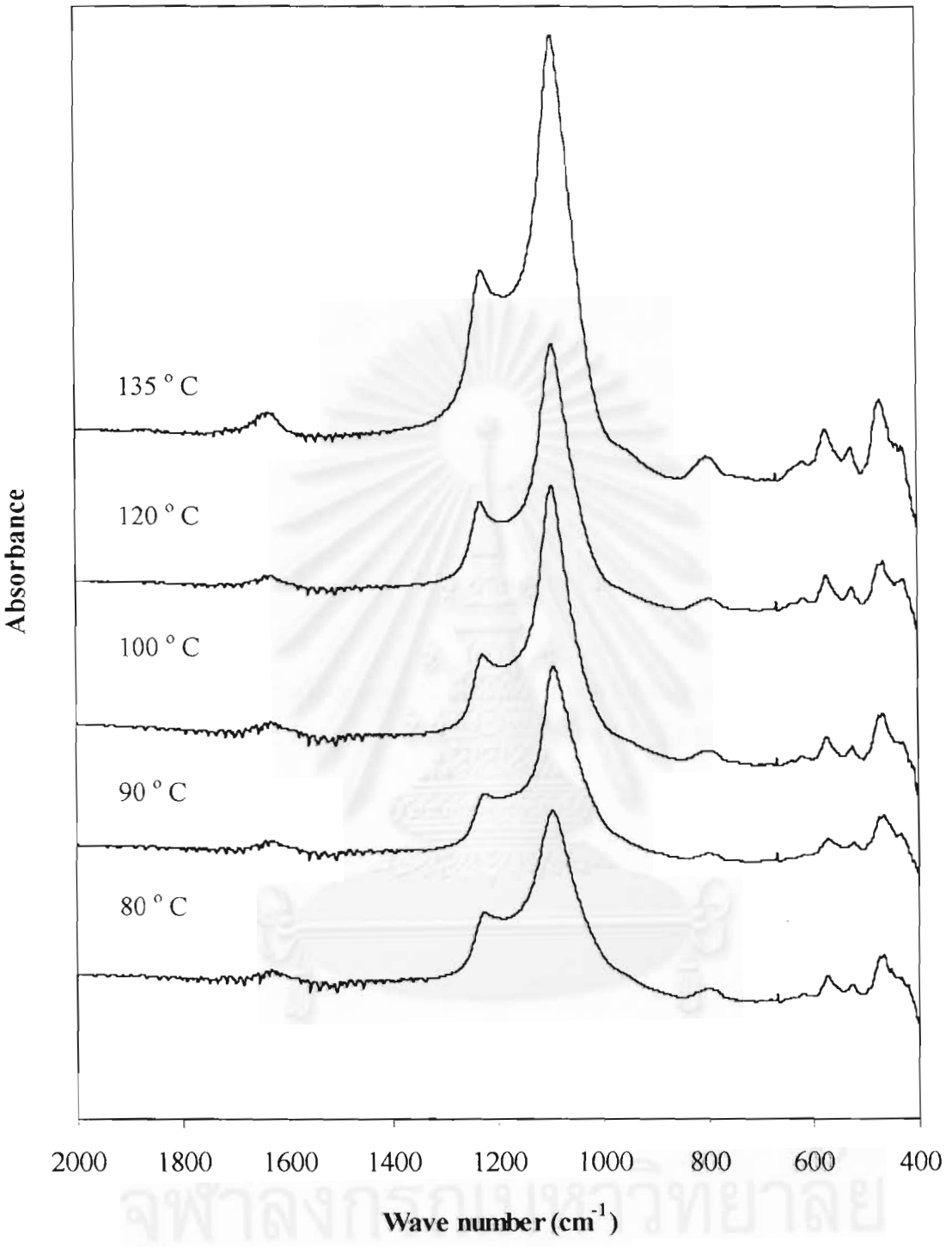

Figure 5.14 FTIR spectra of zeolite beta synthesized from lignite fly ash at various aging temperature

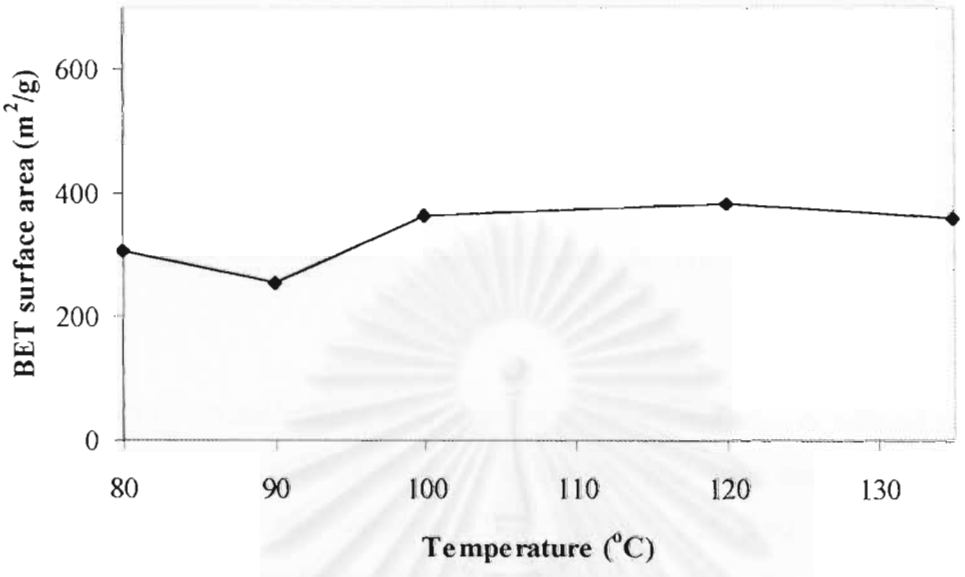

Figure 5.15 BET surface area of zeolite beta synthesized from lignite fly ash at aging temperature ranging from 80 to 135°C

5.1.2.2 Effect of temperatures at crystallization without stirring stage

As shown in the study of effect of aging temperature, crystallization increased with increasing aging temperature. It can be suggested that at high aging temperature the growth of crystal was better. Therefore, in the study of effect of crystallization temperature, aging with stirring stage was proceeded at the temperature higher than 100^{o}C and system was not changed temperature between aging with stirring and crystallization without stirring stage in order that the crystallization was not be disturbed.

The effect of crystallization temperatures at the crystallization without stirring stage to the synthesis of zeolite beta from lignite fly ash were studied by varying crystallization temperature as following: 110, 120, 130, 135, 140, and 150^{o}C. The aging temperatures were similar to the temperature at crystallization without stirring stage because in the study of effect of aging temperature it was found that changing of temperature from aging with stirring to crystallization without stirring stage effect on crystallization. In addition, TEAOH/SiO2 and Si/Al mole ratio were fixed at 0.5 and 50, respectively.

(a) Characterization of product crystal by crystallinty

The XRD patterns of zeolite beta synthesized from various crystallization temperature were shown in Figure 5.16. XRD pattern was similar to XRD pattern of commercial zeolite beta (as shown in Figure 5.4). The intensity of XRD pattern developed from 110 to 140^{o}C which the highest intensity was 98% and intensity of XRD pattern decreased at the temperature of 150^{o}C.

By the calculation, the crystallinity of each pattern were shown in Figure 5.17, the cystallinity increased with increasing crystallization temperature from 110 to 140^{o}C and the crystallinity increased slightly at the crystallization temperature of 150^{o}C. The results of XRD pattern and crystallinity showed that at the crystallization temperature about 140^{o}C the progress of crystallization was better.

(b) External structure (morphoology) analysis by scanning electron microscope

SEM photograph of zeolites Beta synthesized from lignite fly ash at crystallization temperature from 110 to 150^{o}C are shown in Figures 5.18 to 5.23, respectively.

From Figure 5.18, SEM photograph shows that the product crystals are crystalline as cuboid form (about 0.4 μm), similar to commercial zeolite beta, which was showed that there were zeolite beta crystals. Nevertheless, there were much amount of amorphous forms in irregular shape and impurities of Fe_2O_3 crystals like bar shape also presented.

Product crystals of zeolite synthesized from lignite lignite fly ash at crystallization temperature of 120^{o}C showed in Figure 5.19. The crystal size was about 0.4 μm and it showed that as the crystallization temperature increased the progress crystallization was better because of disappearance of amorphous form compared with product crystals synthesized from crystallization temperature at 110^{o}C as showed in Figure 5.18.

For SEM photograph at crystallization temperature of 130^{o}C in Figure 5.20, product crystal almost contained of cuboid form of zeolite beta and the size of cuboid crystals were various, however, amount of product crystal were greater than product crystal synthesized from lower aging temperature. Crystal sizes varied in the range of 0.25 to 1 μm. The crystal of Fe_2O_3 and little impurities also presented.

For SEM photograph at crystallization temperature of 135^{o}C in Figure 5.21, product crystals were almost cuboid form and crystal size was not quite different (about 0.5 μm) and less amount of impurities presented.

In Figure 5.22 and 5.23 were zeolite beta synthesized from lignite fly ash at crystallization temperature of 140 and 150^{o}C respectively. It showed that crystal size at temperature of 140^{o}C closed to crystal size at 150^{o}C about 0.25 μm.

The results indicated that at crystallization temperature of about 140^{o}C which was consistent to result of XRD diffraction pattern was the best condition for the synthesis of zeolite beta from lignite fly ash and crystal size was about 0.25 μm.

.

(c) Functional group analysis

The IR spectra of zeolites Beta synthesized from lignite fly ash at various aging temperature were shown in Figure 5.24. The IR spectra of each band were similar to IR spectra of commercial zeolite beta in Figure 5.13. The progress of IR spectra developed from the crlystallization temperature of 110 to 140^{o}C and decreased slightly at the crystallization temperature of 150^{o}C. The results showed that IR spectra of zeolite beta obtained at crystallization temperature of 140^{o}C showed strong shoulder band at around 1090 and 1230 cm^{-1}.

(d) BET surface area

The results of BET surface area showed in Figure 5.25. BET surface area of obtained crystals increased with increasing crystallization temperature from 110 to 140^{0}C and slightly decreased at crystallization temperature of 150^{o}C. The best condition at 140^{o}C showed BET surface area of about 630 m^2/g which was not lower much than BET surface area of commercial zeolite beta (700 m^2/g).

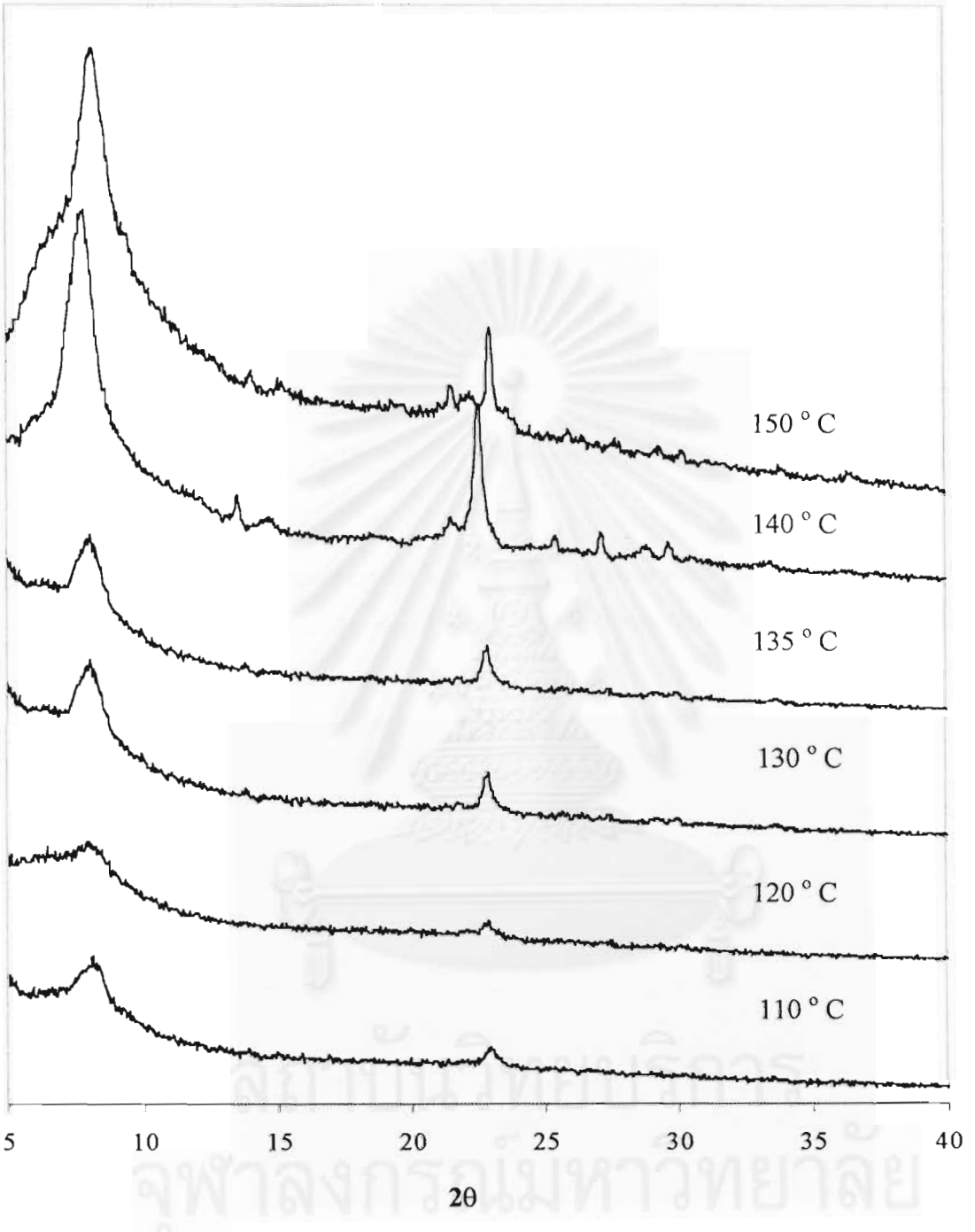

Figure 5.16 X-ray diffraction pattern of zeolite beta synthesized from lignite fly ash at various crystallization temperature

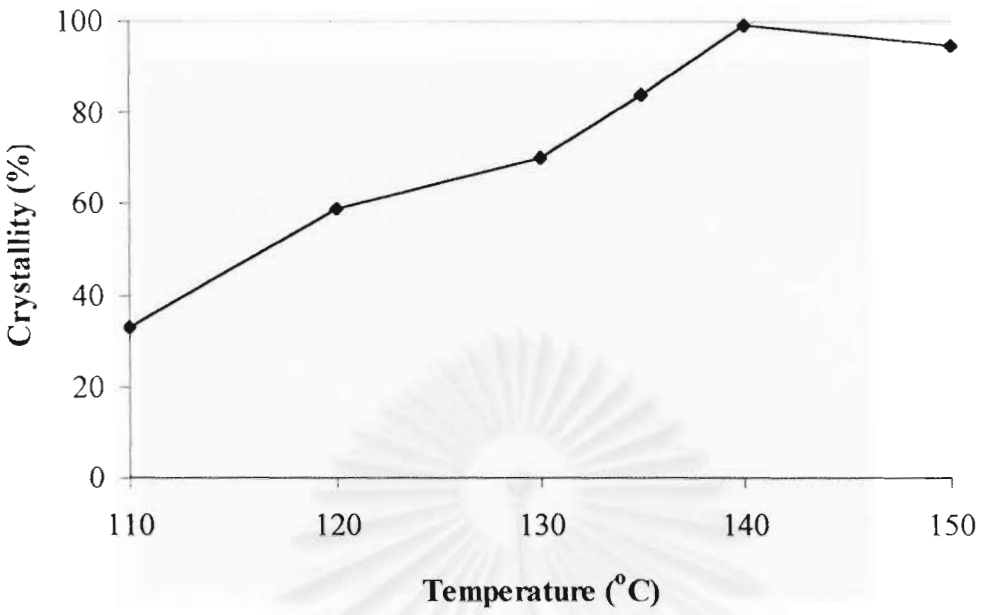

Figure 5.17 Percent crystallinity of zeolite beta synthesized from lignite fly ash at various crystallization temperature in the range of 110 to 150°C

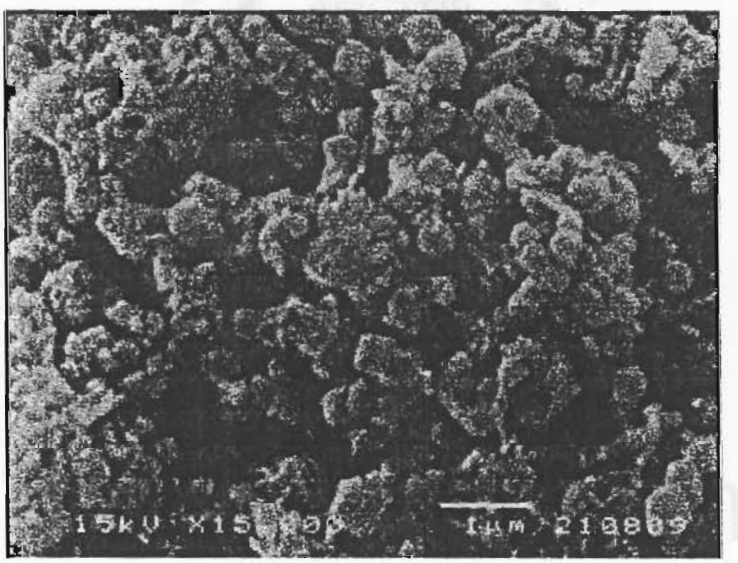

Figure 5.18 SEM photograph of zeolite beta synthesized from lignite fly ash at crystallization temperature of 110°C

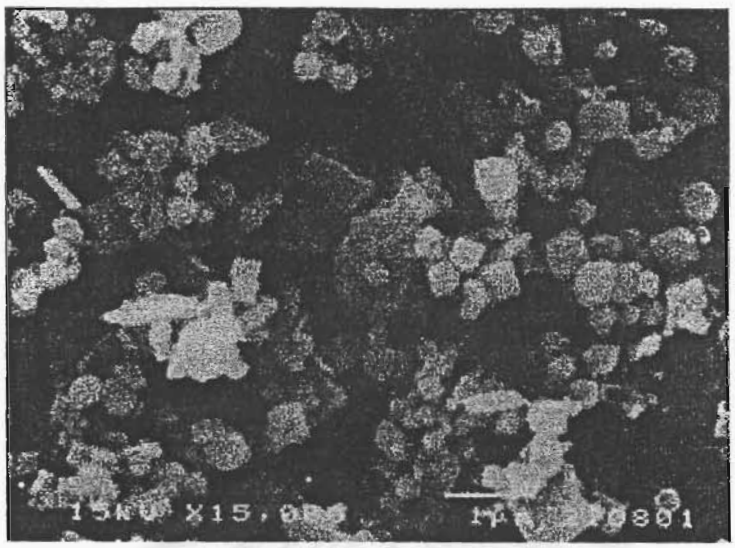

Figure 5.19 SEM photograph of zeolite beta synthesized from lignite fly ash at crystallization temperature of 120°C

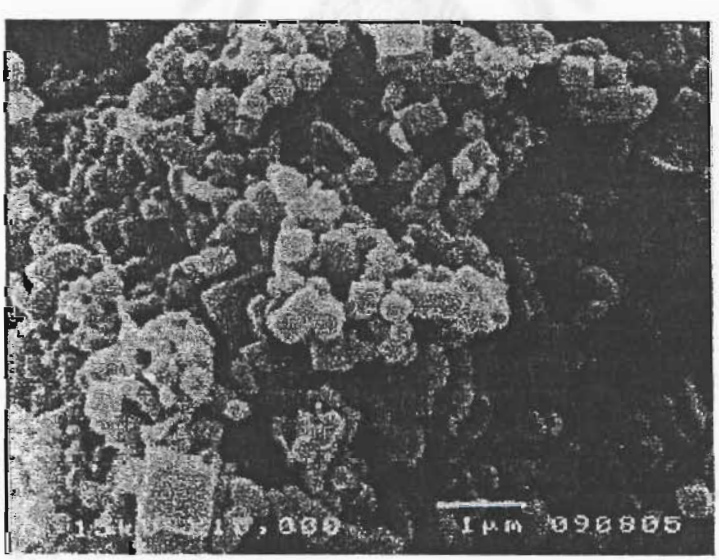

Figure 5.20 SEM photograph of zeolite beta synthesized from lignite fly ash at crystallization temperature of 130°C

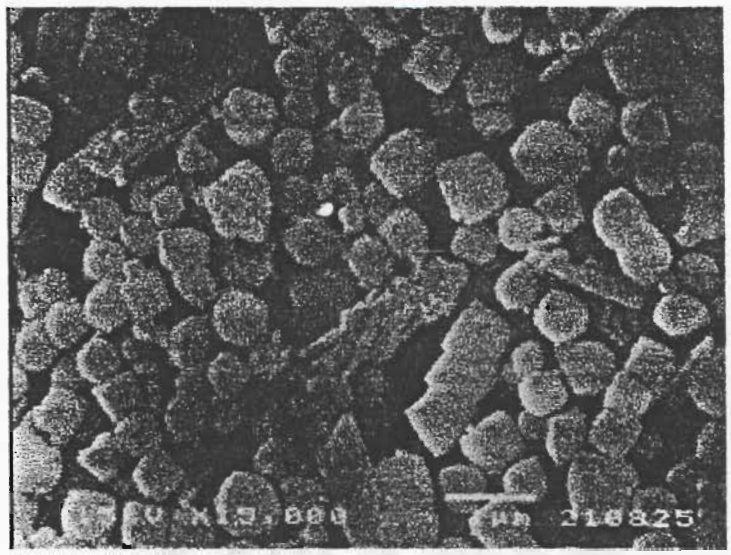

Figure 5.21 SEM photograph of zeolite beta synthesized from lignite fly ash at crystallization temperature of 135°C

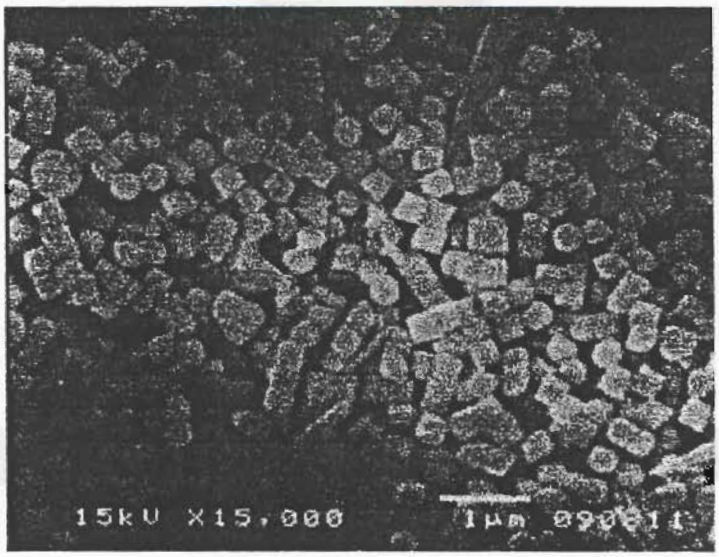

Figure 5.22 SEM photograph of zeolite beta synthesized from lignite fly ash at crystallization temperature of 140°C

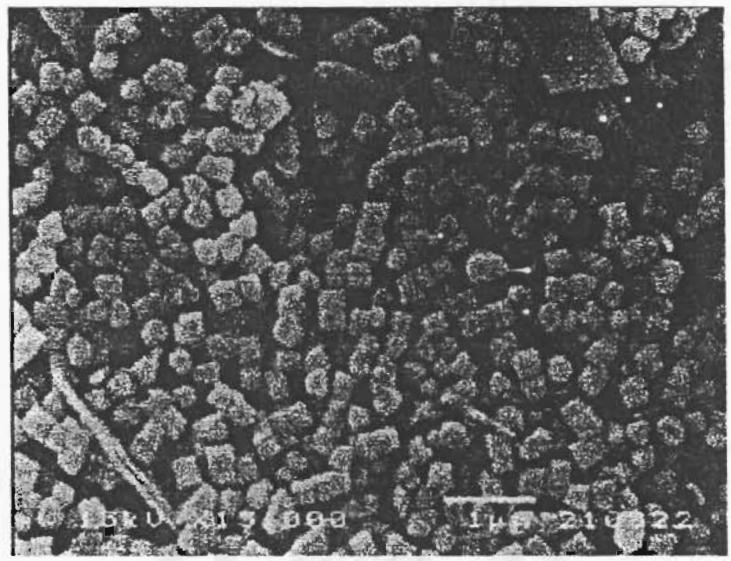

Figure 5.23 SEM photograph of zeolite beta synthesized from lignite fly ash at crystallization temperature of 150°C

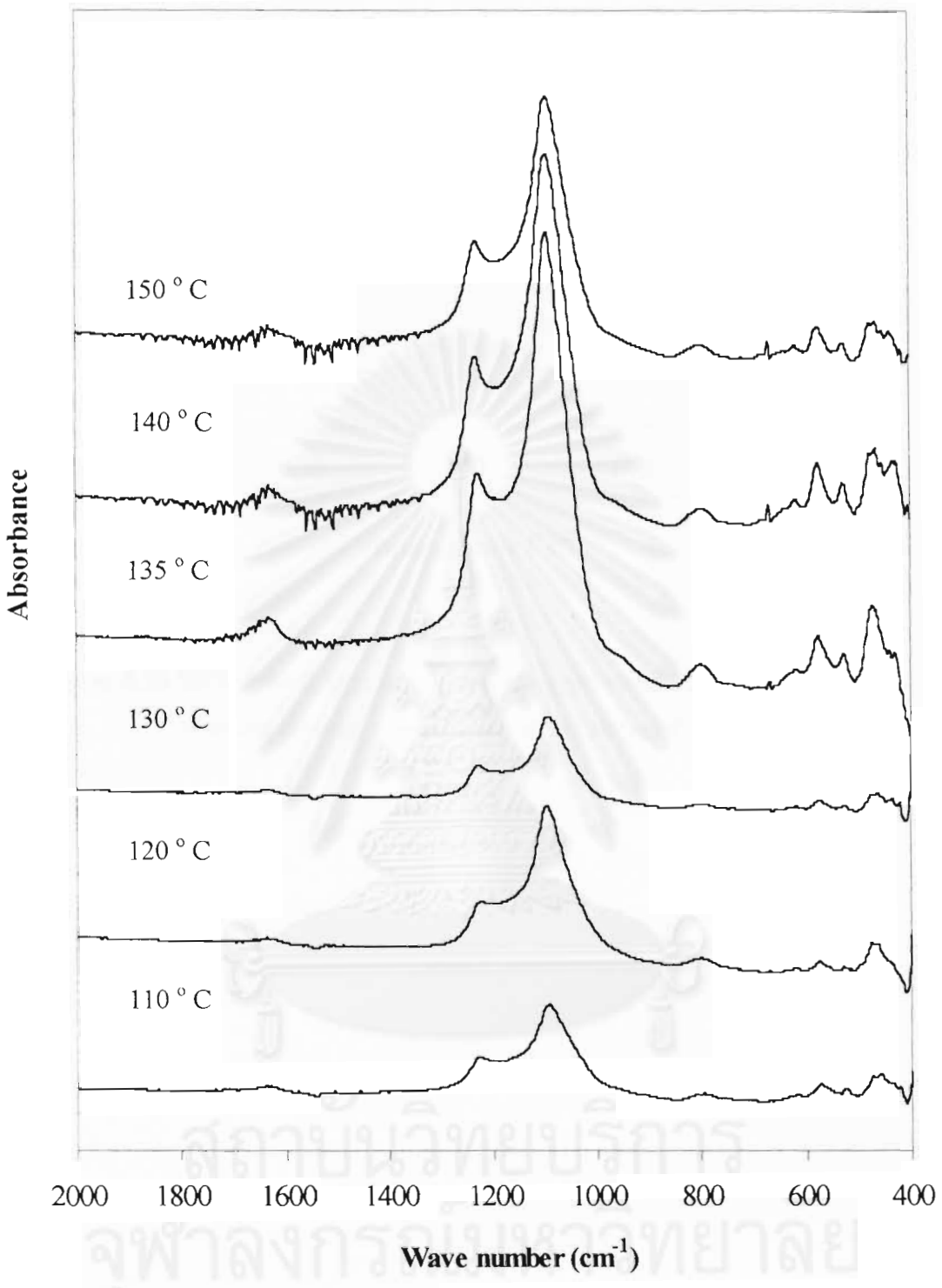

Figure 5.24 FTIR spectra of zeolite beta synthesized from lignite fly ash at various crystallization temperature

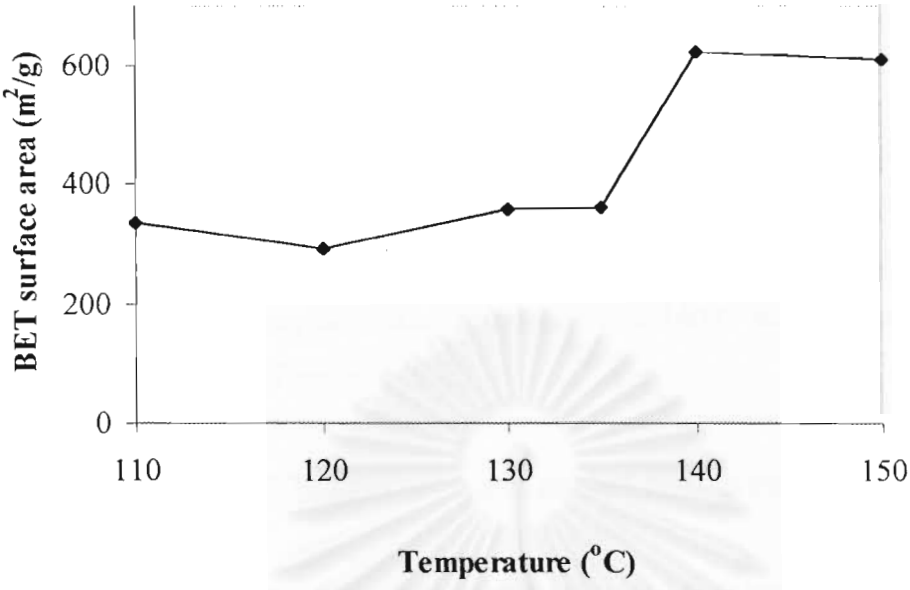

Figure 5.25 BET surface area of zeolite beta synthesized from lignite fly ash at crystallization temperature in the range of 110 to 150°C

5.1.2.3 Effect of amount of template

TEAOH was used as the template of the synthesis of zeolite beta from lignite fly ash in this study and the effect of amount of TEAOH to the characteristics of product was assessed by TEAOH/SiO_2 mole ratio which was varied as following: 0, 0.25, 0.3, 0.4, 0.5, and 0.75. Si/Al atomic ratio was fixed at 50 and as shown in the study of effect aging and crystallization temperature of 140^{o}C was the best condition therefore temperature was fixed at 140^{o}C.

(a) Characterizations of product crystals by crystallinity

As mentioned, X-ray diffraction is approach used for characterization the type of zeolite crystals by comparing with the data of powder diffraction file.

The XRD of pattern zeolites Beta synthesized from lignite fly ash at various TEAOH/SiO_2 mole ratios were shown in Figure 5.26. From each XRD pattern was similar to XRD pattern of commercial zeolite beta as shown in Figure 5.4. The intensity of XRD patterns developed from TEAOH/SiO_2 mole ratio of 0 to 0.5 and the maximum intensity was showed at TEAOH/SiO_2 of 0.5. The intensity of XRD pattern of zeolite beta synthesized from TEAOH/SiO_2 of 0.75 decreased distinctly. In addition, at TEAOH/SiO_2 of product crystal was amorphous form.

The crystallinity of each pattern was calculated. The results of calculation were shown in Figure 5.27, the crystallinity increased with increasing TEAOH/SiO_2 mole ratio from 0 to 0.5. At TEAOH/SiO_2 mole ratio of 0.5 the maximum crystallinity was carried out, which crystallinity was about 98% and the crystallinity at TEAOH/SiO_2 mot ratio of 0.75 was decreased distinctly.

The results indicated that there was influence of amount of TEAOH used as the template of zeolite beta from lignite fly ash. At the TEAOH/SiO_2 mole ratio of 0.5 was the optimum condition for the synthesis. The maximum product crystals were carried out at this ratio. The results also showed that if there was no TEAOH as

template in the synthesis of zeolite beta from lignite fly ash the crystallization can not be occurred.

(b) External structure (morphology) analysis by scanning electron microscope

SEM photographs of zeolite beta synthesized from lignite fly ash at $TEAOH/SiO_2$ mole ratio ranging from 0 to 0.75 were shown in Figure 5.28 to 5.33, respectively.

SEM photograph of zeolite beta synthesized at $TEAOH/SiO_2$ mole ratio of 0 and 0.3 showed in Figure 5.28, 5.29, and 5.30, respectively. They showed that product crystals of these conditions were amorphous forms. Therefore, it illustrated that at mole ratio of $TEAOH/SiO_2$ from 0 to 0.3 was not suitable for the synthesis of zeolite beta from lignite fly ash.

Figure 5.31 showed SEM photograph of zeolite beta synthesized from lignite fly ash at $TEAOH/SiO_2$ mole ratio of 0.4. The cuboid crystals of zeolite beta appeared in the crystal size in the range from 0.25 to 0.6 μm and a little of amorphous form also presented.

Figure 5.32 showed SEM Photograph of zeolite beta synthsized from lignite fly ash at $TEAOH/SiO_2$ mole ratio of 0.5. At this condition, the cuboid crystals in the size of about 0.25 μm occurred, the occurrence of cuboid crystals showed that there were zeolite beta crystals. A little of Fe_2O_3 crystals and impurities also presented.

The structure of zeolite beta crystal synthesized from lignite fly ash was collapsed at $TEAOH/SiO_2$ mole ratio increased to 0.75. Because of cuboid crystals synthesized from this condition were less than condition at $TEAOH/SiO_2$ mole ratio of 0.5 and there were amorphous form occurred, as shown in Figure 5.33.

The SEM photograph From Figure 5.28-5.33 illustrated that at $TEAOH/SiO_2$ mole ratio of 0.5 was the optimum condition for the synthesis of zeolite beta from

lignite fly ash and also found that the synthesis of zeolite beta from lignite fly ash can not be succeeded without TEAOH as template.

(c) Functional group analysis

The IR spectra of zeolites Beta synthesized from lignite fly ash at various $TEAOH/SiO_2$ mole ratios were shown in Figure 5.34. From each IR spectra, bands were similar to IR spectra of commercial zeolite beta in Figure 5.13. The strong band at 1090 and 1230 cm^{-1} increased with increasing $TEAOH/SiO_2$ mole ratio from 0 to 0.5 and slightly decreased with increasing $TEAOH/SiO_2$ mole ratio to 0.75. IR spectra of zeolite beta synthesized from the $TEAOH/SiO_2$ mole ratio of 0 showed strong band around 1000-1300 cm^{-1}, it showed asymmetric stretching mode because of amorphous silica.

IR spectra indicated that at $TEAOH/SiO_2$ mole ratio of 0.5 was the best condition for the synthesis of zeolite beta from lignite fly ash and this results were consistent to the result from XRD patterns.

(d) BET surface area

As discussed above, at $TEAOH/SiO_2$ mole ratio of about 0.5 was the best condition for the synthesis of zeolite beta from lignite fly ash, the results was confirmed by BET surface area. From Figure 5.35, the tend of BET surface area increased with increasing $TEAOH/SiO_2$ mole ratio from 0 to 0.5 and slightly decreased at $TEAOH/SiO_2$ mole ratio increased to 0.75. The BET surface area was achieved about 630 m^2/g at the best condition.

From results in the study of effect of amount of template added into gel as presented above, it was found that, concentration of OH^- species from TEAOH was not enough to dissolve Si from fly ash and cataloid into liquid phase at $TEAOH/SiO_2$ ratio lower than 0.3. Because of every composition in gel must be dissolved to be liquid phase in order to incorporate to be zeolite and transfer to solid phase [39,41,42]. At $TEAOH/SiO_2$ ratio of 0.5 was the optimum amount of OH^- species from TEAOH, which gave highest amount of zeolite beta crystal. Nevertheless, at $TEAOH/SiO_2$

higher than 0.5, there were excess OH^- species from TEAOH after zeolite beta transfered to solid phase , which will dissolve Si and destroy structure of zeolite product [39,41,42]. Therefore, the optimum TEAOH/SiO_2 mole ratio for synthesis of zeolite beta from lignite fly ash was about 0.5.

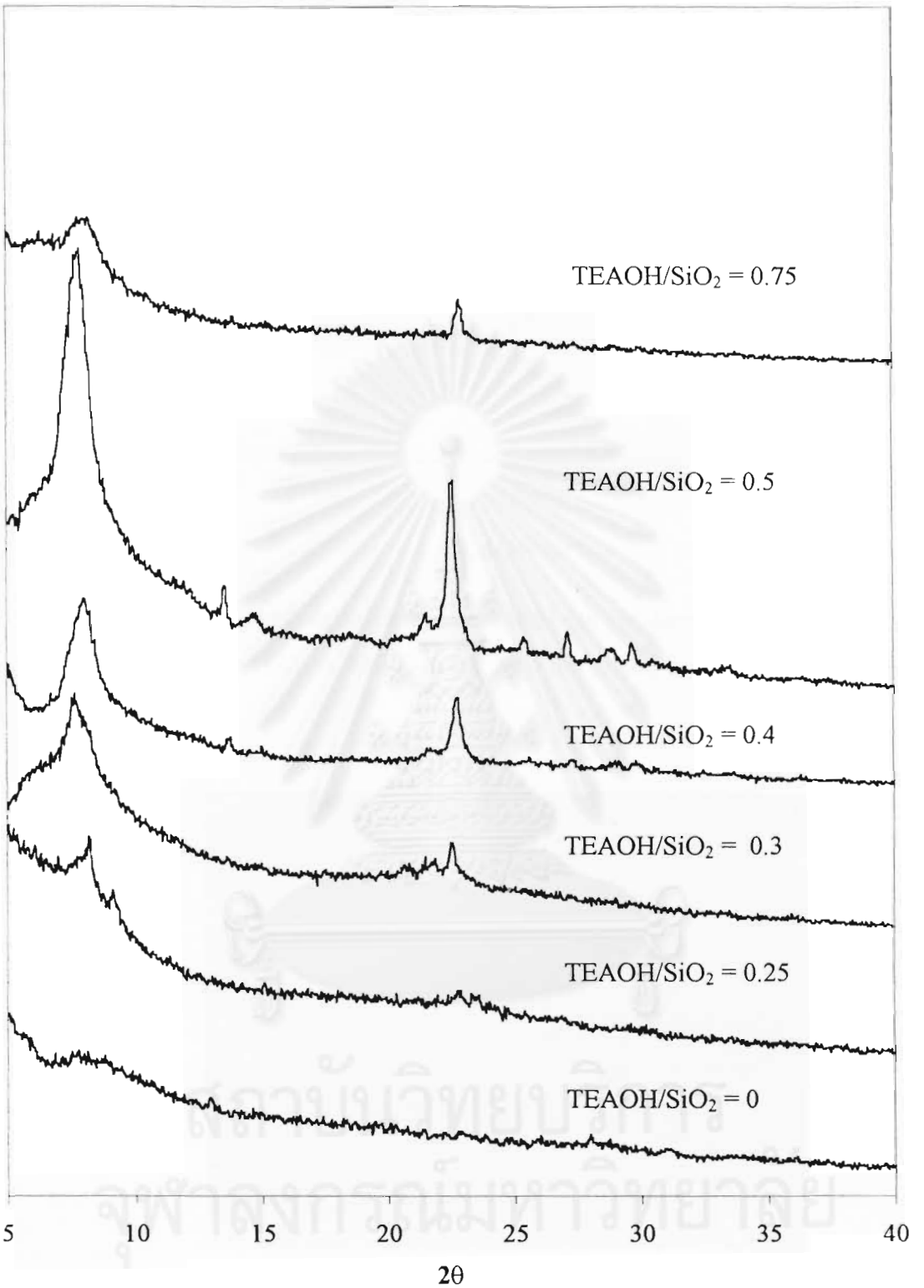

Figure 5.26 X-ray diffraction pattern of zeolite beta synthesized from lignite fly ash at various $TEAOH/SiO_2$ mole ratio

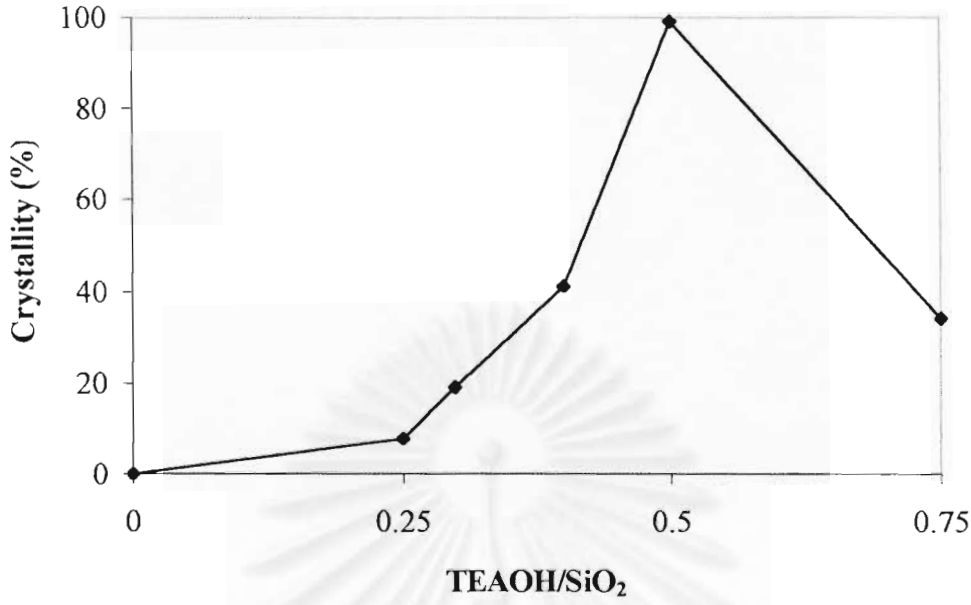

Figure 5.27 Percent crystallinity of zeolite beta synthesized from lignite fly ash at TEAOH/SiO_2 mole ratio in the range of 0 to 0.75

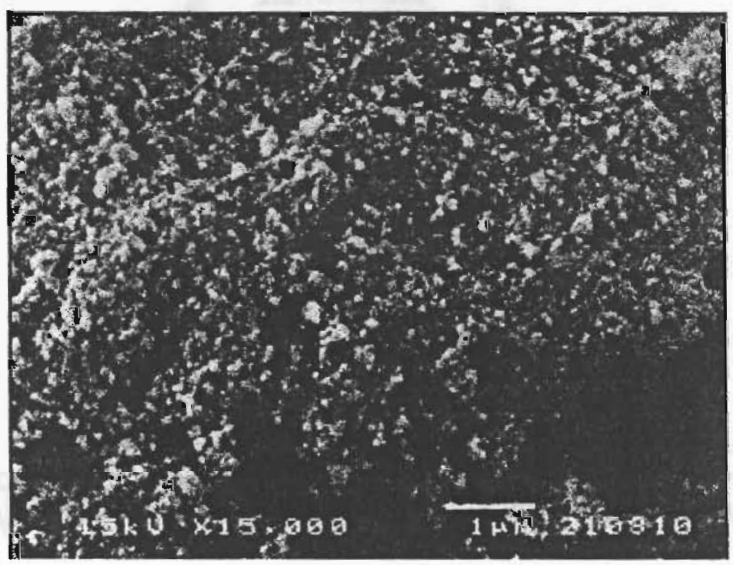

Figure 5.28 SEM photograph of zeolite beta synthesized from lignite fly ash at TEAOH/SiO_2 mole ratio of 0

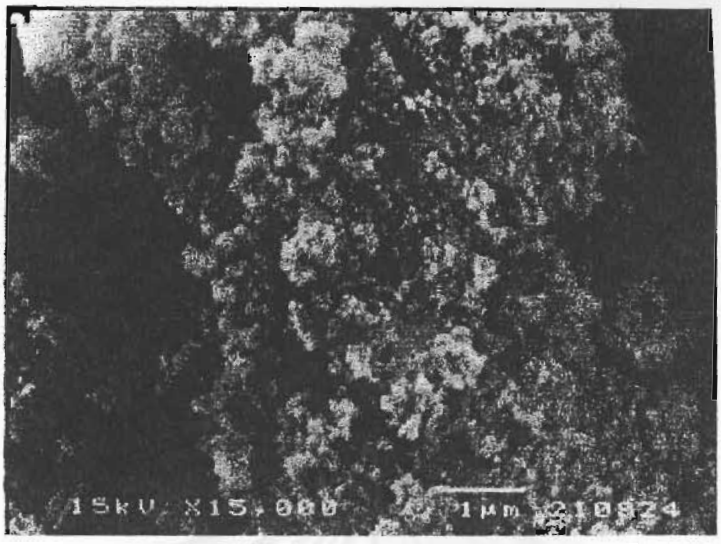

Figure 5.29 SEM photograph of zeolite beta synthesized from lignite fly ash at TEAOH/SiO_2 mole ratio of 0.25

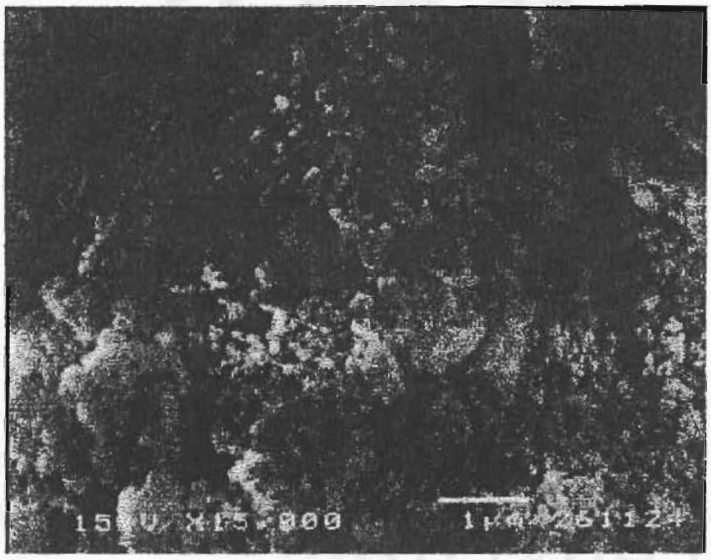

Figure 5.30 SEM photograph of zeolite beta synthesized from lignite fly ash at TEAOH/SiO_2 mole ratio of 0.3

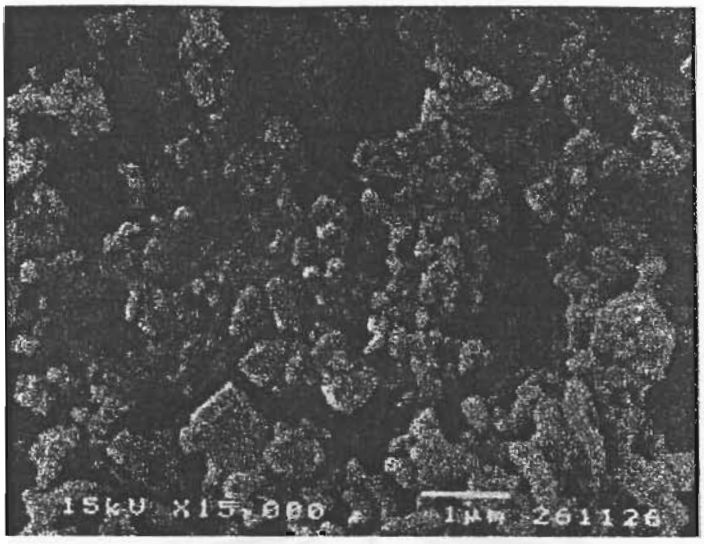

Figure 5.31 SEM photograph of zeolite beta synthesized from lignite fly ash at TEAOH/SiO_2 mole ratio of 0.4

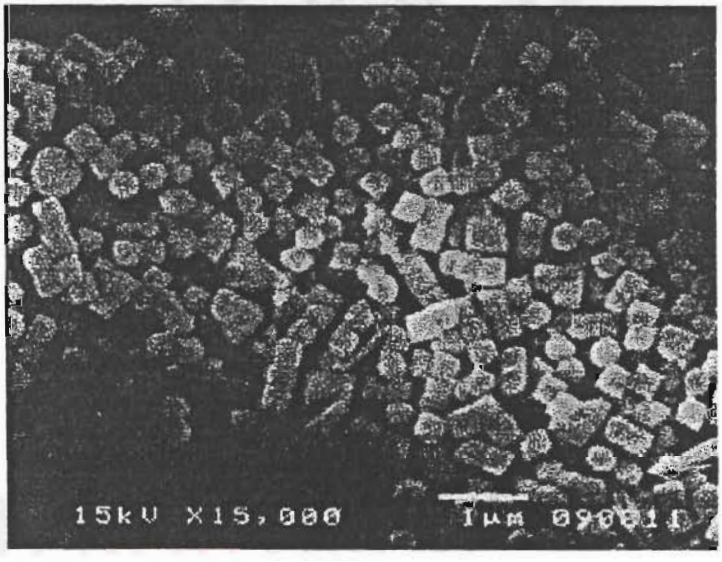

Figure 5.32 SEM photograph of zeolite beta synthesized from lignite fly ash at TEAOH/SiO_2 mole ratio of 0.5

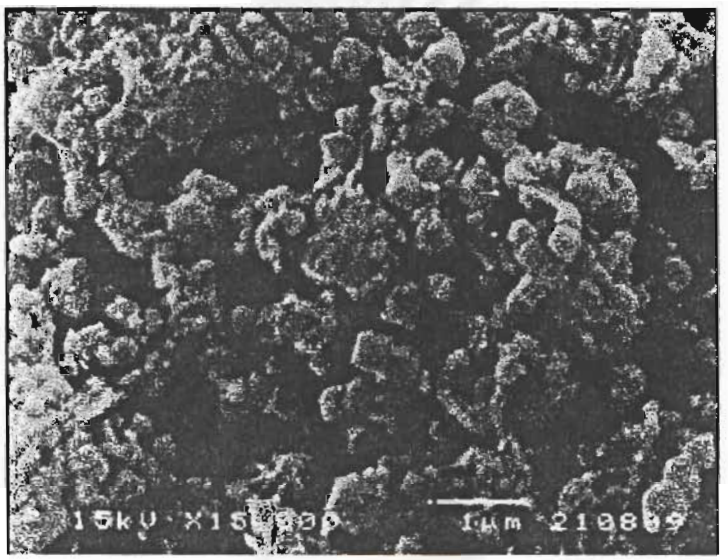

Figure 5.33 SEM photograph of zeolite beta synthesized from lignite fly ash at TEAOH/SiO_2 mole ratio of 0.75

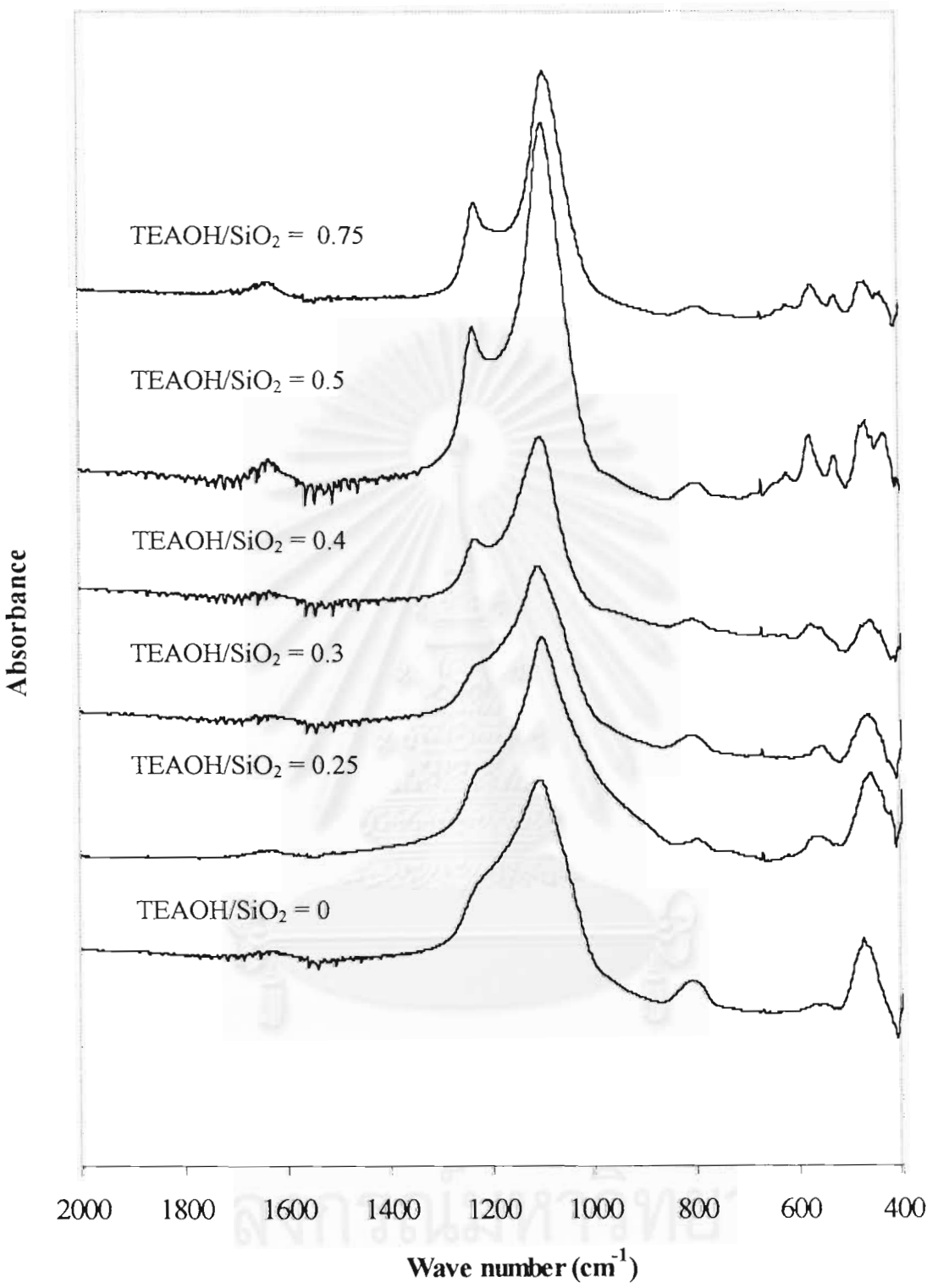

Figure 5.34 IR spectra of zeolite beta synthesized from lignite fly ash at various $TEAOH/SiO_2$ mole ratio

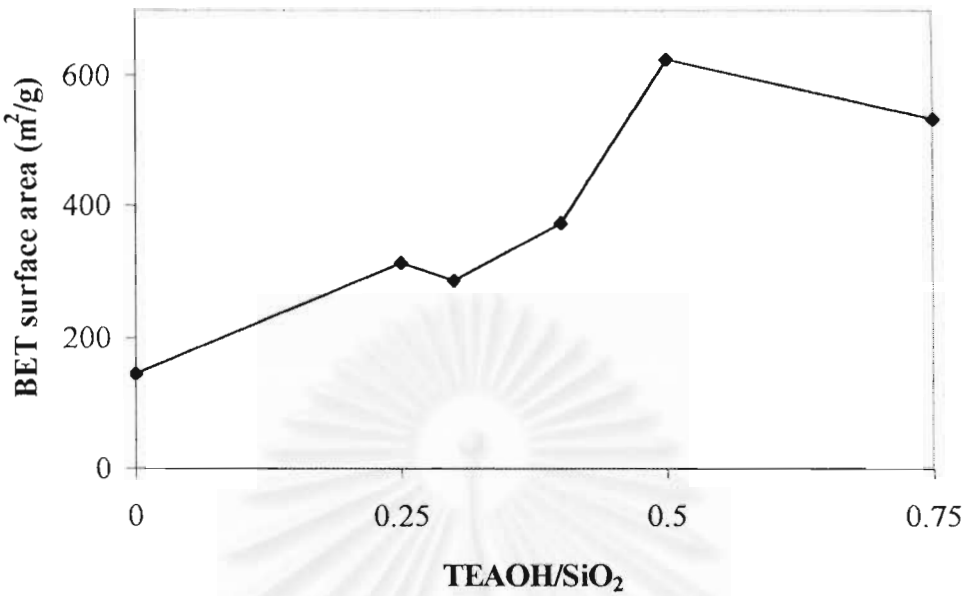

Figure 5.35 BET surface area of zeolite beta synthesized from lignite fly ash at TEAOH/SiO_2 mole ratio in the range of 0 to 0.75

5.1.2.4 Effect of amount of silica

Cataloid was used as source of Si of the synthesis of zeoltes Beta from lignite fly ash in this study and the effect of amount of silica assigned as Si/Al atomic ratio which was varied as following: 5, 25, 50, 60, 75, and 100. As discussed before, it found that at the best conditions were proceeded at temperature of aging with stirring and crystallization without stirring stage at 140^{o}C and TEAOH/SiO_2 mole ratio at 0.5.

(a) Characterization of product crystals by crystallinity

The XRD patterns of zeolite beta synthesized from lignite fly ash at various Si/Al atomic ratios were shown in Figure 5.36. From each XRD pattern was similar to XRD pattern of commercial zeolite beta as shown in Figure 5.4 and there was no peak of impurities because intensity of impurities were concealed by intensity of zeolite beta. The intensity of XRD pattern developed from Si/Al atomic ratio of 5 to 50 and the maximum intensity was carried out at Si/Al atomic ratio at 50. The intensity of XRD pattern decreased, which Si/Al atomic ratio was higher than 50. In addition, the XRD pattern also showed that at Si/Al atomic ratio, crystals obtained were amorphous forms.

The crystallinity of each was calculated, which the results of calculation show in Figure 5.37, the crystallinity increased with increasing of Si/Al atomic ratio from 5 to 50 and decreased at Si/Al atomic ratio higher than 50. The results of crystallinity were consistent to XRD patterns and the maximum crystallinity of 98% was carried out at Si/Al atomic ratio of about 50.

The results of XRD pattern and crystallinity indicated that at the Si/Al atomic ratio of 50 was the optimum condition for the synthesized of zeolite beta from lignite fly ash since the maximum product crystals were carried out at this ratio.

(b) External structure (morphology) analysis by scanning electron microscope

SEM photographs of zeolite beta synthesized from lignite fly ash at Si/Al mole ratio ranging from 5 to 100 were shown in Figure 5.38 to 5.43, respectively.

SEM photograph of zeolite beta synthesized at Si/Al atomic ratio of 5 was shown in Figure 5.38. It showed that product crystal was amorphous form, therefore, it illustrated that at Si/Al atomic ratio of 5 was not suitable for the synthesis of zeolite beta from lignite fly ash.

Figure 5.39 showed SEM photograph of zeolite beta synthesized from lignite fly ash at Si/Al atomic ratio of 25. At this condition, the product crystals almost contained of cuboid form of zeolite beta in size of about 1μm, however there was little amount of impurities in bar and irregular shape such as Fe_2O_3 also presented.

The crystal size of product obtained from Si/Al atomic ratio of 50 to 60 was about 0.25 μm as shown in Figure 5.40 and 5.41, respectively. At this condition, crystal shape was almost cuboid form, whereas, amorphous forms were disappeared. However, little amount of impurities also presented.

At Si/Al atomic ratio increased to 75 amount of cuboid crystal decreased and structure of zeolite beta crystal collapsed as amorphous form with Si/Al atomic ratio increased to 100 as shown in Figure 5.42 and 5.43, respectively.

The result analyzed from SEM photograph indicated that at the optimum Si/Al atomic ratio of about 50 was suitable for the synthesis of zeolite beta from lignite fly ash, which was consistent to results from XRD pattern.

(c) Functional group analysis

IR spectra of zeolite beta synthesized from lignite fly ash at various Si/Al atomic ratios were shown in Figure 5.44. The IR spectra of each band were similar to IR spectra of commercial zeolite beta in Figure 5.1. IR spectra developed from Si/Al atomic ratio from 5 to 50 and decreased with Si/Al atomic ratio higher than 50. The results showed strong shoulder band at around 1090 and 1230 cm^{-1}, which was the

best condition. As analyzed from IR spectra, the result was also consistent to results of XRD pattern and SEM photograph.

(d) BET surface area

The results of BET surface area showed in Figure 5.45. BET surface area of crystal obtained increased with increasing Si/Al mole ratio from 5 to 50 and distinctly decreased with Si/Al mole ratio increased to 100. The Si/Al mole ratio of 50, which was the best condition the BET surface area was about 630 m^2/g.

From results in the study of effect of amount of silica added into gel as presented above, it was found that at Si/Al atomic ratio lower than 5 zeolite beta was not occurred since Si in gel was not suitable to incorporate to be zeolite in liquid phase. As Si/Al atomic increased to 25, Si was enough to incorporate to be zeolite beta and at Si/Al atomic ratio of 50 was the optimum to synthesized zeolite beta from fly ash. However, at Si/Al atomic ratio higher than 0.5, it was not suitable to synthesize zeolite beta from lignite fly ash since at Si/Al atomic ratio higher than zeolite in liquid phase will transfer to other zeolites such as ZSM-12 and ZSM-5 [39,41,42]. Nevertheless, there were no other zeolites in this study.

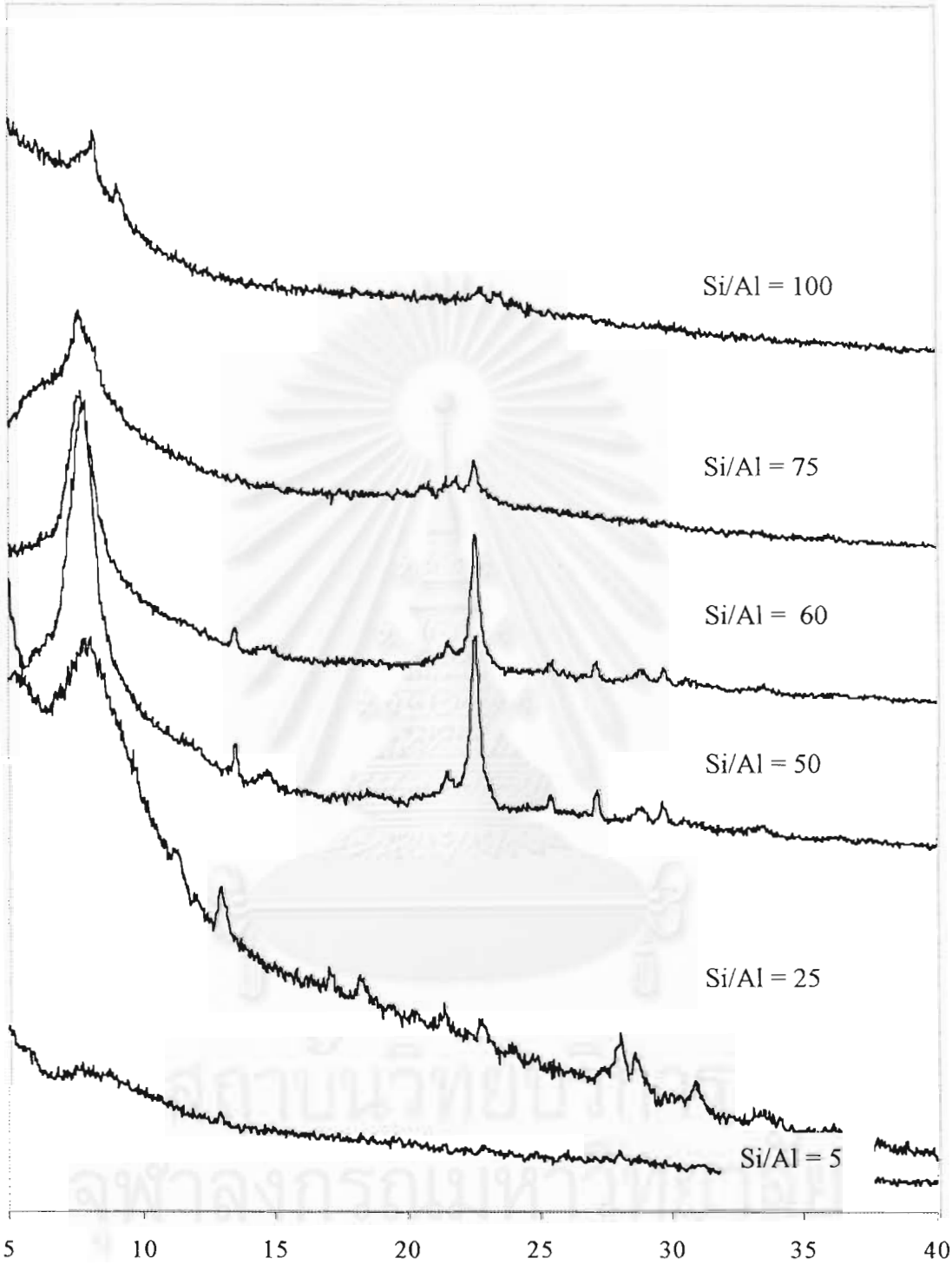

Figure 5.36 X-ray diffraction of zeolite beta synthesized from lignite fly ash at various Si/Al atomic ratio

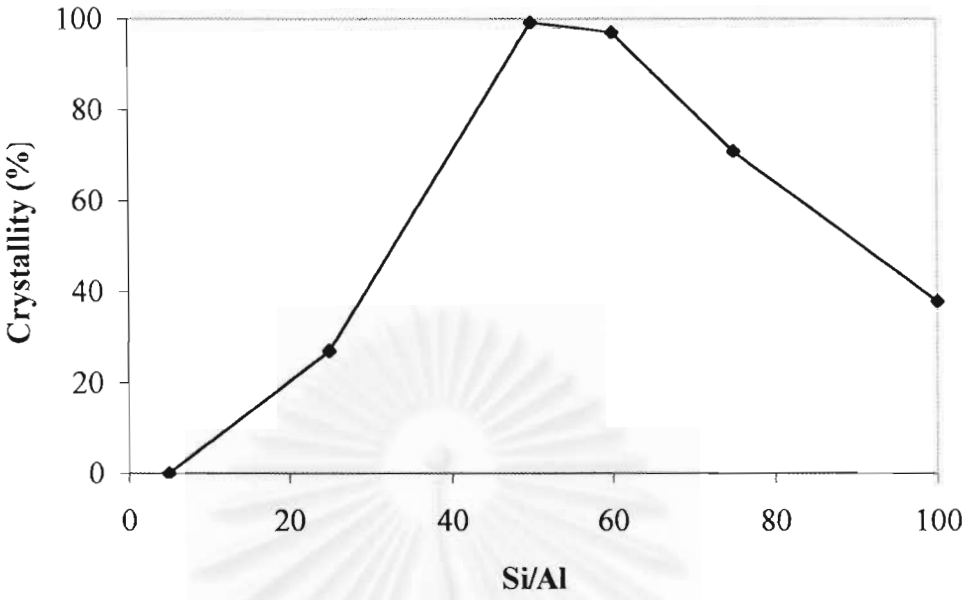

Figure 5.37 Percent crystallinity of zeolite beta synthesized from lignite fly ash at Si/Al atomic ratio in the range of 5 to 100

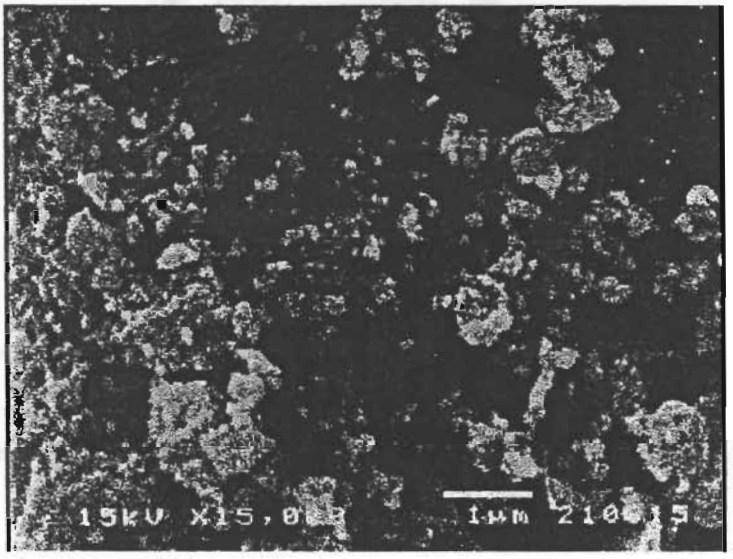

Figure 5.38 SEM Photograph of zeolite beta synthesized from lignite fly ash at Si/Al atomic ratio of 5

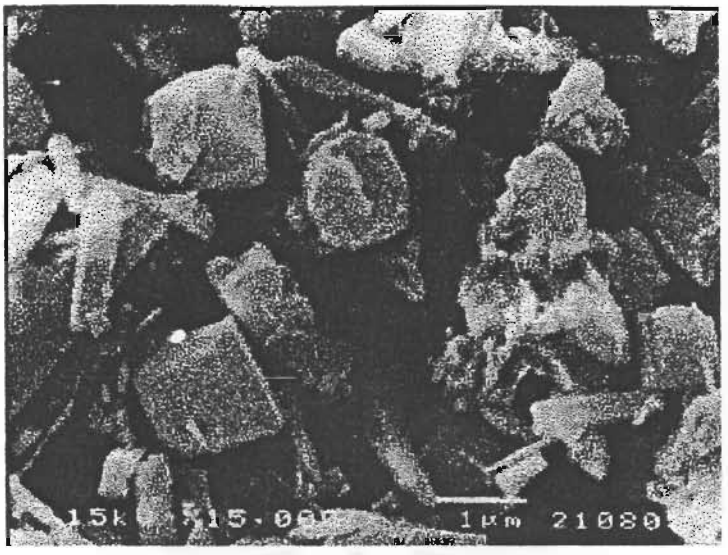

Figure 5.39 SEM Photograph of zeolite beta synthesized from lignite fly ash at Si/Al atomic ratio of 25

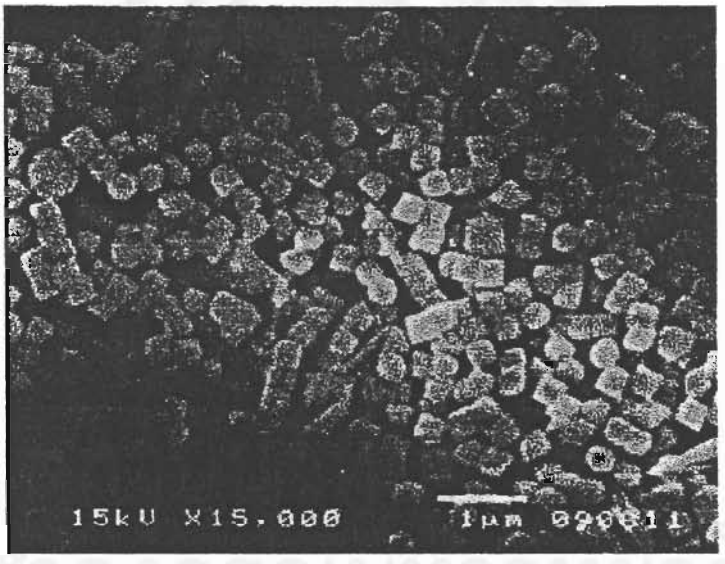

Figure 5.40 SEM Photograph of zeolite beta synthesized from lignite fly ash at Si/Al atomic ratio of 50

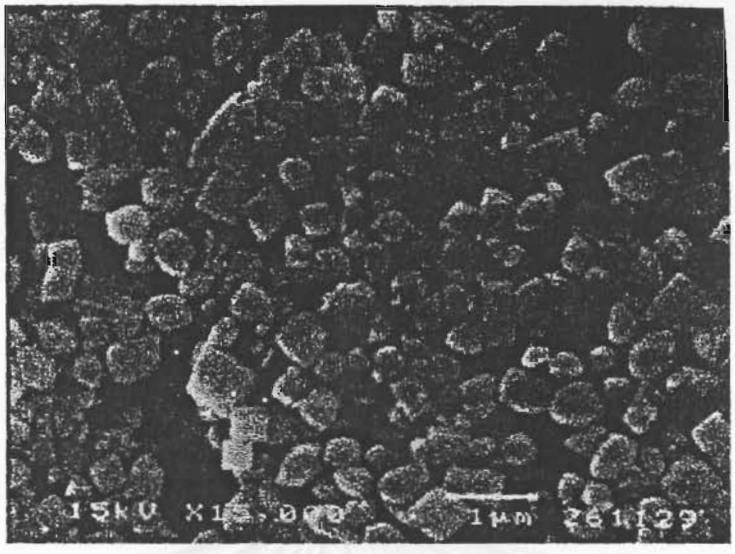

Figure 5.41 SEM Photograph of zeolite beta synthesized from lignite fly ash at Si/Al atomic ratio of 60

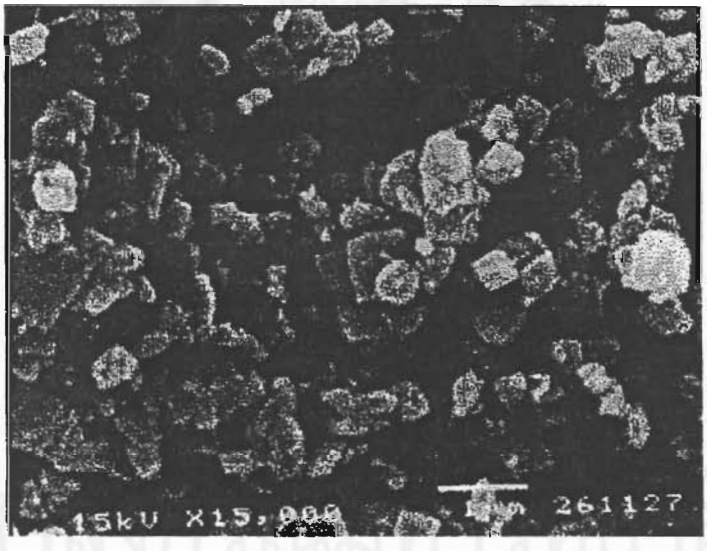

Figure 5.42 SEM Photograph of zeolite beta synthesized from lignite fly ash at Si/Al atomic ratio of 75

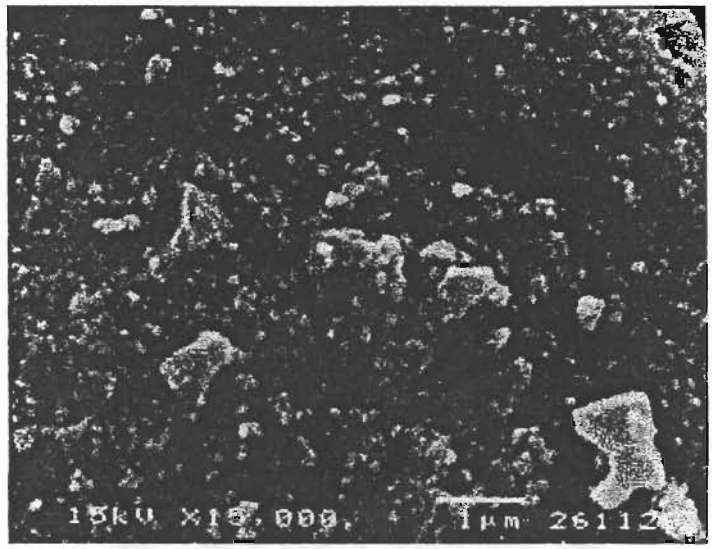

Figure 5.43 SEM Photograph of zeolite beta synthesized from lignite fly ash at Si/Al atomic ratio of 100

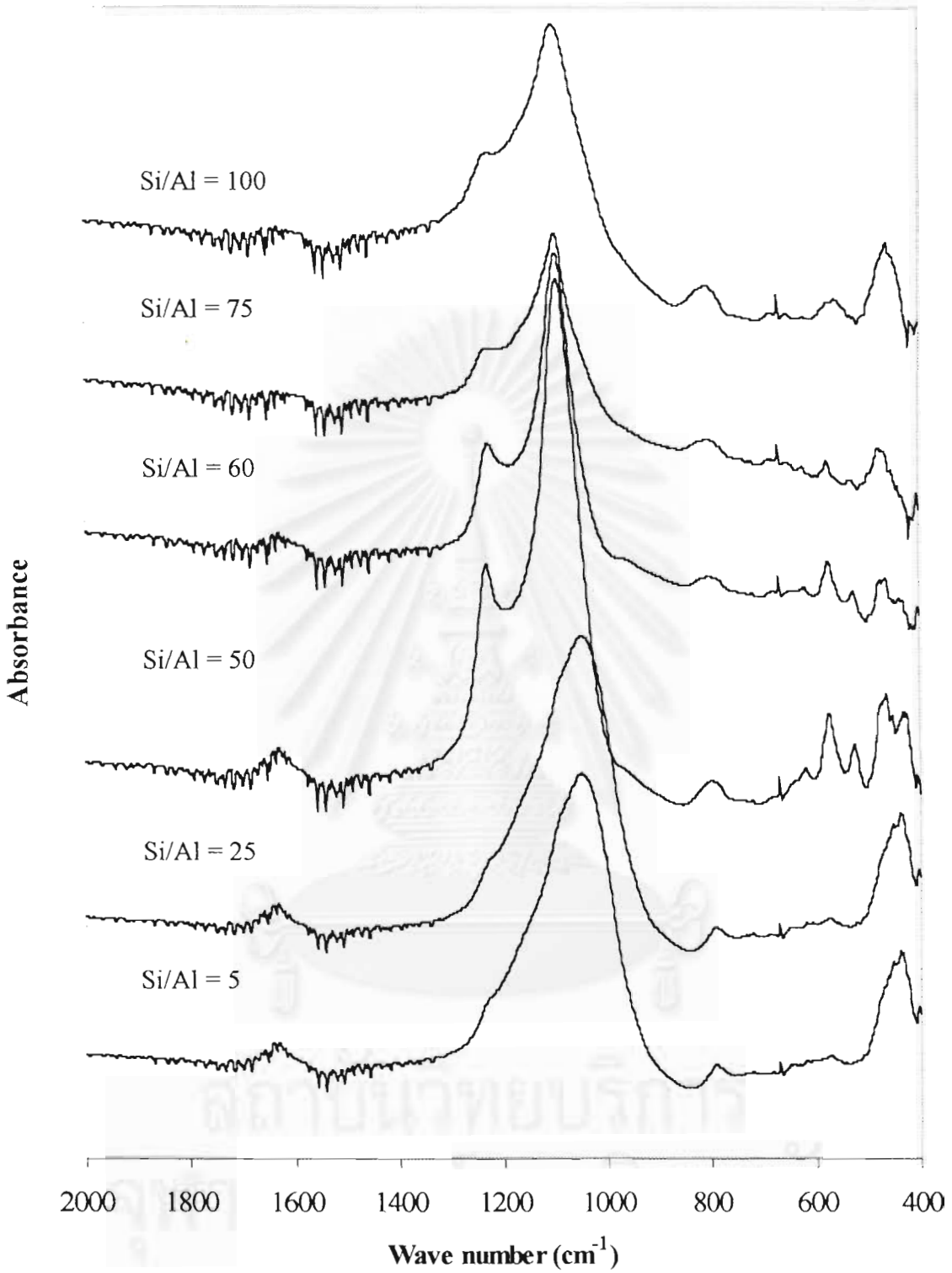

Figure 5.44 IR spectra of zeolite beta synthesized from lignite fly ash at various Si/Al atomic ratio

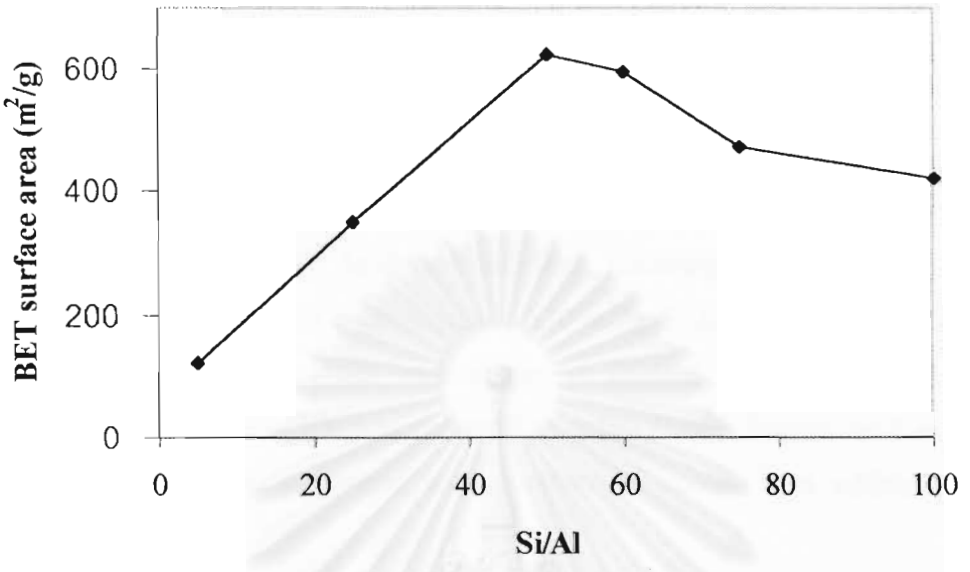

Figure 5.45 BET surface area of zeolite beta synthesized from lignite fly ash at Si/Al atomic ratio in the range of 5 to 100

5.1.3 Reaction Testing

Methanol conversion was used as reaction for testing zeolite beta synthesized from fly ash by comparing with commercial zeolite beta.

From the study, the optimum conditions synthesis of zeolite beta from lignite fly ash were stirring and aging temperature of 140°C, SiO_2/TEAOH mole ratio of 0.5, and Si/Al atomic ratio of 50. At these conditions, obtained crystals had crystallinity about 98 %, BET surface was approximately 630 m^2/g, Si/Al atomic ratio of about 20 and other chemical compositions were shown in Table 5.2. The obtained crystals were exchanged with NH_2NO_3 and calcined to zolite H-beta before used as catalyst Reaction was proceeded compared with commercial zeolite beta which has Si/Al atomic ratio of 15.

The results of reaction were shown in Figure 5.46. Methanol conversion from both catalyst was 100%. Products of methanol conversion were compared between synthesized zeolite beta from lignite fly ash and commercial zeolite beta. The product from both catalyst composed of three group of hydrocarbon which were paraffin, olefin and aromatic hydrocarbon. By comparing of each product amount of paraffin, amount of methane produced from commercial zeolite beta was greater than methane produced from zeolite beta synthesized from lignite fly ash however amount of ethane, propane and buthane were not quite different. Olefin products were composed of ethene, propene and butene. Amount of propene produced from zeolite beta synthesized from lignite flu ash was much greater than commercial zolite beta because it is well-known that Fe will reduce acid site, which can promote olefin formation. However, amount of ethene produced from commercial zeolite beta was slightly greater than zeolite beta synthesized from lignite fly ash. Amount of butene produce from both catalyst was not quite different because the distribution Fe in zeolite beta synthesized from lignite fly ash was not well and other impurities effected on selectivity of olefin formation. In addition, amount of aromatic hydrocarbon produce from both catalyst slightly occurred.

Table 5.2 Chemical composition of zeolite beta synthesized from lignite fly ash

Chemical compositions	Constituent (wt%)
SiO_2	91.15
Al_2O_3	3.97
Fe_2O_3	1.24
Na_2O	0.43
K_2O	1.38
MgO	0.42
CaO	1.32

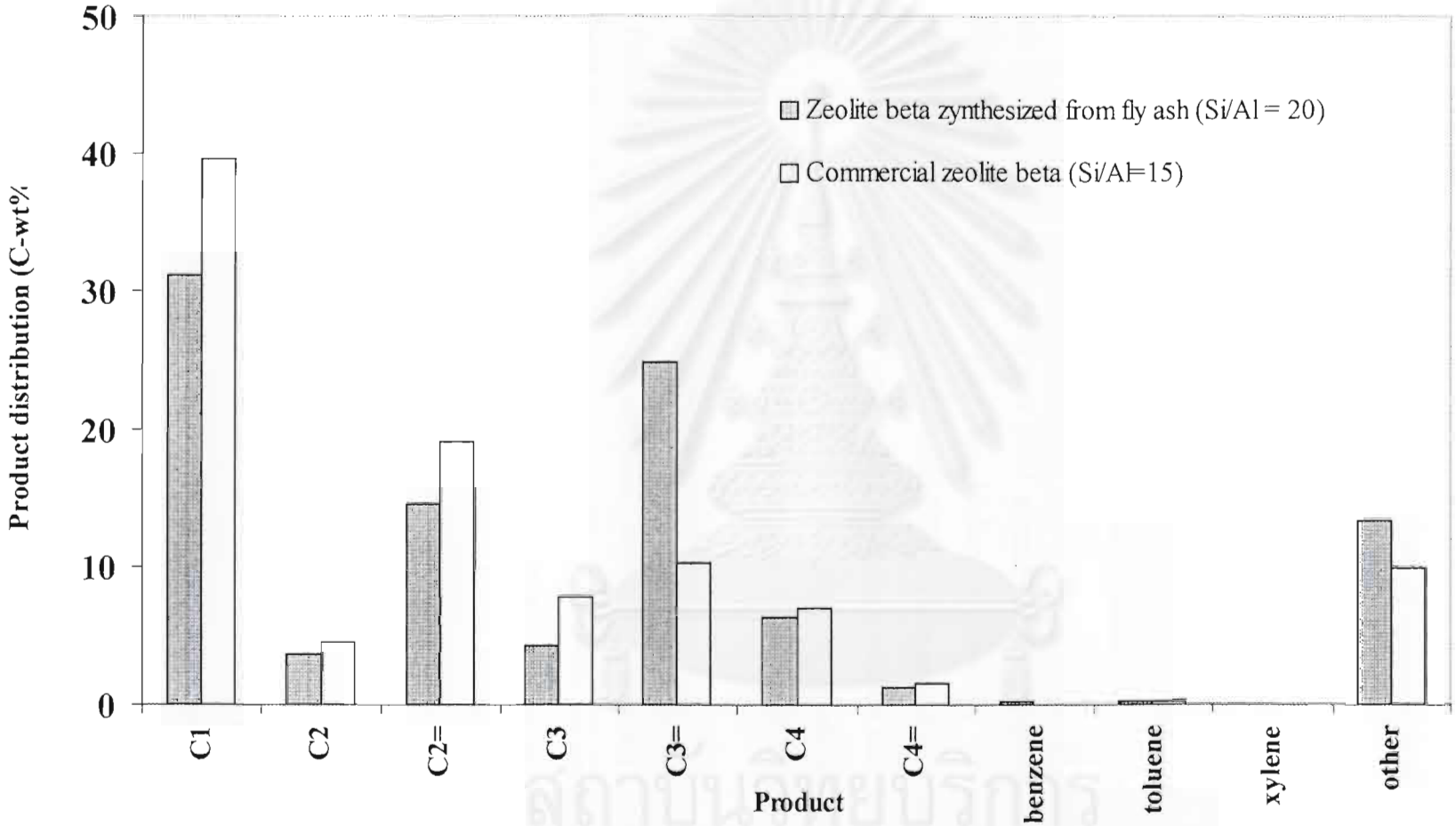

Figure 5.46 Product distribution (C-wt%) of methanol conversion compared between zeolite beta synthesized from lignite fly ash (Si/Al = 20) and commercial zeolite beta (Si/Al = 15)

CHAPTER VI

CONCLUSIONS AND RECOMMENDATIONS

In the study of factors affect to the structure of synthetic zeolite beta from lignite fly ash, the results were as follows:

The temperature of aging with stirring stage effected on the crystallinity of zeolite beta synthesized from fly ash. The optimum temperature at aging with stirring stage and temperature at crystallization without stirring stage was 140^{o}C and the temperature of both stage should be the same temperature since changing of the temperature during crystallization will disturb the crystallization of zeolite. The optimum TEAOH/SiO_2 mole ratio and Si/Al atomic ratio were about 0.5 and 50, respectively. At this condition gave the highest crystallinity of zeolite beta synthesized from lignite fly ash about 98% and BET surface area about 630 m^2/g and uniform crystal size was about 0.25 μm. At this optimum condition the characteristics of zeolite beta synthesized from lignite fly ash are not much different from commercial zeolite beta which has BET surface area and average crystal sized 0.5 about μm and 700 m^2/g, respectively.

Furthermore, the results of methanol conversion between zeolite beta synthesized from lignite fly ash and commercial zeolite beta are quite the same. However, there is Fe also presented in obtained crystal. However, effect of Fe presented in zeolite beta synthesized from fly ash to olefin formation is not clear, it may be because of distribution of Fe and effect of other impurities.

In this study, lignite fly ash which used as source of SiO_2 and Al_2O_3, was untreated and it also has Fe_2O_3 and other metal oxides, which can contaminate zeolite crystals therefore the removal of metal oxide prior to synthesis is necessary. The alternative of using chaff in stead of lignite fly ash may be better since it has less impurity.

REFERENCES

1. Balkema, A. A. Fly Ash as Addition to Concrete, pp. 7-16, Netherlands: A.A. alkema Publishers, 1992.
2. Chen, N.Y.; Garwood, W.E.; Dwyer, F.G. Shape Selective Catalyst in Industrial Applications, 2nd ed., New York: Marcal Dekker, 1996.
3. Cliament, M.J.; Corma, A.; Garcia, H.; Iboraa, S. and Primo, J. "Heterogeneous Catalysis and Fine Chemicals II" Stud. Surf. Sci. Catal. 59 (1991): 557.
4. Croma, A.; Gonzales-Alfaro, V. and Orchilles, A. V. Appl. Catal. 129 (1995): 203-215.
5. Drzaj, B.; Hocevar, S. and Pejovik, S. Zeolites: Synthesis, Structure, Technology and Application, pp.147-154, Elsevier, 1985.
6. Haag, W.O. and Chen N.Y. Catalyst Design: Progress and Perspectives, pp. 163-207, New York: John Wiley & Sons, 1987.
7. Hollman, G.G.; Steenbruggen, G. and Janssen-Jurkovicova, M. Fuel 78 (1999): 1225-1230.
8. Holtermann, D.L. US Patent 5 082 988 (1992).
9. King, R.B. Encyclopedia of Inorganic Chemistry, pp.4365-4391, vol. 7, Wiley & Sons, 1994.
10. Kunavanakit, V. "Lignite Fly Ash" Journal of Electricity Generating Authority of Thailand, Bangkok, 1995.
11. Lopez-Salinas, E.; Salas, P.; Schifter, I.; Moran, M.; Castillo, S. and Mogica, E. Prog. Zeo. Microp. Mat. 105 (1997): 1565-1570.
12. Modica, F. S. US Patent 5 233 121 (1993).
13. Pattanaporn, C. and Chareonwipartchaed, P. Synthesis of Zeolilte from Gaolinite. Senior Project, Department of Chemistry, Faculty of Science, Kasetsart University, Bangkok, 1992 .
14. Phumethum, S. and Siriadhul, V. Synthesis of Zeolite from Gaolinite. Senior Project, Department of Chemistry, Faculty of Science, Chulalongkorn University, Bangkok,1988.
15. Querol, X.; Alastuey, A.; Fernandez-Turiel, J.L. and Lopes-Soler, A. Fuel 74 (1995): 1226-1231.
16. Querol, X.; Plana, F.; Alastuey, A. and Lopes-Soler, A. Fuel 76 (1997): 793-799.

17. Ratnasamg, P.; Bhat, R. N.; Pokhrrigak, S. K.; Hegde, S.G. and Kumar, R. J. Catal. 199 (1989): 65.

18. Samran, M. and Chareonpanich, M. Upgrading of Lignite Fly Ash to Zeolitic Compounds, Proceeding of Thailand Chemical Engineering Conference, 8 th, pp. 176-183, Bangkok, 1998.

19. Satterfield, C.N. Heterogeneous Catalysis in Industrial Practice, 2nd ed., pp. 226-259, New York: McGraw-Hill, 1991.

20. Shigemoto, N. and Hayashi, H. J. Mat. Sci. 28 (1993): 4781-4786.

21. Szostak, R. Handbook of Molecular Sieves, pp. 92-97, New York: Van Nostrand Riengold, 1992.

22. Wesche, K. Fly Ash in Concrete: Properties and Performance, pp. 3-22, London: E & FN SPON, 1991.

23. Yingyuad, R. and Shinaphan, N. Synthesis of Zeolite from Gaolinite. Senior Project,Department of Chemical Engineering, Faculty of Engineering, Kasetsart, Bangkok, 1993-1994.

24. Fukui, K.; Yoshida, H.; Sakaguchi, H. and Arita, M. Kagaku Kogaku Ronbunshu. 25 (1999): 987-991.

25. Yang, G.C.C. and Yang, T.Y. J. Harz. Mat. 62(1998): 75-89.

26. Chang, H.L.; Chun, C.M.; Aksay, I.A. and Shih, W.H. Ind. Eng. Chem. Res. 38 (1999): 973-977.

27. Kang, S.J.; Egashira, K. and Yoshida, A. Appl. Clay. Sci. 13(1998): 117-135.

28. Zhao, X.S.; Lu, G.Q. and Zhu, H.Y. J. Por. Mat. 4(1997): 245-251.

29. Barrer, R.M. Hydrothermal Chemistry of Zeolites, London: Acedamic Press, 1982.

30. Breck, D.W. Zeolite Molecular sieves, New York: Wiley-Interscience, 1974.

31. Bekkum, H.V.; Flanigen. E.M. and Jansen, J.C. Stud. Surf. Sci. Catal: 578 (1991).

32. Szoztak, R. Molecular Sieve Principles of Synthesis and Identification, pp. 1-50, Newyork: Van Nostrand Reingold, 1989.

33. Meier, W.M. and Olson, D.H. Atlas of Zeolite Structure Types, 3rd revised ed., int. Zeolite Assoc., Boston: Butterworth-Heiemann, 1992.

34. Tsai, T.; Lui, S. and Wang, I. Appl. Catal. A 181(1991): 355-3698.

35. Barthoment, D. " Acidic catalysts with Zeolites", Zeolites Science and Techology (Rebeira, F.R. et al.), Matinus Nijhoff Publishers, The Hange, 1984.

36. Ashton, A.G.: Batamanian, S. and Dwyer, J. “Acid in Zeolite” (lmelik, B. et al.), Catalysis by Acid-Bases, Amsterdam: Elesvier, 1985.
37. Sano, T.; Fujisawa, K. and Higiwara, H. “High Stream Stability if H-ZSM-5 Type Zeolite Containing Alkaline Earth Metals” Catalyst Deactivation, (Delmon, B. and Froment, G.R. eds), Stud. Surf. Sci. catal., p 34, Amsterdam: Elsevier, 1987.
38. Tanake, K.; Misona, M.; Ona, Y. and Hattori, H. “New Solid Acids and Bases” (Delman, B. and Yates, J.T. et al.), Stud. Surf. Sci. Catal., p. 51, Tokyo: Elesvier, 1989.
39. Eapen, M.J.; Reddy, K.S.N. and Shiralkar, V.P. Zeolites 14(1994): 295-302.
40. Treacy,M.M.J.; Higgins, J.B. and Ballmoos, R. Collection of Simulated XRD Powder Patterns for Zeolites, 3rd ed., Elesvier, 1996.
41. Perez-Pariente, J., Martens, J.A. and Jacobs, P.A. Appl. Catal., 31(1987): 35.
42. Perez-Pariente, J., Martens, J.A. and Jacobs, P.A. Zeolites, 8(1988): 46.

APPENDICES

APPENDIX A

SAMPLE OF CALCULATIONS

A-1 Calculation of Si/Al Atomic for Beta Zeolite Preparation

The calculation is based on weight of fly ash (Si/Al ≈1.5600)

For fly ash 1 g (Si/Al ≈1.5600):

Amount of Si = 0.0078

Amount of Al = 0.0050

For example, to prepare zeolite Beta at Si/Al atomic ratio of 50 in which, mole ratio of TEAOH/SiO_2 is 0.5, therefore the addition of Si is necessary.

Si/Al = 50 = (0.0078 + X) / 0.0050 (A-1-1)

X = 0.2422 mole

X is equivalent to amount of Si added into the mixture for preparing zeolite Beta at Si/Al = 50. Therefore, 0.2422 mole of Si is equivalent to 0.2422 mole of SiO_2 (In 1 mole of SiO_2 consist of Si 1mole).

Cataloid (SiO_2 30% wt in water) use as the source of silicon.

Molecular weight of SiO_2 = 60.0843

Therefore, weight of added SiO_2 = 0.2422 x 60.0843

= 14.5524 g

And amount of used Cataloid = (14.5524 x 100) / 30

= 48.5080 g

And the calculation of amount of TEAOH For the preparation of zeolite Beta at mole ratio of TEAOH/SiO_2 = 0.5 as following:

TEAOH (TEAOH 40% wt in water) use as the template of zeolite Beta.

Molecular weight of TEAOH = 147.2600

And

Mole ratio of TEAOH/SiO_2 = 0.5000 (A-1-2)

From Equation (A-1-1), the total mole of Si in the mixture is

Total mole of Si = 50 x 0.0050

= 0.2500 mole

From Equation of (A-1-2), amount of TEAOH used preparation of zeolite Beta at Si/Al atomic ratio of 50 in which, mole ratio of TEAOH/SiO_2 is 0.5, is:

Total mole of TEAOH = 0.25 x 0.50

= 0.1250 mole

And, equivalent to weight of TEAOH:

Weight of TEAOH = 0.125 x 147.260

= 18.4075 g

Amount of used TEAOH solution

= (18.4075 x 100) / 40

= 46.0186 g

This is the amount of Cataloid and TEAOH used for preparation of zeolite Beta at Si/Al = 50 and TEAOH/SiO_2 = 0.5.

A-2 Calculation of Reactant Flow Rate

The used catalyst = 0.3000 g

Packed catalyst into quartz rector (inside diameter = 0.6 cm).

Determine the average height of catalyst bed = H cm, so that,

Volume of bed = $\pi(0.3)^2$ x H ml-cat.

Use Gas Hourly Space Velocity (GHSV) = 2000 h^{-1}

$$GHSV = \frac{\text{Volumetric flow rate}^1}{\text{Volume of bed}}$$

$$= \frac{2000 \times \text{Volume of bed}}{2000\pi(0.3)^2 \times H} \quad \text{ml/h}$$

$$= \frac{2000\ \pi\ (0.3)^2 \times H}{60} \quad \text{ml/min}$$

at STP condition:

$$\text{Volumetric flow rate} = \text{Volumetric flow rate}^1 \times \frac{(273.15 + T)}{273.15}$$

Where T = room temperature, ^oC

A-3 Calculation of Percent Crystallinity

For calculation of percent crystallinity, selected 5 order of intensity of XRD pattern.

$$\% \text{ crystallinity} = \frac{\text{Sum of peak intensity (unknown)}}{\text{Sum of peak intensity (standard)}}$$

Commercial zeolite beta which had Si/Al atomic ratio of 55 was used as standard

A-4 Calculation of Conversion and Hydrocarbon Distribution of Methanol conversion reaction

Methanol conversion was evaluated in term of the conversion of methanol into other hydrocarbons.

For example : Synthesized Zeolite H-beta (Si/Al = 20)

Reaction condition: Reaction temperature 450^{o}C, GSHV = 2000 h^{-1}, feed 20% methanol N_2 balanced, 1 h time on steam.

Methanol conversion activity was evaluated in term of conversion of methanol into other hydrocarbons.

$$\text{Methanol conversion (\%)} = \frac{(\text{methanol}_{in} - \text{methanol}_{out}) \times 100}{\text{methanol}_{in}}$$

From data of Shimadzu GC 8A (Porapack-Q column)

$$\text{Mthanol comversion (\%)} = \frac{(248421 - 0) \times 100}{248421}$$

$$= 100\ \%$$

From data of Shimadzu GC 14B (VZ-10 column)

Area of C_1 = 2233145

Area of C_2 = 258913

Area of $C_2^{=}$ = 1042315

Area of C_3 = 309211

Area of $C_3^{=}$ = 1779053

Area of C_4 = 458168

Area of $C_4^{=}$ = 94951

Area of C1-C4 = 2233145 + 258913 + 1042315 + 309211 + 1779053 + 458168 + 94951

= 6175756

From data of Shimazdu GC 14A (OV-1 column)

The first part of data area is C_1-C_4.

Area of C_1-C_4 = 60019

Total area = 69620

So that: compared area from Shimazdu GC 14B (VZ-10 comlumn) and Shimazdu GC 14A (OV-1 column)

$$\text{area of } C_1 \text{ (OV-1)} = \frac{\text{area of } C_1 \text{ (VZ-10) x area of } C_1\text{-}C_4 \text{ (OV-1)}}{\text{area of } C_1\text{-}C_4 \text{ (VZ-10)}}$$

$$= (2233145 \times 60019) / 6175756$$

$$= 21703$$

The other were calculated as the same way

Area of C_2 (OV-1) = 2516

Area of $C_2^=$ (OV-1) = 10130

Area of C_3 (OV-1) = 3005

Area of $C_3^=$ (OV-1) = 17290

Area of C_4 (OV-1) = 4453

Area of $C_4^=$ (OV-1) = 923

Hence: Product distribution (C-wt%)

C_1 = [area C_1 (OV-1) x 100] / total area of OV-1

= [21703 x 100] / 69620

= 31.17 %

C_2 = 3.61 %

$C_2^=$ = 14.55 %

C_3 = 4.31 %

$C_3^=$ = 24.83 %

C_4 = 6.39 %

$C_4^=$ = 1.32 %

and,

benzene= 0.23

toluene= 0.30

xylene = 0

APPENDIX B

DATA OF EXPERIMENT

Table B1 Data of Figure 5.6

Temperature (^{o}C)	% Crysallinity
80	48
90	50
100	55
120	62
135	75

Table B2 Data of Figure 5.17

Temperature (^{o}C)	%Crystallinity
110	33
120	59
130	70
135	84
140	99
150	95

Table B3 Data of Figure 5.27

TEAOH/SIO2 mole ratio	%Crystallinity
0	0
0.25	8
0.3	19
0.4	41
0.5	99
0.75	34

Table B4 Data of Figure 5.37

Si/Al atomic ratio	%Crystallinity
5	0
25	27
50	99
60	97
75	71
100	38

Table B5 Data of Figure 5.15

Temperature (^{o}C)	BET surface area (m2/g)
80	306
90	256
100	364
120	385
135	362

Table B6 Data of Figure 5.25

Temperature (^{o}C)	BET surface area (m2/g)
110	607
120	292
130	359
135	362
140	624
150	612

Table B7 Data of Figure 5.35

TEAOH/SIO2 mole ratio	BET surface area (m2/g)
0	146
0.25	314
0.3	287
0.4	375
0.5	624
0.75	533

Table B8 Data of Figure 5.45

Si/Al atomic ratio	BET surface area (m2/g)
5	121
25	350
50	624
60	595
75	472
100	422

Table B9 Data of Figure 5.46

Product	Product distribution (C-wt%) of commercial zeolite beta	Product distribution (C-wt%) of zeolite beta synthesized from lignite fly ash
C_1	39.61	31.17
C_2	4.55	3.61
$C_2^=$	19.05	14.55
C_3	7.83	4.31
$C_3^=$	10.22	24.83
C_4	6.97	6.39
$C_4^=$	1.59	1.32
Benzene	0	0.23
Toluene	0.29	0.30
Xylene	0	0
other	9.89	13.29

VITA

Mr. Panusit Turatum was born in Phare, Thailand on August 1,1976. He received Bachelor' s Degree of Chemical Engineering from Department of Chemical Engineering, Faculty of Engineering Srinakarinwirote University in 1999.